SAPIENZA
UNIVERSITÀ DI ROMA

Faculty of Mathematical, Physical, and Natural Sciences

PhD PROGRAMME IN
GENETICS AND MOLECULAR BIOLOGY

XXXVIII Cycle
(A.A. 2025/2026)

Architecture of light-independent seed germination: a multi-layered regulation in the model plant *Cardamine hirsuta*

PhD Candidate
Andrea Lepri

Supervisor
Prof. Paola Vittorioso

Tutor
Prof. Raffaele Dello Ioio

Coordinator
Prof. Isabella Saggio

Index

1. Glossary

Symbol	Definition
$^1O_2$	Singlet oxygen
ABA	Abscisic acid
ABA1	ABA DEFICIENT 1
ABA8'OH-1	ABA 8′-HYDROXYLASE 1
ABI3/4/5	ABSCISIC ACID INSENSITIVE 3/4/5
AHG1/3	ABA HYPERSENSITIVE GERMINATION 1 and 3
AL	ALFIN-LIKE readers
ATP	Adenosine triphosphate
AUX1	AUXIN RESISTANT 1
bHLH	Basic helix–loop–helix
BL	Blue light
ChIP	Chromatin immunoprecipitation
CHO1	CHOTTO 1 - AINTEGUMENTA-like 5
CLF	CURLY LEAF E(Z) homolog
COP1	CONSTITUTIVE PHOTOMORPHOGENIC 1
CRY1/2	CRYPTOCHROMES 1-2
CYP	Cyprus accession of *Aethionema arabicum*
CYP707A1/2/3	CYTOCHROME P450, FAMILY 707, SUBFAMILY A, POLYPEPTIDE 1/2/3
DAG1	DOF AFFECTING GERMINATION 1
DAP	Days After Pollination
DELLA	Group of GRAS Transcription Regulators mediating GA Signaling
DMSO	Dimethyl sulfoxide
DOF	DNA binding with one finger
DOG1	DELAY OF GERMINATION 1
E(Z)	ENHANCER OF ZESTE PRC2 core subunit
ELIPs	EARLY LIGHT-INDUCIBLE PROTEINs

EMF2	EMBRYONIC FLOWER 2 SU(Z)12 homolog
ESC	EXTRA SEX COMBS PRC2 core subunit
EZH1/2	Methyltransferase catalytic subunits of PRC2
FIE	FERTILIZATION-INDEPENDENT ENDOSPERM ESC homolog
FIS2	FERTILIZATION-INDEPENDENT SEED SU(Z)12 homolog
FLC	FLOWERING LOCUS C
FR	Far-Red light
FR-HIR	Far Red-High Irradiance Response
FUS3	FUSCA3
GA	Gibberellin/Gibberellic acid
GA20OX1/2/3	GIBBERELLIN 20-OXIDASE 1/2/3
GA2OX2/3	GIBBERELLIN 2-OXIDASE 2/3
GA3OX1/2	GIBBERELLIN 3 BETA-HYDROXYLASE 1/2
GAI	GIBBERELLIC ACID INSENSITIVE
gRNA	guide RNA
H2Aub	Monoubiquitination of histone H2A
H_2O_2	Hydrogen Peroxide
H3ac	Acetylation of histone H3
H3K27me3	Tri-methylation at the 27th lysine residue of histone H3
H3K4me3	Tri-methylation at the 4th lysine residue of histone H3
H3K9me2	Di-methylation at the 9th lysine residue of histone H3
HAI	Hours After Imbibition
HD2A/B	HISTONE DEACETYLASE 2A/B
HDA6/19	HISTONE DEACETYLASE 6/19
HDACs	HISTONE DEACETYLASEs
HIR	High Irradiance Response
HY5	ELONGATED HYPOCOTYL 5
koy1	Koyash1 mutant for the HEME OXYGENASE 1 gene
koy2	Koyash2 mutant for the PHYA gene

leaflets	Dissected leaves divided into individual units
LEC1	LEAFY COTYLEDON 1
LHCII	Antenna complex of PSII
lncRNAs	long non-coding RNAs
MEA/FIS1	MEDEA E(Z) homolog
miRNAs	Micro RNAs
MSI1/5	MULTIPLE SUPPRESSOR OF IRA 1/5 p55 homolog
mya	Million years ago
NADPH	Nicotinamide Adenine Dinucleotide Phosphate
NCED1/6/9	NINE-CIS-EPOXYCAROTENOID DIOXYGENASE 1/6/9
OX	Oxford ecotype of *Cardamine hirsuta*
p55	55 kDa WD40 repeat-containing histone remodelling factor PRC2 core subunit
PAC	Paclobutrazol
PAR1/2	PHY RAPIDLY REGULATED 1/2
PcG	Polycomb group
Pfr	Active phytochromes form
PHOT1/2	PHOTOTROPINS 1-2
phyA-E	Phytochromes A-E holoprotein
PIF1	PHYTOCHROMES INTERACTING FACTOR 1
PIFs	PHYTOCHROMES INTERACTING FACTORs
PP2C	PROTEIN PHOSPHATASE TYPE 2C
Pr	Inactive phytochromes form
PRC1/2	POLYCOMB REPRESSIVE COMPLEX 1/2
PSI-II	PHOTOSYSTEM I-II
PTMs	Post-Translational Modifications
qE	Non-photochemical quenching
R	Red light
RCO	REDUCED COMPLEXITY
RdDM	RNA-directed DNA methylation

RDS 3434	1,5-bis-(3-bromo-4-methoxyphenyl)penta-1,4-dien-3-one
RGA	REPRESSOR OF GA
RNAPII-S2P	RNA Polymerase II, Ser2-phosphorylated form
RNAPII-TOT	RNA Polymerase II, total amount
ROS	Reactive Oxygen Species
RT-qPCR	Real-Time quantitative PCR
RUP	REPRESSOR OF UV-B PHOTOMORPHOGENESIS
SET domain	SU(var)3-9, Enhancer-of-zeste and Trithorax domain
SNL1/2	SIN3-LIKE 1/2 corepressors homologs of the transcriptional repressor SIN3
SU(Z)12	SUPPRESSOR OF ZESTE 12 PRC2 core subunit
SUVH	SU(var)3-9 homologue
SWN	SWINGER
SWR1	SWI2/SNF2-Related 1 chromatin remodeling complex
TFs	Transcriptional Factors
TRX	Trithorax complex
TUR	Turkey accession of *Aethionema arabicum*
UHPLC-MS/MS	Ultra-high performance liquid chromatography tandem mass spectrometry
UNC1999	N-[(6-methyl-2-oxo-4-propyl-1H-pyridin-3-yl)methyl]-1-propan-2-yl-6-[6-(4-propan-2-ylpiperazin-1-yl)pyridin-3-yl]indazole-4-carboxamide
UV-B	Ultraviolet-B radiation
VDE	VIOLAXANTHIN DE-EPOXIDASE
VLFR	Very Low Fluence Response
VRN2	VERNALIZATION 2 SU(Z)12 homolog
WS	Wassilewskija ecotype of *Arabidopsis thaliana*
ΔpH	Transmembrane pH gradient

2. Summary

Light is a pivotal environmental factor in plant life cycle, which integrates energy and information on the surrounding environment, affecting many developmental processes. One example is represented by seed germination which, in the model system *Arabidopsis thaliana*, is induced by light; however, seeds of several plant species can germinate regardless of this stimulus. While the molecular mechanisms underlying light-dependent seed germination are well understood, those governing the light-independent one are still vague, mostly due to the lack of suitable model systems. In this study, we employ *Cardamine hirsuta*, a close relative of *Arabidopsis*, as a powerful model to uncover both the molecular and epigenetic mechanisms underlying light-independent germination. In *Arabidopsis*, the two phytohormones gibberellins (GA) and abscisic acid (ABA) are proved to be antagonistic key regulators in the germination process, with the establishment of a high GA/ABA ratio allowing germination. In our study we show that a high GA/ABA ratio is fundamental also for the germination of *Cardamine* seeds, in both light and dark conditions, and that the DOF transcriptional repressor ChDAG1, homologous of AtDAG1, a repressor of seed germination able to control both GA and ABA levels, is involved in this process, mitigating GA levels in both conditions and being induced by GAs in darkness, allowing to hypothesize a feedback control. Given the involvement of PRC2 and of its mark H3K27me3 in germination of *Arabidopsis* seeds, we also investigate how an alternative deployment of this PTM might support *Cardamine* light-independent germination. Our data reveal a progressive increase of H3K27me3 during the developmental steps preceding germination, and a reduction of this mark uncoupled from light stimulus during early germination. Finally, a time-resolved nuclear profiling reveals a light-independent nuclear reorganization during early germination. Altogheter, our data support *Cardamine* as a new model system suitable for studying light-independent germination, resolving a long-standing question on the molecular mechanisms controlling it, opening new frontiers for future research on the epigenetic cues driving this process.

3. Introduction

3.1. Light: a key environmental cue in plant life

In the life cycle of plants, many developmental and growth processes are strictly dependent on light. Throughout evolution plants developed a wide set of photoreceptors to perceive different types of light (Fig. 1), and translate them into changes in transcription and metabolism, thus influencing different developmental stages. The R and FR lights are perceived by the photoreceptors named phytochromes. In angiosperm, phytochromes are classified into two classes, according to their activity and biochemical properties. Type I phytochromes, represented by phyA in *Arabidopsis*, are light-labile and promote germination and de-etiolation when light is scarce (VLFR) or when the R/FR ratio is very low (FR-HIR). Type II phytochromes (phyB–phyE in *Arabidopsis*) accumulate at lower levels in the dark relative to phyA, but are light-stable and become the predominant phytochrome species in light-grown plants; nevertheless, their molecular form, subcellular localization and signaling outputs change dramatically between dark and light conditions. A brief red pulse converts phyB into its active Pfr form, while a subsequent far-red pulse reverses this effect by regenerating the inactive Pr form; this photoreversibility characterise the five phytochromes molecules [1]. Within the blue/UV-A range, CRY1/CRY2 and PHOT1/PHOT2 are the main photoreceptors [2-5], while UV-B is perceived by UVR8, a tryptophan-based protein photoreceptor [6, 7]. Taken together, these receptors provide a diversified input system in which spectral quality and quantity are transduced into signals at the transcriptional and metabolic levels [8].

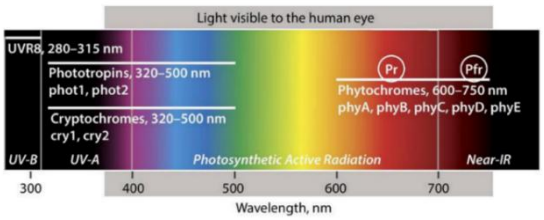

Figure 1. Range of wavelengths sensed by plant photoreceptors (adapted from [8]).

3.2. Light and plant development

Light plays a pivotal role throughout the life cycle of a plant, from seed germination to flowering; indeed, light quantity and quality are sensed and transduced into decisions about when to germinate, when to flower and how to modulate plant growth and plasticity.

As for flowering, light is a key seasonal cue that plants translate into the decision to flower, aligning reproduction with favourable conditions. In species such as *Arabidopsis thaliana*, the transition to flowering is coordinated by integrating light quality, intensity and the photoperiod, in a multi-layered molecular control, acting at transcriptional, post-transcriptional, translational and epigenetic levels. This molecular mechanism allows plants to determine both "what time of day" and "what time of year" it is, starting the flowering process accordingly [9].

Another example of the importance of light quality and quantity is represented by the shade avoidance response: in plant canopies, a low R/FR ratio is the condition that triggers this response, with phyB being the central sensor [10]: under a low R/FR ratio, phyB reverts to its inactive form, PIFs accumulate, and the elongation program is induced, prioritizing the axial growth; upon perception of red light, active phyB promotes phosphorylation and turnover of the PIFs transcription factors, restraining elongation [10-12].

Moreover, chloroplast photo-relocation movement is an archetypal light-driven response that integrates light dual-role, both as energy provider and informative tool: under low fluence rates, chloroplasts accumulate along periclinal walls to maximize photon capture, whereas under excessive irradiance they rapidly vacate the illuminated face and align along anticlinal walls to minimize photodamage [4, 13, 14].

3.3. Light as a stressor

Light can also represent a major abiotic stress. Indeed, sustained or burst high irradiance or prolonged light limitation and UV-B irradiance exemplify stress conditions by light, and although differing in kinetics, sites of ROS generation and photoreceptors are involved.

Under high irradiance, stress occurs as absorbed energy exceed the range that the photosynthetic and regulatory systems can safely process, causing an excessive excitation at PSII and, under some conditions, an over-reduction at PSI, both increasing the probability of ROS formation and photoinhibition [16]. A first defensive response is the energy-dependent component of qE. Strong illumination increases proton pumping, establishing a ΔpH across the thylakoid lumen. The resulting lumen acidification is sensed by the LHCII, whose role in normal conditions is to absorb photons and convey excitation to the PSII reaction centre. Protonation promotes a conformational switch in a subset of these antenna complexes into a dissipative state that converts excess excitation into heat, observed as a fast, reversible decline in chlorophyll fluorescence. Low lumen pH concurrently activates the xanthophyll cycle enzyme VDE, producing zeaxanthin that stabilizes and amplifies the dissipative state while irradiance remains high [17]. When light and ΔpH decrease, zeaxanthin is epoxidized back and the antennae return to their light-harvesting configuration, restoring efficient energy transfer to PSII (Fig. 2) [15, 17]. Moreover, high light stress was also proved to trigger chloroplast-to-nucleus retrograde signalling: H_2O_2 exits chloroplasts and accumulates in nuclei in a light-dependent manner, providing a direct ROS-based feedback for transcriptional control of specific TFs, so that gene expression matches the magnitude and duration of energy imbalance [19]. In parallel, $^1O_2$ generated in PSII can initiate the EXECUTER-dependent program, a response identified in *Arabidopsis thaliana* in which the proteins EXECUTER1/2 enable higher plants to perceive

singlet oxygen as a stress signal in plastid, activating a genetically determined nuclear stress response program aimed at reconfiguring nuclear transcription and promoting acclimation [20]. At the same time ELIPs, a family of protein induced early by light, and related one-/two-helix thylakoid proteins, are rapidly induced and contribute to protection of pigments and PSII during sustained exposure, a role supported by classic induction studies and by *Arabidopsis* transgenics lines expressing bryophyte ELIPs [21]. Functionally these strategies allow plants to translate photon excess into acclimation rather than cumulative photodamage.

By contrast, prolonged low light imposes a different constraint: limited excitation energy limits ATP/NADPH supply and growth, while LHCII make leaves especially vulnerable to sudden irradiance increases; the same sensing circuits that detect excess light also tune acclimation to light scarcity, so the two regimes are physiologically coupled [21, 22]. In the short term, state transitions rebalance excitation between PSI and PSII by reallocating the LHCII, while over longer periods plants adjust the photosystem stoichiometry and chlorophyll composition to optimize energy transfer in a light-limited environment [24]. Such adjustments preserve electron-transport continuity, sustain redox homeostasis, and temper oxidative spikes that otherwise accompany sun-shade transitions.

Light quality, in particular UV-B, can directly damage DNA and photosynthetic proteins, but plants possess the dedicated photoreceptor UVR8, that transduces UV-B photons perception into developmental and protective program. Upon UV-B exposure, UVR8 monomers bind COP1, repressor of photomorphogenesis and as an activator of etiolation in darkness, to stabilize the transcription factor HY5, a transcription factor that acts downstream of the light receptor network and directly affects transcription of light-induced genes, establishing a photomorphogenic transcriptome; COP1–UVR8 association is later reversed by RUP proteins to reset the system [6, 7, 24]. In parallel, UV-B induces photolyase genes that

repair UV lesions, ensuring that the photoreceptor pathway couples with the genome-maintenance machinery [26]. UV-B information also cross-checks with other light cues: under canopies, UV-B antagonizes auxin-driven shade-avoidance growth, preventing unnecessary elongation thus integrating quality signals with growth control [26, 27].

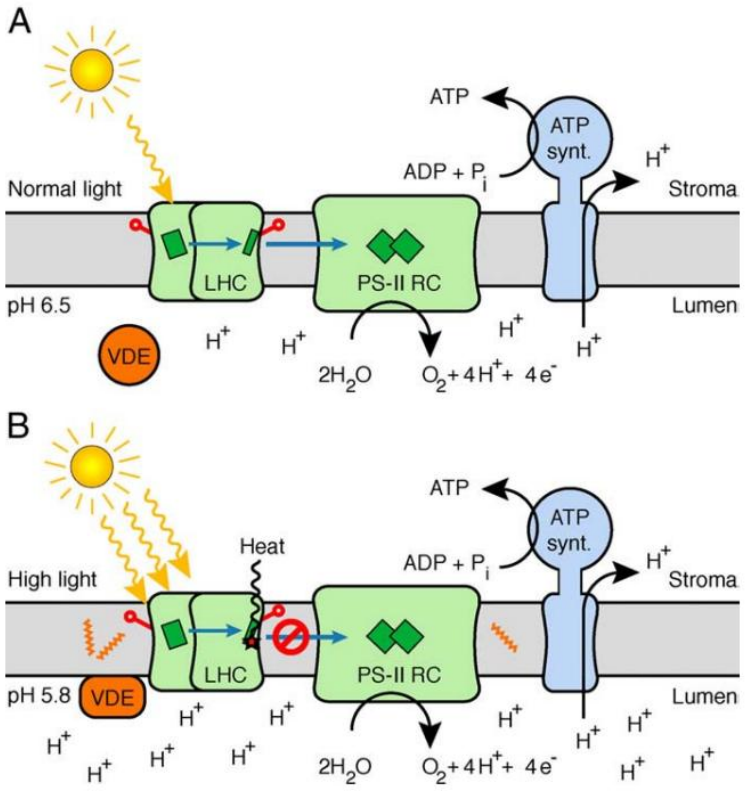

Figure 2. Scheme of non-photochemical quenching (qE).
(A) Under normal light conditions, LHCs collect energy and transmit it to the reaction centres of the photosystems. (B) Under high-light stress, the antenna of PSII switches to a quenched state, by which photodamage is prevented and excess energy is safely dissipated as heat (adapted from [17]).

3.4. Seed development and germination

The first process in plants life cycle is seed germination, which comprises two major phases: embryo development and seed maturation.

Once embryogenesis is complete, the seed undergoes maturation during which food reserves accumulate and dormancy and desiccation tolerance are established [29]. Seed dormancy has been defined as the inability of a viable seed to germinate under favourable conditions, and is hormonally driven by an increase of ABA level [29, 30]. In *Arabidopsis thaliana*, DOG1 is a major determinant of seed dormancy; indeed, *dog1* loss-of-function seeds are largely non-dormant [32].

Under the proper environmental conditions, and upon seed imbibition, germination begins. Indeed, seeds are able to perceive multiple exogenous cues to determine when to release seed dormancy and start germination; light, temperature and water availability are among the most important environmental signals controlling seed germination [32-37]. In plant species characterized by light-dependent germination (positive photoblastism), such as *Arabidopsis thaliana* and *Lactuca sativa*, light perception via phyB is transduced into reprogramming of gene expression and metabolic changes through the balancing of two main phytohormones, GA and ABA. Specifically, in light-dependent seed germination, a high GA/ABA ratio induces the germination process (Fig. 3).

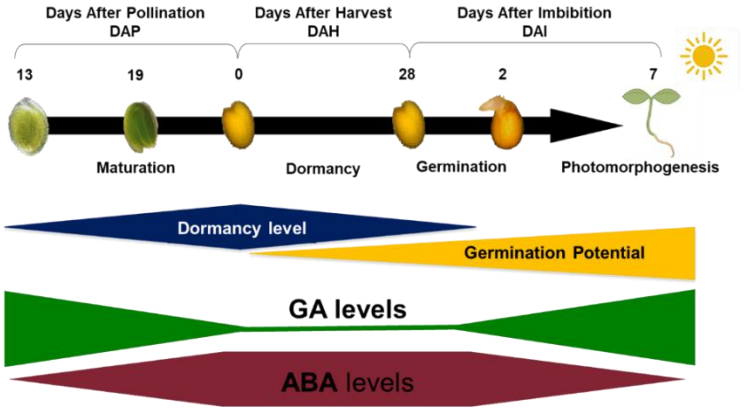

Figure 3. Scheme of seed development and germination.
The scheme highlights the progression of dormancy and germination potential levels (in blue and yellow), controlled by the GA/ABA ratio (in green and red).

Plants evolved different germination strategies that match this hormonal balance with the environmental light conditions. Indeed, the presence of light doesn't always represent the optimal condition to germinate. For instance, plant species characterized by light-inhibited seed germination (negative photoblastism) share a common pattern in terms of ecogeographical distribution, mainly due to climatic conditions. Thus, photo-inhibited plant taxa are mainly present in regions with arid climates (Fig. 4) [39].

As for plants displaying light-independent seed germination, their seeds are able to germinate in both light and dark conditions. Although the molecular mechanisms underlying the light-dependent germination process have been deeply studied, how the light-independent germination process is controlled is still vague.

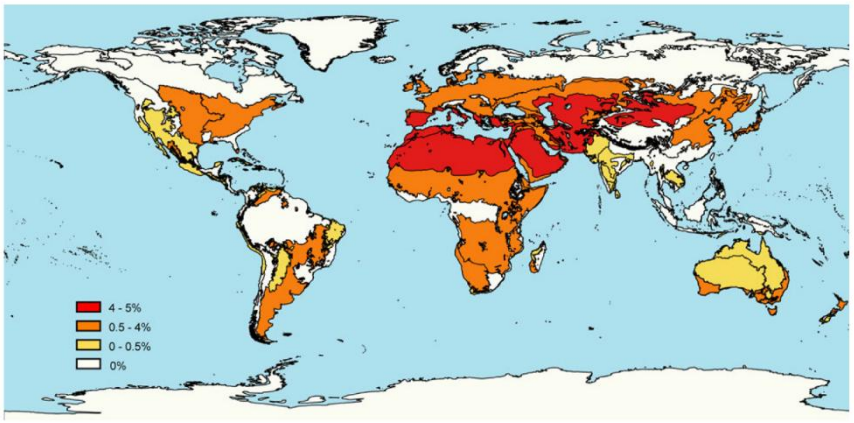

Figure 4. Photo-inhibited plant taxa distribution in regions with arid climates. Percentage of photo-inhibited taxa in each climatic region within each biogeographical realm (adapted from [39]).

3.4.1. Light-dependent seed germination

The light-dependent seed germination has been extensively studied in *Arabidopsis thaliana*, where five phytochromes (phyA–phyE) coordinate light responses in a partially redundant yet distinct manner. phyA primarily responds to FR light, phyB to R light, and phyE contributes to seed germination under continuous FR light and alternating R/FR conditions. The requirement of a light pulse to germinate implies the evolution of a strong germination repression system in dark conditions; in *Arabidopsis* seeds this occurs through a multitude of transcription factors that control both hormone metabolism and signaling, resulting in a low GA/ABA ratio (Fig. 5). A central hub is the basic helix–loop–helix factor PIF1, which accumulates in darkness and induces the expression of germination repressors such as *DAG1* and the *DELLA* genes *GAI* and *RGA* [39,

40]. This results in the induction of the ABA biosynthetic genes (e.g., *NCED6*, *NCED9*, *ABA1*), while repressing GA biosynthesis (*GA3OX1*, *GA3OX2*) and promoting GA catabolism (e.g., *GA2OX2*), thereby lowering bioactive GAs [41-43]. Upon light perception, phyB is activated in its Pfr form, and translocate in the nucleus [45]. Red light perceived by phyB induces the phosphorylation and degradation of PIF1, through the 26S proteasome, resulting in increased levels of GA biosynthetic genes and ABA catabolic ones [43, 45-47].

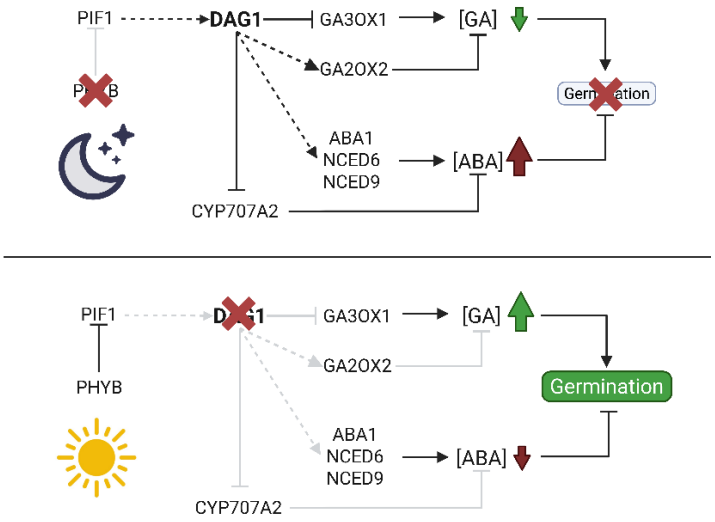

Figure 5. Model of the light-mediated germination signalling network in *A. thaliana*.
On top, the molecular mechanism guiding the germination repression in absence of light; in the bottom, the molecular mechanisms allowing the germination upon light perception. Arrows show positive regulation and bars indicate negative regulation. Dark lines show regulation and light lines show missing regulation.

3.4.1.1. The role of the germination repressor DAG1

DAG1 is an *Arabidopsis* transcription factor belonging to the DOF family. It binds the highly conserved (T/A)AAAG consensus motif [49], and function as a repressor of seed germination, with its expression being induced in dark-imbibed seeds by PIF1. The isolation of *dag1* knock out mutant allowed to highlight its role in the modulation of both GA and ABA during seed germination.

Fresh *dag1* seeds display reduced primary dormancy and increased germination potential, as in monochromatic red light *dag1* seeds require significantly lower fluence to achieve 50% germination respect to the wild type [49, 50]. *dag1* seeds have been also shown to germinate with a faster germination kinetics in light (Fig. 6A) and to partially germinate in dark conditions (Fig. 6B) [52].

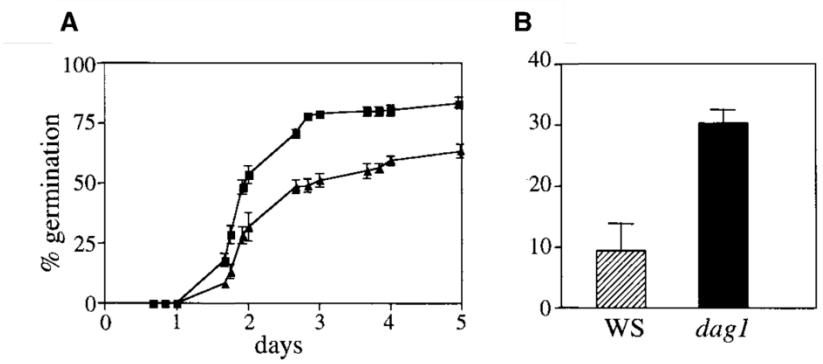

Figure 6. Germination kinetics of *dag1* seeds.
Germination kinetics of WT (closed triangles) and *dag1* (closed squares) lines in light condition (A) and in dark after 5 days (B). The histogram reports germination percentages (adapted from [52]).

DAG1 binds the promoters of both *GA3OX1* and *CYP707A2*, repressing their transcription [52, 53], consistently with higher GA (Fig. 7A) and lower ABA content (Fig. 7B) in the *dag1* mutant line. Furthermore, DAG1 and GAI have been proved to physically and functionally cooperate to repress *GA3OX1*: in seeds, ChIP experiments showed promoter occupancy over *GA3OX1* regions enriched in DOF-binding sites, and absence of GAI compromises DAG1-dependent repression of *GA3OX1* [55].

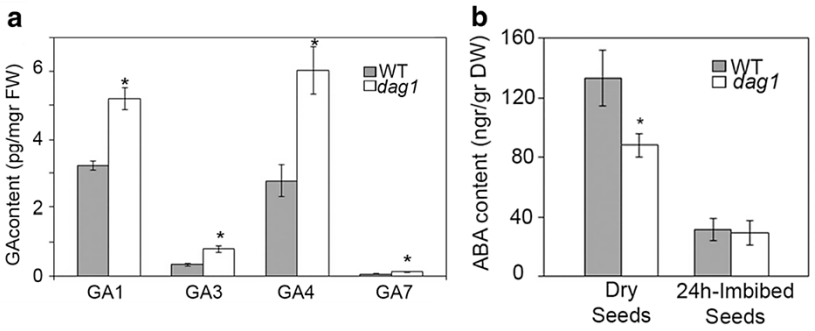

Figure 7. *DAG1* inactivation affects both GA and ABA levels. (A) Bioactive GAs (GA_1, GA_3, GA_4 and GA_7) content in 24 h imbibed seeds, determined by UHPLC-MS/MS and (B) ABA content in dry or 24 h imbibed seeds determined by HPLC analysis, in *Arabidopsis* wild type (WT) and *dag1* mutant line (adapted from [54]).

It has also been demonstrated that GAs create a feedback loop on *DAG1* expression and protein stability during the early hours of imbibition: indeed, exogenous GA_{4+7} significantly induce *DAG1* transcripts and stabilize DAG1 protein in imbibed seeds (Fig. 8) [54].

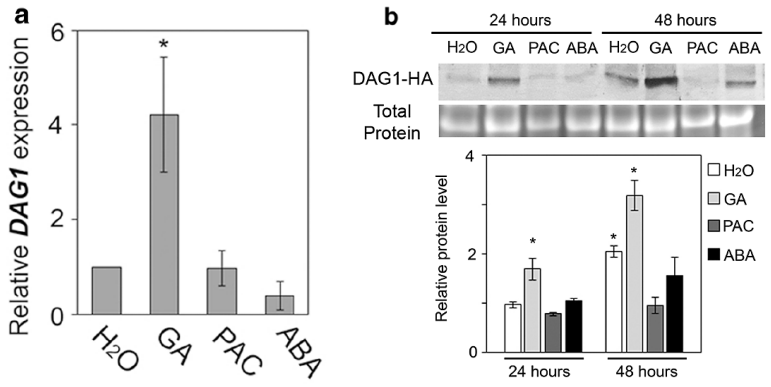

Figure 8. GAs enhance *DAG1* transcription and stabilize DAG1 protein.
The relative expression of *DAG1* is induced specifically by exogenous GA_{4+7} (A) and the DAG1 protein results stabilized specifically by GA_{4+7} at 24 and 48 h, as demonstrated by the immunoblot results using the DAG1-HA tagged line (adapted from [54]).

DAG1 is also regulated at the epigenetic level: in seeds, *DAG1* locus displays an H3K4me3 enrichment during maturation and early imbibition, whereas H3K27me3 accumulates in seedlings and correlates with *DAG1* silencing. In imbibed seeds, GA increases *DAG1* transcript and protein abundance and is associated with a rise in H3K4me3 across the locus, indicating hormone-responsive tuning of this permissive mark [54].

Taken together, these data indicate that DAG1 functions as a repressor of seed germination that is induced in darkness downstream PIF1, directly targeting *GA3OX1* and *CYP707A2* to lower the GA/ABA ratio and cooperating with GAI to repress *GA3OX1* repression. *DAG1* inactivation both lowers the red-light requirement and increases the germination potential, consistent with DAG1 role as a key integrator of light and hormone control in the seed.

3.4.2. Light-inhibited and -independent seed germination

Seed germination can be repressed by light, mainly in habitats where darkness constitutes a more reliable condition for a safe establishment; this occurrences have likely favoured the evolution of negative photoblastism in diverse coastal and arid-adapted species, including Mediterranean maritime plants and halophytes, [55-57].

In crops, light-inhibited germination has been documented, for instance, in tomato and watermelon, since their seeds exhibit delayed or repressed germination under particular spectral regimes, often most strongly under continuous white or specific wavelength [58, 59]. These studies enforce the negative photoblastism a context-dependent strategy: in open, sun-exposed habitats, repression by light prevents dangerous emergence at the surface until burial, shading, or seasonal light are perceived [56, 57].

In tomato, phyA and phyB can exert opposing effects depending on light conditions: continuous high-irradiance red light inhibits germination through phyA, while low-fluence red pulses promote germination through phyB, demonstrating that the same light spectra can either repress or promote the process via distinct phytochrome pathways. These antagonistic behaviours explain how continuous light at the soil surface can block germination, whereas a transient or attenuated light environment, for example beneath a thin soil layer, can relieve the repression [60, 61].

BL can also be strongly inhibitory, especially in cereals. In barley, wheat and *Brachypodium*, BL repression is tightly related to dormancy and progressively weakens with after-ripening. Genetic and physiological analyses in barley identified CRY1 as the key receptor mediating BL inhibition: BL irradiation increases *NCED1*, an ABA biosynthetic gene, and represses *ABA8'OH-1*, related to ABA catabolism, preventing germination [63].

However, light-inhibited, as well as light-independent germination, has primarily been documented in ecologically disparate non-model species, whose genetics and transformation methods are limited, leaving the molecular cues behind it largely unresolved. In a recent study [64], *Aethionema arabicum* has been proposed as a model system, because it presents both light-independent (TUR) and light-inhibited (CYP) accessions (Fig. 9).

TUR germinates robustly in darkness and under continuous light across broad spectral and intensity ranges, maintaining a high GA/ABA ratio regardless of light conditions, as a light-independent germination species, while in CYP light lowers the GA/ABA ratio, consistent with its light-inhibited germination. The fact that genetic analyses indicate that phytochrome sequences are largely conserved between accessions, and no accession-specific non-synonymous variants were detected in PIF1, suggests a remodelling of downstream signalling rather than impaired photoperception [63, 64].

Transcriptome comparisons strengthen this view, as TUR exhibits a comparatively restrained light-responsive program. Upon light exposure, the repression of the GA-biosynthetic gene *AearGA3OX1* and the induction of the GA-deactivating gene *AearGA2OX3* are markedly stronger in CYP than in TUR, consistent with bioactive GAs maintenance in TUR [64]. Upstream modules appear conserved with *Arabidopsis*, where PIF1 promotes dormancy establishing a low GA/ABA ratio. Mérai et al. showed differential expression of the bHLH factors PAR1 and PAR2 between TUR and CYP under both light and dark conditions. Given that PAR1/2 can modulate PIF activity as transcriptional cofactors, their accession-specific expression offers a likely cue through which light fails to repress GA in TUR [41, 63, 65].

Additional results further support the light-inhibited and -independent behaviour: accession-specific alternative isoforms and antisense transcripts in *ABI3*, *ABI4*, and *DOG1*, and lower light-

induced *NCED6* in TUR, align with its reduced ABA accumulation [63, 66].

Further genetic analyses also implicate phytochromes in germination repression: the *koy1* mutant of the CYP accession, lacking the chromophore, loses R/FR inhibition, while the *koy2* mutant shows that phyA mediates HIR-type inhibition while permitting VLFR promotion. Thus, outcome depends on fluence and response mode; classic R/FR reversibility and blue-light effects are conserved but hormonally wired in a species- and accession-specific manner [60, 62, 63, 67, 68].

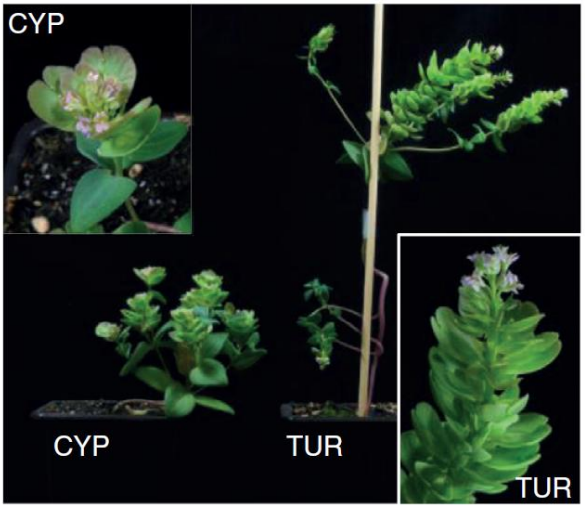

Figure 9. Comparison between *A. arabicum* Cyprus and Turkey. Eight-week-old *Aethionema arabicum* CYP (Cyprus) and TUR (Turkey) plants (adapted from [64]).

3.4.3.1. *Cardamine hirsuta* as a new model system

In plants as in animals, comparative studies might be particularly informative, enabling knowledge gained in model species to be exploited in new contexts, to explain the origin of traits not present in the model species and to provide evolutionary and ecological perspectives [69, 70]. The Brassicaceae comprise more than 2,000 primarily herbaceous species with flowers bearing six stamens and four petals arranged in a cross, hence the alternative name "Cruciferae." Within this family, beside species closely related to the model system *Arabidopsis thaliana*, such as *Arabidopsis halleri*, or *Arabidopsis lyrata*, *Cardamine hirsuta* has emerged as an especially valuable system. This species represents a powerful genetic model to dissect the molecular bases of plant morphological evolution (Fig. 10) [72]. *Cardamine hirsuta* is a small invasive plant, probably native to Europe, and distributed in both hemispheres [72, 73]. Fossil-based analyses estimate that *Cardamine hirsuta* and *Arabidopsis thaliana* diverged approximately 14 mya, within a relatively short interval [74, 75].

Figure 10. Comparison between *A. thaliana* and *C. hirsuta*.
Adult *A. thaliana* (left) and *C. hirsuta* (right) wild-type plants (adapted from [77]).

Like *Arabidopsis*, *Cardamine* was selected for laboratory study based on practical attributes, including short generation time, small size, abundant progeny, and ease of large-scale cultivation. *C. hirsuta* is a diploid annual with a small genome (1.5× the size of that of *Arabidopsis*), which retains the ancestral Brassicaceae genome structure and is organized into eight chromosomes. It has a short generation time (about 5–7 weeks), is self-fertilizing, and produces large numbers of seeds [77]. It is also transformable using the same *Agrobacterium tumefaciens*–mediated methods developed for *A. thaliana* [74]. These characteristics allowed to establish *C. hirsuta* as a promising model system, as for the study of leaves dissection: in contrast to *Arabidopsis*, which has simple leaves, *Cardamine* produces leaflets arranged along both sides of a central rachis. This trait is controlled by *RCO*, absent in *A. thaliana* [78]. *RCO* has been shown to suppress growth at the flanks of initiating leaflets, contributing to leaf complexity [77, 78]. Recent studies have generated new alleles of *rco*, further elucidating its role in leaf development [80].

From a molecular-evolutionary perspective, a huge advancement was constituted by the assembly and annotation of the *Cardamine hirsuta* "Oxford" ecotype genome [81]. A phylogeny based on the complete set of protein-coding genes from *Cardamine hirsuta*, *Cardamine rubella*, *Arabidopsis thaliana*, *Arabidopsis lyrata*, *Arabidopsis arabicum*, *Brassica rapa*, *Schrenkiella parvula*, and *Eutrema salsugineum* placed the divergence between *C. hirsuta* and *A. thaliana* at roughly 32 mya, within the range of prior estimations; also, the *C. hirsuta* genome results largely syntenic with the *Arabidopsis* one (Fig. 11) [72].

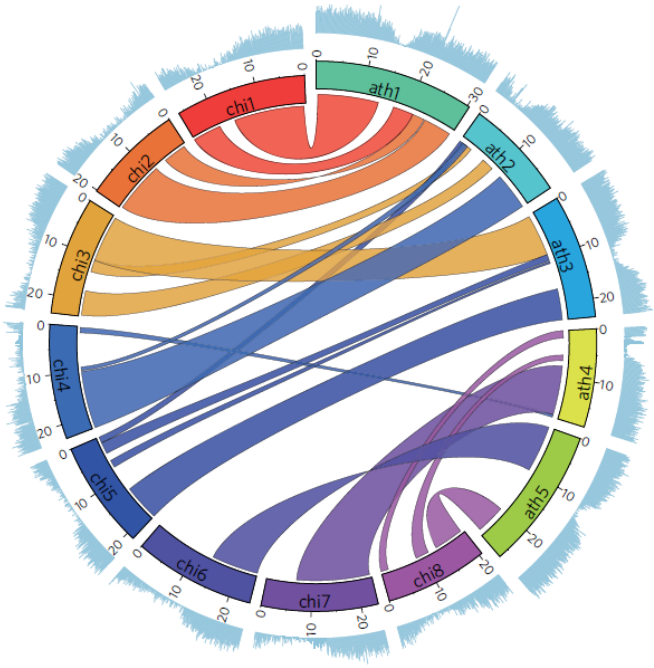

Figure 11. Synteny between *A. thaliana* and *C. hirsuta* genomes. Circos plots showing synteny between the genomes of *A. thaliana* (ath) and *C. hirsuta* (chi) (adapted from [72]).

Preliminary results from our research group identified *Cardamine hirsuta* as a plant species characterised by light-independent seed germination, allowing us to further expand its employment in comparative studies, possibly establishing *C. hirsuta* as a new valuable plant model system for studying the molecular aspects of seed germination.

3.5. Epigenetics during seed germination

Seed germination in *Arabidopsis thaliana* is controlled through coordinated changes across several epigenetic layers that integrate environmental light cues with hormonal pathways, resulting in a rapid reprogramming of gene expression. At the RNA level, lncRNAs and miRNAs mediate light-responsive switches in ABA and GA pathways; at the DNA level, RdDM and active demethylation fine-tune dormancy; at the chromatin level, histone variants and PTMs remodel accessibility and promoter competence as seeds commit to germination. Together these layers provide a phased transition from seed maturation programs to seed germination [82].

As for histone PTMs, activating marks such as H3ac and H3K4me3 accompany transcriptional engagement at germination-promoting loci, whereas repressive PTMs, including H3K9me2 and H3K27me3, enforce the repression of the seed-specific program as germination proceeds. During germination, targeted histone deacetylation removes H3ac from embryogenesis and dormancy regulators to consolidate the transition: HDA6 and HDA19 are required to repress *LEC1*, *FUS3* and *ABI3* after germination, consistent with H3ac removal from these loci; HD2A and HD2B reduce H3ac at *DOG1* to facilitate dormancy release; SNL1/2, acting through HDAC-associated deacetylation, dampen *AUX1* to modulate the germination kinetic [82-85]. In parallel, ubiquitin-based histone marks contribute: PRC1-mediated H2Aub, recruited by AL readers of H3K4me3, promotes the switch from a permissive H3K4me3 mark to the PRC2-dependent H3K27me3 at seed-specific loci [86-88]. At the same time, H3K9me2 deposited by SUVH-class methyltransferases collaborates with deacetylation to restrain dormancy regulators; notably, SUVH5 acts as a positive regulator of light-dependent germination, linking H3K9me to photoregulatory control [89, 90]. Together, these PTMs ensure the coordinated repression of maturation genes and the timely activation of growth

programs that enable germination and photomorphogenic seedling establishment [82, 85-88].

A key element of the epigenetic control of seed germination is PRC2, a complex of the PcG proteins, initially discovered in *Drosophila* and proved to be highly conserved across evolutionarily distant organisms and across diverse lineages. In *Drosophila*, the PRC2 core comprises four subunits: E(Z), ESC, p55, and SU(Z)12. E(Z), which contains a SET domain, and catalyzes histone methylation. In *Arabidopsis thaliana*, there are three E(Z) homologs: *CLF* [92], *MEA/FIS1* [92, 93], and *SWN* [95]; three SU(Z)12 homologs: *EMF2* [96], *VRN2* [97], and *FIS2* [94]; five p55 homologs: *MSI1/5* [97-99]; a single ESC homolog: *FIE* [100-103]. Combinatorial assemblies of these twelve proteins form three PRC2 complexes in plants, active specifically during different developmental stages, from seed germination to flowering [105] (Fig. 12).

The silencing mark H3K27me3 is partially counteracted by the activating mark H3K4me3, deposited by the Trithorax complex, which is highly conserved in both animals and plants, similarly to PRC2. During germination, PRC2 catalyses and maintains the repressive mark H3K27me3 to silence seed-specific genes, in a partially antagonistic interplay with H3K4me3. In germinating seeds exposed to light after dormancy release, these two marks are dynamically spread across the genome to regulate key loci related to dormancy, hormone metabolism, and growth, establishing a chromatin landscape prone to germination [104, 105]. Genetic dissection of PRC2 function demonstrates its pivotal role during the seed-to–seedling transition phase. Mutants for the FIE core PRC2 component lose H3K27me3 genome-wide and show enhanced dormancy and germination defects; transcriptome analysis of *fie* mutants shows that when H3K27me3 repression is relieved, expression of seed-specific genes persist during post-germinative development, resulting in defects in seedling establishment and growth. Therefore, PRC2-mediated deposition of H3K27me3 is

required to lower seed traits and consolidate a light-responsive seedling state [106].

The dormancy-to-germination transition involves reprogramming between H3K4me3 and H3K27me3 on seed-specific master regulators. When dormancy is released by stratification and seeds are exposed to light, loci such as *FLC*, *DOG1*, *ABI3, DAG1* and other dormancy/seed maturation genes progressively lose H3K4me3 while gaining H3K27me3, to be silenced. Conversely, genes whose products promote germination and seedling growth acquire H3K4me3 and are expressed [106]. *DAG1* has been proved to be one of the genes whose locus is enriched in H3K4me3 during seed maturation, acquiring the H3K27me3 repressive mark during seedlings establishment, consistently with its role as germination repressor [54].

Overall, the antagonistic redistribution of both H3K4me3 and H3K27me3 is a hallmark of germination and underscores the necessity for a functional PRC2. Notably, the same mechanism was observed in gymnosperms, indicating evolutionary conservation of the H3K4me3/H3K27me3 interplay during seed life-cycle transitions [105].

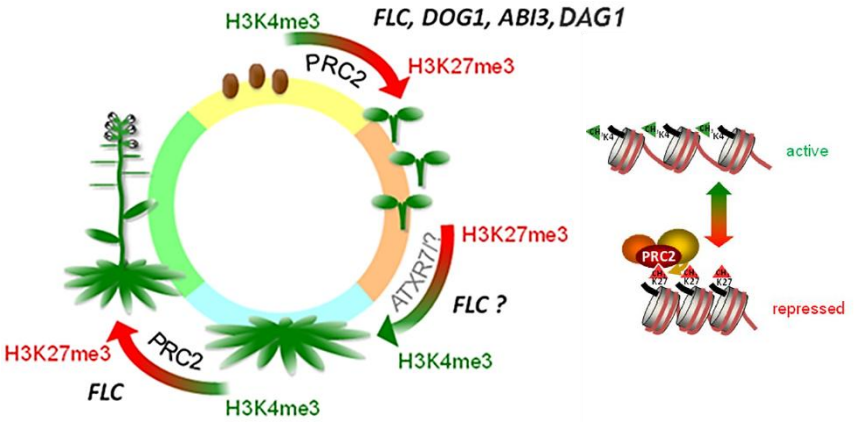

Figure 12. Role of histone PTMs during germination and vegetative-to-reproductive phase transitions. Repressive H3K27me3 marks on genes encoding key regulators of dormancy are deposited through the PRC2 complex and replace the activating H3K4me3 mark in response to the environmental cues (adapted from [105]).

3.5.1. Epidrugs applications in plants

Given that PRC2 is a key regulator of the epigenetic control during germination, the development of alternative approaches to study its function were required, since PRC2 activity is essential for seed development: indeed, maternal loss of PRC2 results in embryo-lethal phenotype, hampering the classic mutant analysis of post-embryonic germination [106].

A useful approach, not yet extensively used in plant biology, is chemical genetics: small molecules (*epidrugs*) are employed to modulate the activity of epigenetic regulators *in vivo*, enabling dose- and time-controlled alterations. Given that the EZH2 methyltransferase is deeply conserved, several classes of mammalian inhibitors provide a practical lead compound for plants, such as 2-pyridone–based compounds (e.g., UNC1999), that inhibit EZH1/2 and lower H3K27me3 with minimal effects on enzyme abundance[106, 107]. By repurposing such compounds to *Arabidopsis thaliana*, it is possible to carry out a focused dissection of PRC2-dependent repression during germination and seedling establishment, without the constraint of generating multiple mutant alleles [109].

In this context, in a recent study carried out in our laboratory, the compound RDS 3434 was showed to be a powerful *epidrug* to study PRC2 function in seeds. Originally developed as a selective EZH2 inhibitor in human leukaemia cells, where it reduces global

H3K27me3 levels without lowering EZH2 protein level [110], RDS 3434 was proved to be effective in plants: *Arabidopsis* seeds exposed to the compound show a dose-dependent decrease of total H3K27me3 and a reciprocal, modest increase of H3K4me3, consistent with the partial antagonism between these marks. Consistently, PRC2 target genes, such as *DAG1*, are transcriptionally derepressed, linking the chemical inhibition of H3K27 trimethylation to functional outputs. At the physiological level, PRC2 inhibition delays germination, aligning with genetic evidence that PRC2-mediated silencing accelerates the exit from the embryonic program toward a light-responsive seedling state [87, 105, 110].

Thus, *epidrugs* offer several practical advantages: first the timing, since compound exposure can be restricted for instance to the imbibition phase, when light perception and hormone rebalancing initiate germination, allowing to test whether PRC2 activity is required before, during, or after specific checkpoints. Second, reversibility, since the removal of the compound allows recovery experiments to distinguish transient requirements for PRC2-dependent repression from irreversible developmental commitment. Third, tunability: dose-dependent inhibition can reveal thresholds at which H3K27me3 loss begins to destabilize the repression of seed programs. Finally, and most importantly, comparative studies: indeed, epidrugs can be applied across accessions or related species, as in the case of *Arabidopsis thaliana* and *Cardamine hirsuta*, enabling comparative tests of PRC2 contribution to photoblastic behaviour. Taken together, the chemical-genetics approach described broadens the experimental repertoire to study the possible different epigenetic landscape behind different germination behaviours, such as light-dependent and -independent.

3. Aim of the thesis

Seed germination is a key developmental process in plants, where precise molecular and hormonal regulation ensures a successful seed-to-seedling transition under favourable environmental conditions. Among the environmental factors driving germination, light has a central role: indeed, plant species can be characterized by a light-dependent, -inhibited or -independent germination. While the molecular mechanisms underlying the light-dependent germination have been deeply investigated, how the light-independent germination process is controlled is still vague.

To address this gap, the first aim of this thesis was to shed light on the hormonal and transcriptional networks that allow light-independent germination in *Cardamine hirsuta*, exploiting the central role of the repressor of germination DAG1, characterized in *Arabidopsis thaliana*, where it exerts its role by modulating both GA and ABA levels.

Moreover, since seed germination in *Arabidopsis* is controlled through coordinated epigenetic changes integrating environmental light factors with hormonal pathways, the second aim of this thesis was to gain insights into the epigenetic mechanisms possibly determining the light-independent germination behaviour. The study focuses on the role of PRC2 during early germination steps, while also presenting preliminary data on the epigenetic landscape underlying early seed developmental stages.

5. Results and discussion

In order to study the molecular mechanisms governing light dependency for seed germination, we look for feasible model systems for comparative studies. To this end, we analysed the germination properties of close relatives of *Arabidopsis thaliana* (light-dependent germination) and *Lepidium sativum* (light-independent germination), such as *Cardamine hirsuta*, *Capsella rubella*, and *Camelina sativa*, finding both *Camelina* and *Cardamine* able to germinate regardless of the light conditions [112]. Germination kinetics experiments using ABA or PAC suggested that, despite the light independence for germination, the GA/ABA ratio is fundamental for *Lepidium*, *Cardamine* and *Camelina* germination [112]. Given the availability of the genome sequence, as well as of a successful transformation method and short life cycle [71, 76], we decided to employ *Cardamine hirsuta* to gain insights in the light-independent germination, at both physiological and molecular level.

5.1 The molecular side

5.1.1 GA levels are key for germination of *C. hirsuta* seeds

Adapted from Lepri et al., 2025

In *Arabidopsis*, GAs and ABA levels are controlled by light during phyB-dependent seed germination, through the action of several downstream effectors [42, 65]. Indeed, the GAs biosynthetic genes *AtGA3OX1* and *AtGA3OX2* are repressed in the dark, whereas the catabolic gene *AtGA2OX2* is induced. In contrast, in the same conditions the expression of the ABA biosynthetic genes, *AtABA1*, *AtNCED6* and *AtNCED9*, is promoted, while the catabolic *AtCYP707A2* gene is downregulated [42, 65]. Given the light-independent germination of *Cardamine* seeds, we wondered whether the GA and ABA metabolic genes could have a different trend of expression in seeds imbibed in the dark.

Since it is not yet known which GA and ABA metabolic genes are expressed in *Cardamine* seeds, we assessed the expression profiles of a number of both GA and ABA genes, on wild-type dry seeds and on seeds imbibed 12 or 24 hours, either in light or in darkness, via RT-qPCR. The results of this analysis revealed that the GA and ABA metabolic genes mainly involved in seed germination are those reported in *Arabidopsis* (*ChGA20OX3*, *ChGA3OX1*, *ChGA3OX2*, *ChGA2OX2* and *ChGA2OX3* for GA, *ChABA1*, *ChNCED6*, *ChNCED9* and *ChCYP707A2* for ABA) with the sole exception of the catabolic gene *ChGA2OX3*, which in *Arabidopsis* is not expressed, while the others were very low or not expressed (Fig. 13). Interestingly, expression of the GA biosynthetic gene *ChGA20OX3* was high irrespectively of light conditions, while *ChGA3OX1* and *ChGA3OX2* were significantly upregulated during imbibition in dark, compared to light condition, where expression increased only at 24 HAI. Conversely the mRNA levels of the catabolic genes *ChGA2OX2* and *ChGA2OX3* were low, both in light and dark conditions, compared to dry seeds (Fig. 13A). In addition, expression of ABA genes showed an opposite trend, with the catabolic gene *ChCYP707A2* significantly upregulated during imbibition irrespective of the light conditions, while the biosynthetic genes were downregulated respect to dry seeds (Fig. 13B). These data show a similar trends of expression for GA and ABA metabolic genes regardless of light condition during imbibition, with an overall best performance in dark.

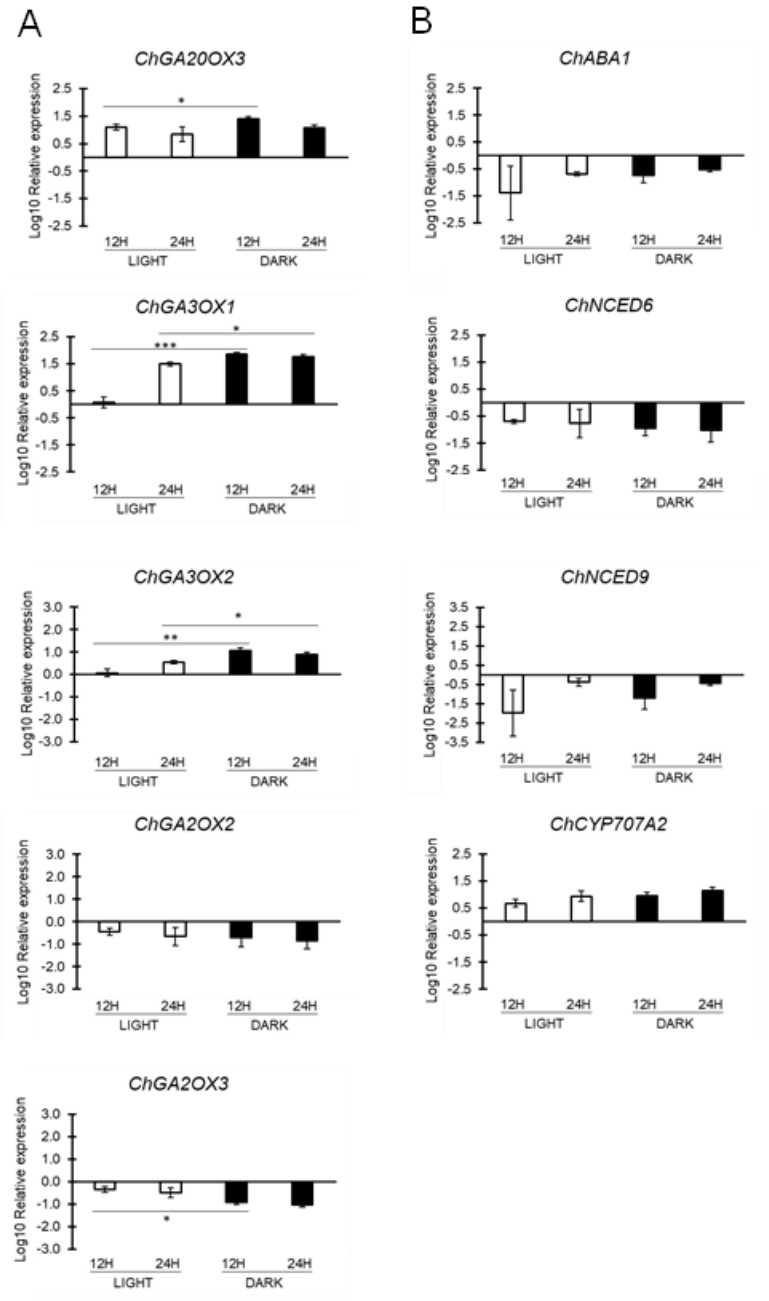
A
B
ChGA20OX3
ChABA1
ChGA3OX1
ChNCED6
ChGA3OX2
ChNCED9
ChGA2OX2
ChCYP707A2
ChGA2OX3
Log10 Relative expression
12H
24H
LIGHT
DARK

Figure 13. Expression profiles of GA and ABA metabolic genes in *Cardamine* seeds.
Relative expression levels of: *ChGA20OX3, ChGA3OX1, ChGA3OX2, ChGA2OX2, ChGA2OX3 (A), ChABA1, ChNCED6, ChNCED9, ChCYP707A2* (B) in *Cardamine* wild-type (Ox) seeds at 12 and 24 HAI, under light and dark conditions. Expression levels are presented as $\log_{10}$ respect to the dry condition, set to 0 (X axis). The values are means of three biological replicates, with SD values. Significant differences were analysed by t-test (***$p < 0.001$, **$p < 0.005$, *$p < 0.05$) (adapted from [112]).

Given the expression profile of the GA biosynthetic and catabolic genes, we reasoned that overexpression of *ChGA2OX2*, encoding a GA-2 oxidase [113], would lower GA levels in seeds and, in turn, possibly reduce the germination ability in the dark. To verify this hypothesis, we crossed the *Cardamine* transgenic lines expressing the transcriptional activator GAL4 under the control of the constitutive promoter *UBIQUITIN10* (*ChUBQ10::GAL4*), with lines bearing the *UAS::GA2OX2* construct (*ChUBQ10>>GA2OX2*) [114]. Germination in darkness of seeds issued from these crosses was significantly reduced in *ChUBQ10>>GA2OX2* in comparison to the *UBQ10-GAL4* control line and the wild-type (48.9 vs 100%) (Fig. 14A), corroborating the idea that control of GA levels is required to enable *Cardamine* to germinate in the dark.

As our data support the idea that GA levels must be increased during seed imbibition to allow germination in dark conditions, we measured GAs levels in dry seeds of *Cardamine,* as well as in 24 hours imbibed seeds under light or dark conditions. Given that the GA/ABA ratio influence seed germination, rather than the absolute levels of GAs, we also assessed ABA levels under the same conditions. Consistent with the ability to germinate in darkness, GAs levels in seeds imbibed in the dark were similar to those in light-imbibed seeds, as well as the amount of ABA in light-imbibed seeds

was comparable to that of dark-imbibed seeds. This evidence suggests that light does not influence the metabolism of these phytohormones as it does in *Arabidopsis* seeds [66]. Interestingly, and in contrast to dry seeds, the ratio of GA/ABA, based on the average of bioactive GAs (GA_1, GA_4, GA_7, GA_5 and GA_6), was surprisingly high in both dark- and light-imbibed seeds (Fig. 14B). Our data suggest that increased levels of GAs during imbibition are key for triggering the germination of *Cardamine* seeds in a light-independent fashion.

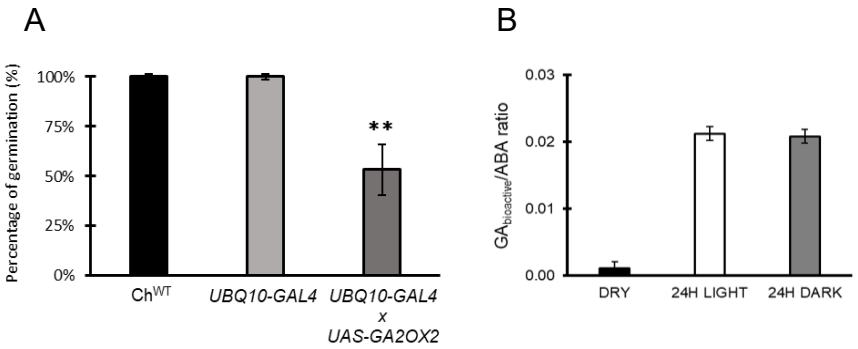

Figure 14. A high GA/ABA ratio enables germination of *Cardamine* seeds in darkness.
(A) Germination of seeds *ChUBQ10>>GA2OX2*, issued from the cross *UBQ10::GAL4 x UAS::GA2OX2*, under dark conditions, compared with the wildtype (Ox) and the *UBQ10-GAL4* line. Germination rates were measured at 120 HAI. The values are means of three biological replicates, with SD values. Significant differences were analysed by one-way ANOVA with post hoc Tukey multiple comparison test (**$p < 0.005$). (B) Ratio of bioactive GAs/ABA in wild-type Ox seeds; the analyses were performed on dry and 24-h imbibed seeds in light and dark conditions. The values are the mean of three biological replicates, with SD values (adapted from [112]).

Our data provide compelling evidence that dark germination in *Cardamine* is enabled by the maintenance of proper GA content in dark-imbibed seeds, which results from highly expressed GA biosynthetic genes and downregulated catabolic ones. These results are quite consistent with those obtained by Merai et al. [64], in two accessions of *Aethionema arabicum*. Indeed, they showed that *AearGA3OX1* and *2* were more expressed in the dark, both in seeds of the accession with dark-dependent germination (CYP) as in the one with light-neutral germination (TUR). In contrast, the catabolic *AearGA2OX3* gene was downregulated [64], thus strengthening the notion that GA levels are crucial for germination in the absence of light. Consistently, overexpression of *GA2OX2* in *Cardamine* seeds results in a significant decrease of the germination percentage. Interestingly, inactivation of *AtGA2OX2*, the only gibberellin 2-oxidase encoding gene expressed in *Arabidopsis* seeds in darkness [47], resulted in increased germination rate in dark conditions [44]. This evidence enables to posit that fine-tuning GA levels might be a conserved mechanism, which would then have evolved in plants with light-dependent germination. Corroborating this hypothesis, GA signaling pathway and their molecular mechanism are conserved in seed plants [118, 119]. Differently several spore plants such as *Physcomitrella patens* do not present functionally conserved GA signaling elements, supporting our evolutionary hypothesis [117].

Intriguingly, GA levels are unusually high in dry seeds, compared to *Arabidopsis*, and consequently the amounts might seem inconsistent with the transcript levels of the biosynthetic genes at 24 HAI. In the future, it will be interesting to measure the amount of GAs and transcript levels during seed maturation. What is fundamental to control germination is the GA/ABA ratio, which is definitely consistent with the expression data. In addition, it should be noted that, even in *Aethionema*, the data of bioactive GAs are not really consistent, since if GA_4 is coherent with *GA3OX1* transcript level and with the germination rates of the two accessions, GA_6 is

extremely higher in dark and light CYP seeds, inconsistently with the germination rates [64].

Also, the results concerning ABA, which counteracts the germination-promoting function of GAs, are extremely consistent with the dark germination ability of *Cardamine* seeds. Indeed, ABA biosynthetic genes are downregulated during imbibition, regardless of light conditions, in contrast to dry seeds which show high transcript levels of *ChABA1*, *ChNCED6* and *ChNCED9.* On the other hand, the transcript levels of *ChCYP707A2*, the main catabolic gene in *Cardamine* seeds as in *Arabidopsis* [48], are elevated during seed imbibition, similarly in the dark and in the light. In agreement with these expression data, ABA levels in dry seeds are extremely high, then at 24 HAI they decrease, both in dark and in light. Presumably, this is necessary to establish and maintain seed dormancy, which in *Cardamine* seeds is similar to *Arabidopsis*. We cannot exclude that ABA might act through the downstream PP2C phosphatases encoded by *AHG1/3* [120, 121], nor that the dormancy-promoting factor DOG1 may function on a pathway parallel to ABA converging on these phosphatases, as has been recently proved in *Arabidopsis* [120, 121].

5.1.2 ChDAG1 affects germination fine-tuning GA levels

Adapted from Lepri et al., 2025

In *Arabidopsis* and most annual plants, a number of negative regulators work to prevent germination in the dark, such as the master repressor AtPIF1, which positively controls downstream negative regulators of GA signaling and metabolism such as the DELLA proteins AtGAI and AtRGA and the DOF transcription factor AtDAG1 [40, 42, 53]. Given that these genes are highly conserved among Brassicaceae, studying their function in light-independent species represents a crucial step to unravel the molecular mechanisms underlying this process when not mediated

by light. Interestingly *ChPIF1* showed a low expression level during imbibition of *Cardamine* seeds, except at 24 HAI in darkness, when *ChPIF1* transcript level was significantly increased compared to 24 HAI in light (Fig. 15), similarly to the *Arabidopsis AtPIF1* gene. With respect to the expression profiles of the *DELLA* genes *ChGAI* and *ChRGA*, the transcript level of both genes was significantly higher during imbibition in dark than in light conditions (Fig. 15).

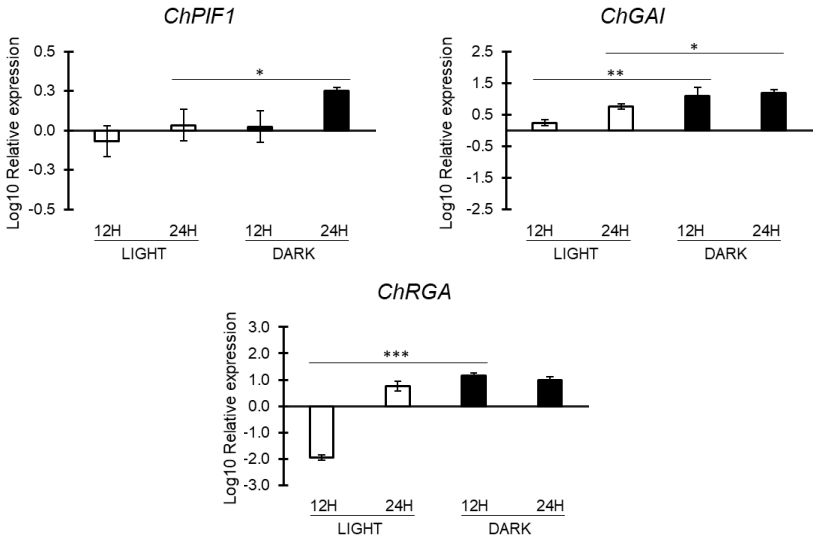

Figure 15. Expression profiles of negative regulators in *Cardamine*.
Relative expression level of *ChPIF1*, *ChGAI*, and *ChRGA* in *Cardamine* wild-type (Ox) seeds at 12 and 24 HAI under light and dark conditions. Expression levels as log10 respect to the dry condition, set to 0 (X axis). The values are means of three biological replicates, with SD values. Significant differences were analysed by t-test (**$p < 0.005$, *$p < 0.05$) (adapted from [112]).

However, in contrast to *Arabidopsis* seeds, where *AtDAG1* expression levels raise during imbibition in darkness (Fig. 16A), *ChDAG1* expression was maintained low in both light- and dark-imbibed seeds respect to dry seeds (Fig. 16B), as shown by both the the RT-qPCR analysis and the GUS histochemical assays, using the *pChDAG1::GUS Cardamine* transgenic line and the *pAtDAG1::GUS Arabidopsis* transgenic lines, with the *GUS* reporter gene under the control of 2.15 kb of the physiological promoter region (Fig. 16).

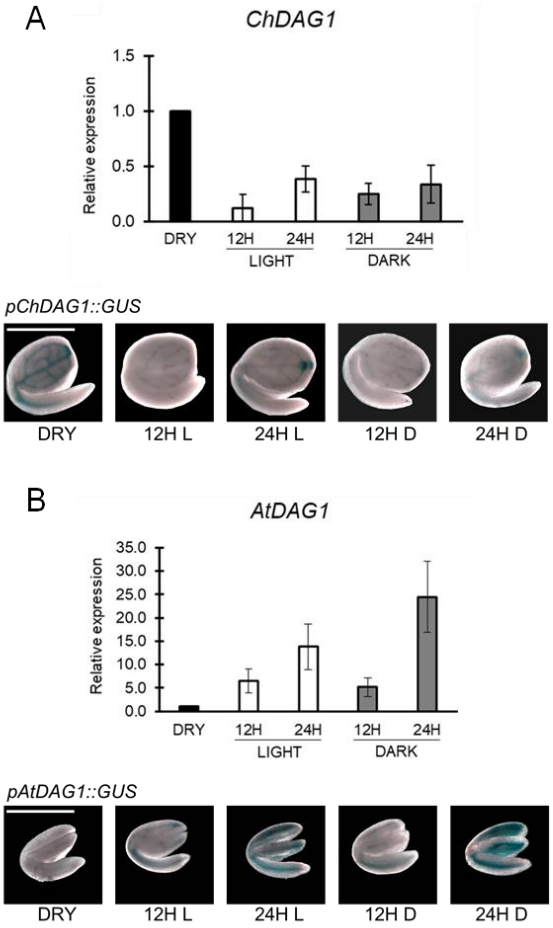

Figure 16. Expression of *DAG1* in *Cardamine* and *Arabidopsis*.
(A) Relative expression levels of *ChDAG1* and histochemical staining of *pChDAG1::GUS* and (B) relative expression levels of *AtDAG1* and histochemical staining of *pAtDAG1::GUS* in *Cardamine* and *Arabidopsis* wild-type (Ox, Ws, respectively) seeds at 12 and 24 HAI, under light and dark conditions. Expression levels are presented as the ratio of the corresponding mRNA level in dry, which was set to 1. The values are means of three biological replicates, with SD values. Scale bar, 1 mm (adapted from [112]).

Our results showed that, although *ChDAG1* is expressed in the vascular tissue of the hypocotyl and cotyledons, similarly to *Arabidopsis*, the expression profile during germination is quite diverse, as only the steady-state level of the *ChDAG1* transcript is significantly higher in dry seeds than in imbibed ones. This is in contrast to *Arabidopsis*, where *AtDAG1* is induced during imbibition, thus suggesting a putative role of ChDAG1 in the control of seed germination independently of both PIF1 and light. On the other hand, *ChPIF1* expression was extremely low in all conditions, except at 24 HAI in the dark, which does not rule out that it may have post-translational regulation as in *Arabidopsis*, and as it has also been presumed in *Aethionema arabicum* [64]. Also *ChGAI* and *ChRGA* have a similar expression profile in *Cardamine* than in *Arabidopsis* seeds, which is consistent with their role as repressor of the GA-mediated germination process [40, 122].

Given the role of AtDAG1 in the control of the GA/ABA ratio during seed germination in *Arabidopsis* [54], we investigated the role of ChDAG1 in light-independent seed germination of *Cardamine*.

By using the Crispr-Cas9 methodology [80], we generated a loss-of-function *Chdag1* mutant, designing a gRNA immediately after the start codon of the *ChDAG1* locus. Two independent *dag1* mutant

alleles (*Chdag1-1* and *Chdag1-2*) were isolated and characterized by the insertion of a single base in the seventh codon starting from the ATG, A in the *Chdag1-1* allele and T in the *Chdag1-2*, resulting in a frameshift and the formation of a premature stop codon. A seed germination assay revealed that inactivation of *ChDAG1* results in faster germination kinetics, as 25% of *Chdag1-1* seeds and 14% of *Chdag1-2* seeds germinated at 24 HAI and 78% and 60% at 36 HAI, compared to 4 and 35% of wild-type seeds, respectively (17A). Even in dark germination, inactivation of *ChDAG1* results in faster germination compared to wild-type (10 and 8%, and 30% and 41% germination rate for the two alleles at 24 and 36 HAI, compared to 0 and 13% of the wild-type, respectively) (Fig. 17B). Since the lack of *AtDAG1* in *Arabidopsis* seeds results in a reduced requirement of GAs to germinate [52], and considering that germination of *Cardamine* seeds requires GAs, we investigated whether inactivation of *ChDAG1* could reduce the GA requirement also in *Cardamine*. For this, we performed a germination assay in the presence of an inhibitory amount of PAC (100 μM) and increasing concentrations of exogenous GAs. Conversely to the phenotype of *Atdag1* seeds [52], inactivation of *ChDAG1* results in a slight but significant decrease of germination at 10 μM GA, as *Chdag1-1* and *Chdag1-2* seeds showed 45% and germination rate, compared to 63% of wild-type seeds (Fig. 17C), suggesting a slightly different control of the GA/ABA ratio by DAG1 between the two species.

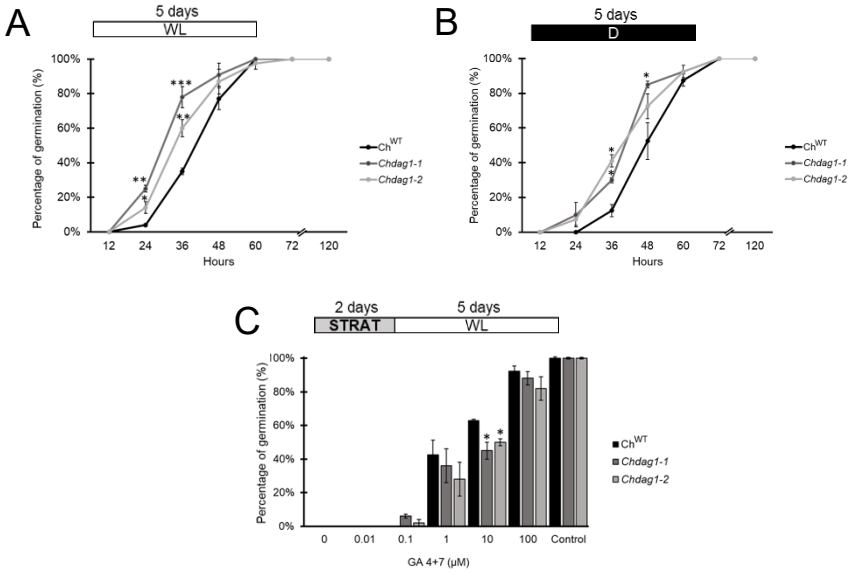

Figure 17. ChDAG1 is involved in light-independent seed germination.
Germination rates of wild-type (Ox) and both *Chdag1-1* and *Chdag1-2* mutant seeds: in white light (A), in total darkness (B), and in the presence of PAC 100 mM + increasing concentrations of GA_{4+7} (C). Germination rates were measured at different HAI (12, 24, 36, 48, 60, 72, and 120) in (A and B), and at 120 HAI in (C). The values are means of three biological replicates, with SD values. Significant differences were analysed by t-test (***$p < 0.001$, **$p < 0.005$, *$p < 0.05$). Control is referred to ‘‘mock treatment control’’ with ethanol. The diagram on top depicts the light treatment scheme (adapted from [112]).

Given that ChDAG1 is a transcription factor and its homolog AtDAG1 functions as repressor of *AtGA3OX1* and *CYP707A2* [53, 54], we wondered whether inactivation of *ChDAG1* could affect the expression of GA and ABA metabolic genes. Therefore, the transcript levels of *ChGA20OX3*, *ChGA3OX1*, *ChGA3OX2*, *ChGA2OX2* and *ChGA2OX3* for GA, and of *ChABA1*, *ChNCED6*, *ChNCED9* and *ChCYP707A2* for ABA were measured in dry conditions, and in 12 or 24 hours imbibed wild-type and both *Chdag1-1* and *Chdag1-2* mutant seeds, either exposed to white light or kept in total darkness. The results of this analysis showed that lack of DAG1 results in the upregulation of the GA biosynthetic genes *ChGA3OX1* and *ChGA3OX2* (Fig. 18A). In particular, in *Chdag1-1* seeds *ChGA3OX1* transcript level was extremely higher at 12 HAI in light (23-fold, compared to the wild-type) and increased 2-fold also at 24 HAI, and at both 12 and 24 HAI in the dark, although to a lesser extent (2.3- and 2-fold, respectively). Surprisingly, the transcript level of *ChGA3OX2* showed an even more relevant upregulation compared to the wild-type, with a 50- and 63-fold increase at 12 and 24 HAI in the light, and a 6- and 61-fold increase under dark conditions at 12 and 24 HAI, respectively (Fig. 18A). These results were corroborated by the expression profile of these genes in the *Chdag1-2* allele, which perfectly matched the one of *Chdag1-1.* Indeed, *ChGA3OX1* transcript level increased 3-fold at 12 and 24 HAI in the light, and 6 and 12-fold in dark conditions, while expression of *ChGA3OX2* raised 8- and 9-fold in the light, and 7- and 11-fold in the dark (12 and 24 HAI, respectively) (Fig. 18A).

On the other hand, expression of ABA metabolic genes was not affected by the inactivation of *ChDAG1*, as the transcript level of *ChABA1*, *ChNCED6*, *ChNCED9* and *ChCYP707A2* was comparable in *Chdag1* mutant alleles and wild-type seeds (Fig. 18B), suggesting that ChDAG1 activity is specifically aimed at controlling GA levels.

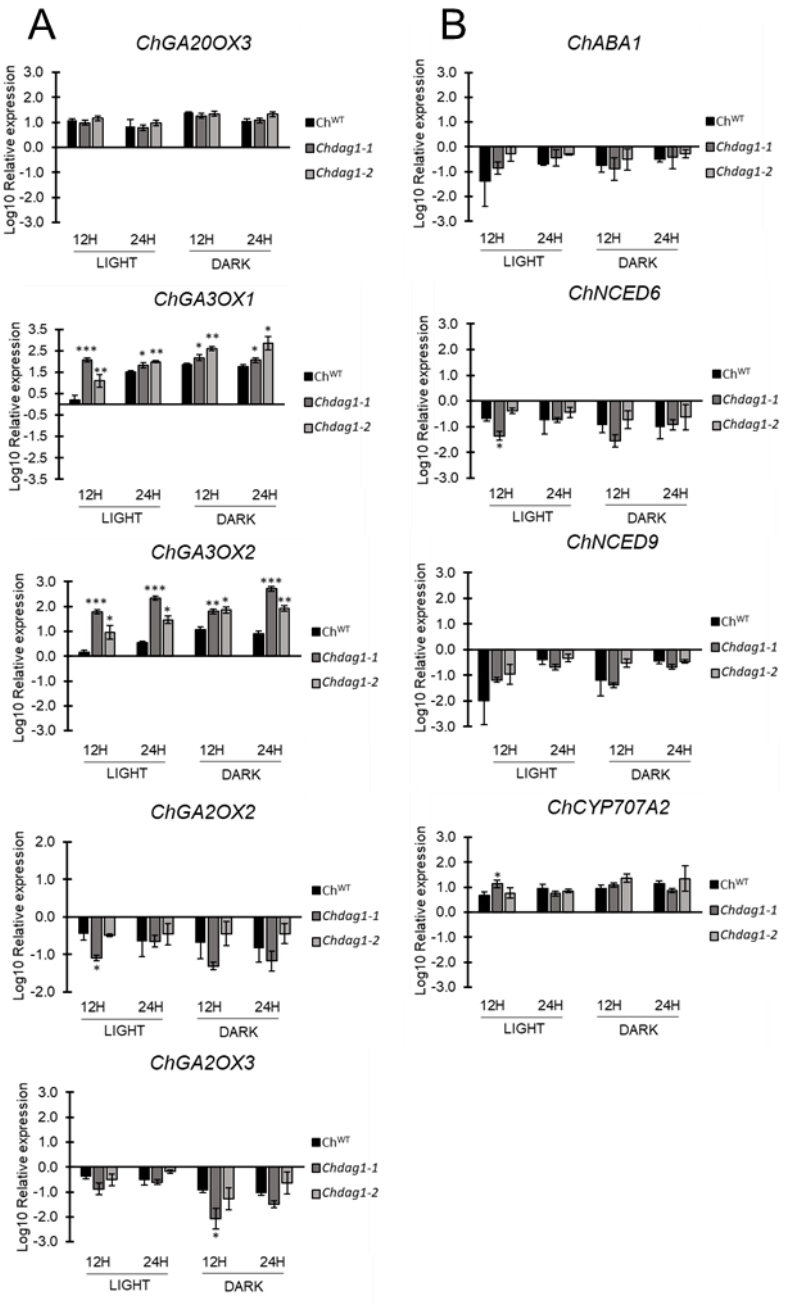
A
ChGA20OX3
ChGA3OX1
ChGA3OX2
ChGA2OX2
ChGA2OX3
B
ChABA1
ChNCED6
ChNCED9
ChCYP707A2
Log10 Relative expression
ChWT
Chdag1-1
Chdag1-2
12H
24H
LIGHT
DARK

Figure 18. Expression profiles of GA and ABA genes in *Chdag1* mutant alleles.
Relative expression levels of: *ChGA20OX3, ChGA3OX1, ChGA3OX2, ChGA2OX2, ChGA2OX3* (A), *ChABA1, ChNCED6, ChNCED9, ChCYP707A2* (B) in *Chdag1-1* and *Chdag1-2* mutant seeds compared to the wild-type, at 12 and 24 HAI under light and dark conditions. Expression levels are presented as log_{10} respect to the dry condition, set to 0 (X axis). The values of relative expression levels are means of three biological replicates, with SD values. Significant differences were analysed by t-test (***p < 0.001, **p < 0.005, *p < 0.05) (adapted from [112]).

To test this hypothesis, we measured the GAs levels in *Chdag1-1* seeds compared to wild-type seeds. This experiment revealed a complex fine-tuning of GAs levels, with lack of ChDAG1 resulting in increased levels of bioactive GA_5 and GA_6, unlike GA_1 or GA_4. Nevertheless, the GA/ABA ratio was increased in *Chdag1-1* imbibed seeds in dark and light conditions, compared to wild-type seeds (Fig. 19B). These data indicate that a differential fine-tuned regulation of the levels of GAs by ChDAG1 contributes to the different germination activity of *Arabidopsis* and *Cardamine* seeds. This hypothesis is also supported by the expression profile of *ChGAI* and *ChRGA* in the *Chdag1* mutant background, as these *DELLA* genes are upregulated in light-imbibed seeds at 12 HAI, suggesting that ChDAG1 is required to repress their expression. Intriguingly, the inactivation of *ChDAG1* results in higher steady-state level of *ChGAI* and *ChRGA* at 12 HAI in the light, making the expression in light- and dark-imbibed seeds not significantly different as it is in wild-type seeds (Fig. 19A).

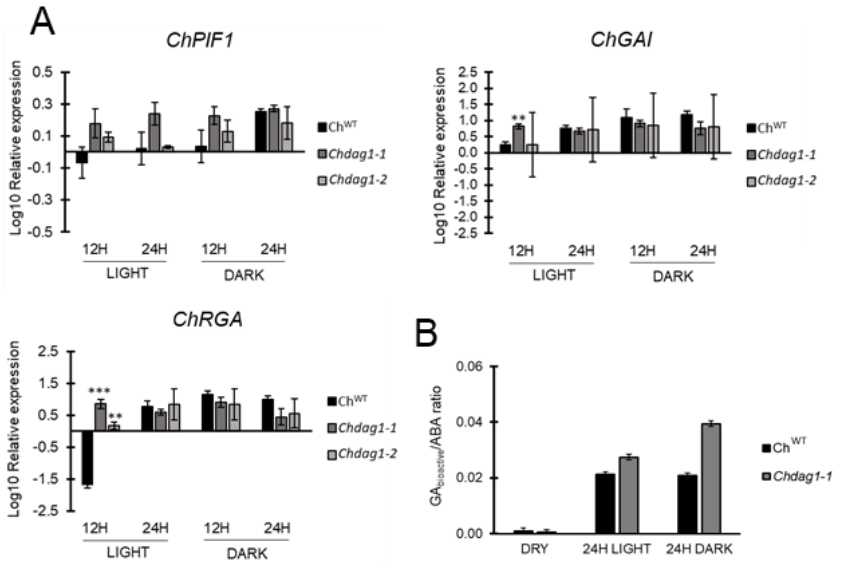

Figure 19. Expression profiles of negative regulators in *Chdag1* mutant alleles.
(A) Relative expression levels of *ChPIF1, ChGAI, ChRGA* in *Chdag1-1* and *Chdag1-2* mutant seeds compared to the wild-type, at 12 and 24 HAI under light and dark conditions. Expression levels are presented as $\log_{10}$ respect to the dry condition, set to 0 (X axis). The values of relative expression levels are means of three biological replicates, with SD values. Significant differences were analyzed by t-test (**p < 0.001, **p < 0.005, *p < 0.05). (B) Ratio of bioactive GAs/ABA in *Chdag1-1* mutant seeds compared to Ox seeds. The analyses were performed on dry and 24-h imbibed seeds in light and dark conditions. The values are the mean of three biological replicates, with SD values (adapted from [112]).

In *Arabidopsis* seeds, DAG1 fine-tunes the GA/ABA balance irrespective of light conditions, as well as the GA homeostasis, through a feedback loop on *AtGA3OX1* [54]. Of 29 *Cardamine* putative *DOF* genes, only the protein encoded by the single-copy gene *ChDAG1* shares 91.4% amino acid identity with AtDAG1, thus we hypothesized that ChDAG1 might be involved in the control of light-independent seed germination in *Cardamine*. Indeed, the inactivation of *ChDAG1* affects seed germination: *Chdag1* seeds display a faster germination kinetics, similarly to *Atdag1* seeds [50], while having an increased GA requirement, in contrast to *Atdag1* [52]. As for ABA, ChDAG1, unlike AtDAG1, is not likely to function on ABA levels, as revealed by the similar expression of ABA metabolic genes as well as by the comparable amount of ABA in *Chdag1-1* and wild-type seeds. Thus, ChDAG1 seems to be committed only to the repression of the two key GAs biosynthetic genes which, in the absence of ChDAG1, are upregulated, particularly in light-imbibed seeds.

5.1.3 *ChDAG1* expression is induced by GAs in the dark

Adapted from Lepri et al., 2025

As a fine-tuning of GA metabolism is fundamental for germination in dark conditions and ChDAG1 is able to control GA homeostasis, we questioned whether GAs might influence *ChDAG1* levels, as observed for *Arabidopsis AtDAG1* [54], to permit light-independent germination.

Therefore, we used RT-qPCR to measure *ChDAG1* transcript level in seeds imbibed in the presence of GAs, in white light or in total darkness. Interestingly, expression of *ChDAG1* was significantly increased by GAs in seeds kept in the dark (up to almost 8-fold compared to the control set to 1), while it was downregulated by GAs in light-imbibed seeds (up to 5.3-fold) (Fig. 20A). Conversely, *AtDAG1* was induced to the same extent (8-fold) in *Arabidopsis*

wild-type seeds imbibed in the presence of GAs in white light, as expected [54], while *AtDAG1* transcript level decreased (almost 2-fold) when seeds were imbibed with GAs in the dark (Fig. 20B). To further examine this result, we exploited *pChDAG1::GUS Cardamine* and *pAtDAG1::GUS* transgenic lines and we analysed the whole mount expression of *ChDAG1* and *AtDAG1* on seeds imbibed 24 hours in the presence/absence of GAs (GA_{4+7} 100 mM), in light or dark conditions. Consistently, GUS staining was notably expanded in all the vascular tissue in late embryos of *pChDAG1::GUS* seeds imbibed in the presence of GAs in the dark, compared to seeds with GAs in white light, or with those without GAs regardless of light conditions, whereas *pAtDAG1::GUS* showed increased GUS staining in light-imbibed seeds (Fig. 20C).

Our data suggest that GA enhances *ChDAG1* expression. Since ChDAG1 is a potential repressor of *ChGA3OX1* and *2*, while its expression is induced by GAs, a feedback control of GAs levels can be hypothesized.

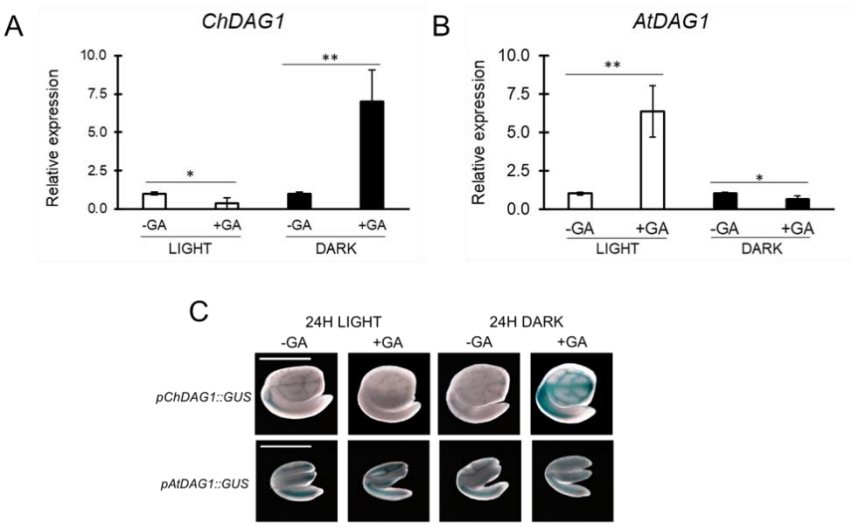

Figure 20. GAs promote *ChDAG1* expression in dark-imbibed seeds.
Relative expression levels of *ChDAG1* (A) and *AtDAG1* (B) in 24-h imbibed wild-type seeds (Ox and Ws, respectively), in the presence of water (control) or GA_{4+7} (100 mM), in white light or in darkness. Expression levels were normalized with that of the *ChUBQ10* and *AtUBQ10* genes for *Cardamine* and *Arabidopsis* samples, respectively. Expression levels are presented as the ratio of the corresponding mRNA level in the -GA control, which was set to 1. The values are the mean of three biological replicates, with SD values. Significant differences were analysed by t-test (**$p < 0.005$, *$p < 0.05$). (C) Histochemical staining of *pChDAG1::GUS* and of *pAtDAG1::GUS* seeds imbibed 24 h, with/without addition of GAs, under white light (WL) or in dark (D). Scale bar, 1 mm (adapted from [112]).

5.1.4 Assessing ChDAG1/AtDAG1 functional homology

Adapted from Lepri et al., 2025

Given the high amino acidic identity between AtDAG1 and ChDAG1 and the common target gene *GA3OX1* in *Arabidopsis* and *Cardamine*, we then investigated whether ChDAG1 and AtDAG1 might have a conserved function, at least to a certain extent, between the two Brassicaceae species. To evaluate this potential functional homology, we produced the transgenic lines expressing on one hand *ChDAG1* in the *Arabidopsis dag1* mutant, and on the other hand the fully complementing *AtDAG1* in the same background as control. The two constructs contained the *ChDAG1* and *AtDAG1* genomic loci under the control of 2.15 kb of their own promoters. Four transgenic lines for each construct have been selected and analysed. The phenotypic analysis for seed germination of the *Atdag1* mutant expressing *ChDAG1* (named *Atdag1*,*pChDAG1::ChDAG1*) revealed that ChDAG1 was unable to complement the phenotype of *Atdag1* in the light. Indeed, as expected [50], *Atdag1* mutant seeds germinated faster than *Arabidopsis* wild-type seeds (23% vs 5% at

24 HAI), while mutant seeds expressing *ChDAG1* showed an even increased germination rate at 24 HAI (60%) (Fig. 21A; Fig. 17A). Conversely, expression of *ChDAG1* in the *Atdag1* background was able to complement the dark germination mutant phenotype [50], since germination dropped to 0, as in wild-type seeds (Fig. 21B). With respect to GA requirement, *Atdag1* mutant seeds showed increased germination frequencies compared to wild-type seeds (17% vs 1% and 62% vs 35% at 0.01 and 0.1 μM GA, respectively), consistently with previous results [52]. Similarly, *Atdag1* expressing *ChDAG1* showed a similar germination trend, although with a slightly reduced germination rate at 0.1 μM GA (41%), indicating that again ChDAG1 was unable to revert the *Atdag1* phenotype (Fig. 21C).

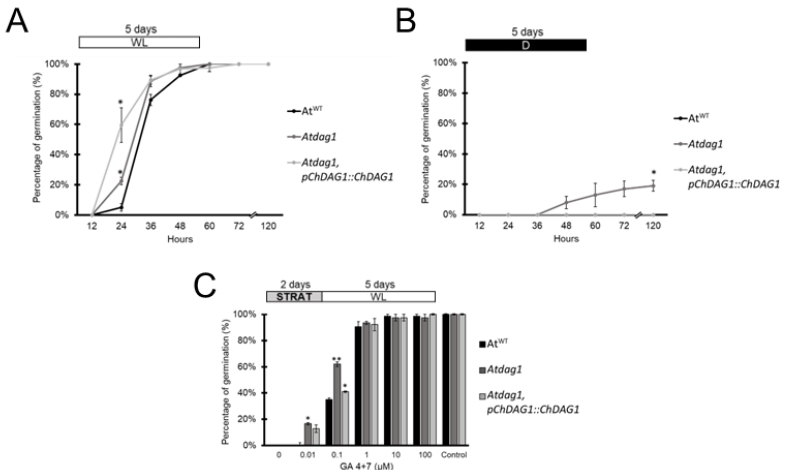

Figure 21. Effect of ChDAG1 in the *Atdag1* background.
Germination rates of *Atdag1,pChDAG1::ChDAG1*, *Atdag1*, and wild-type (Ws) seeds in white light (A), in total darkness (B), and in the presence of PAC 100 mM + increasing concentrations of GA_{4+7} (C). Germination rates were measured at different HAI (12, 24, 36, 48, 60, 72, and 120) in (A and B), and at 120 HAI in (C). The values are the mean of three biological replicates, with SD values. Significant differences were analyzed by t-test (**p < 0.005, *p < 0.05). Control is referred to treatment with ethanol. The diagram on top depicts the light treatment scheme (adapted from [112]).

We analysed the expression of *ChDAG1* and found that, in the *Atdag1* mutant background, it was lower during imbibition in the light respect to dry seeds, while it was higher in the dark (Fig. 22), suggesting a different transcriptional control of *ChDAG1* compared to *AtDAG1*. This would explain the inability of ChDAG1 to complement the white light phenotypes of the *Atdag1* mutant. Also, to verify whether ChDAG1 can complement the function of AtDAG1 in repressing *AtGA3OX1* and *AtCYP707A2*, we measured the expression level of these genes in *Atdag1*,*pChDAG1::ChDAG1* and in the *Atdag1*,*pAtDAG1::AtDAG1* complemented line, as a control. In addition, the expression of *AtGA3OX2*, *AtGA2OX2*, *AtGA2OX3, AtABA1*, *AtNCED6*, *AtNCED9* was also evaluated. Surprisingly, in the dark, *AtGA3OX1* was upregulated in the *Atdag1*,*pChDAG1::ChDAG1* lines (Fig. 22A) while, as expected, it was repressed in the *Atdag1*,*pAtDAG1::AtDAG1* complemented line (Fig. 22B). This indicates that, despite the high amino acid identity between AtDAG1 and ChDAG1, the latter is unable to repress *AtGA3OX1*. Expression of *AtCYP707A2* was downregulated by ChDAG1 in *Atdag1*,*pChDAG1::ChDAG1* seeds, both in light and dark conditions (Fig. 22A), compared to the complemented line (Fig. 22B), suggesting an over-repression by ChDAG1 on this ABA catabolic gene. On the other hand, expression of *ChDAG1* in the *Atdag1* background did not affect expression of any other GA and ABA metabolic genes, as the expression profiles in *Atdag1*,*pChDAG1::ChDAG1* (Fig. 22A) were similar to the ones in the *Atdag1*,*pAtDAG1::AtDAG1* complemented line (Fig. 22B).

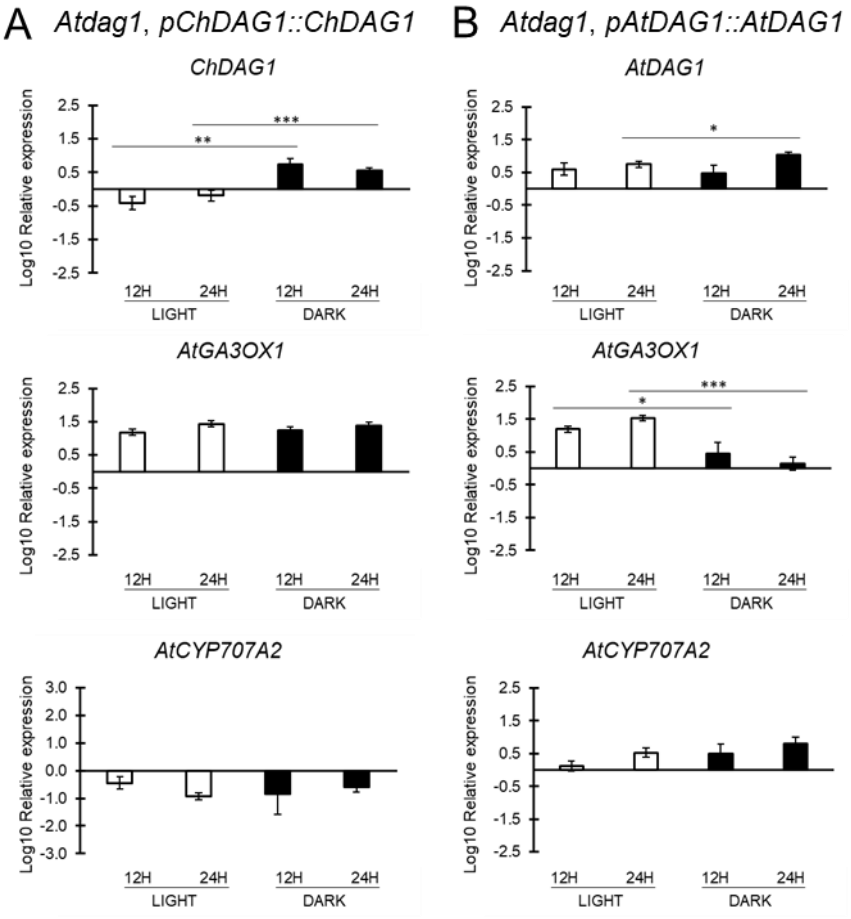

Figure 22. Activity of ChDAG1 in the *Atdag1* background.
Relative expression level of *ChDAG1* and *AtDAG1* (A and B) and of *AtGA3OX1* and *AtCYP707A2*. Seeds of *Atdag1,pChDAG1::ChDAG1* (A) and *Atdag1,pAtDAG1::AtDAG1* (B) at 12 and 24 HAI, under light and dark conditions. Expression levels are presented as $\log_{10}$ respect to the dry condition, set to 0 (X axis). The values of relative expression levels are means of three biological replicates, with SD values. Significant differences were analysed by t-test (***$p < 0.001$, **$p < 0.005$, *$p < 0.05$) (adapted from [112]).

To further characterize whether AtDAG1 and ChDAG1 could be functional homologs, a transgenic line expressing *AtDAG1* under 2.15 kb of its physiological promoter in the *Chdag1* mutant background (*Chdag1,pAtDAG1::AtDAG1*) was also generated, as well as a fully complementing control line expressing the *Cardamine* genomic *ChDAG1* under its own promoter in the same background (*Chdag1,pChDAG1::ChDAG1*) as a control. Expression analyses of *AtDAG1* in the *Cardamine Chdag1* background displayed a profile comparable to the *ChDAG1* one in the complementing line (Fig. 23A). As for the GA biosynthetic gene, *ChGA3OX1*, AtDAG1 in the *Cardamine* background mirrored the expression profile in the light observed in the complementing line, whereas in darkness *ChGA3OX1* was repressed at both 12 and 24 HAI (4- and 12-fold, respectively) in the *AtDAG1* expressing line respect to the complementing line (Fig. 23B). This observation sounds consistent with the role of AtDAG1 in repressing *AtGA3OX1*. Interestingly, also *ChGA3OX2* showed a repression at 12 and 24 HAI in darkness (6- and 7-fold, respectively) respect to the complementing line (Fig. 23C), although AtDAG1 was proved not to regulate this gene in *Arabidopsis.* As for the ABA catabolic gene *ChCYP707A2*, expression analyses showed a mild repression in the *AtDAG1* expressing line respect to the complementing line, where *ChCYP707A2* was found to be expressed to the same extent in dark as in light, as expected (Fig. 23D). Notably, despite the partial repression of GA biosynthetic genes in the dark, *Chdag1,pAtDAG1::AtDAG1* seeds retained a germination potential of 100% under both light and dark, suggesting that, despite AtDAG1 activity, the transgenic line maintains a sufficiently high GA/ABA ratio, allowing light-independent germination.

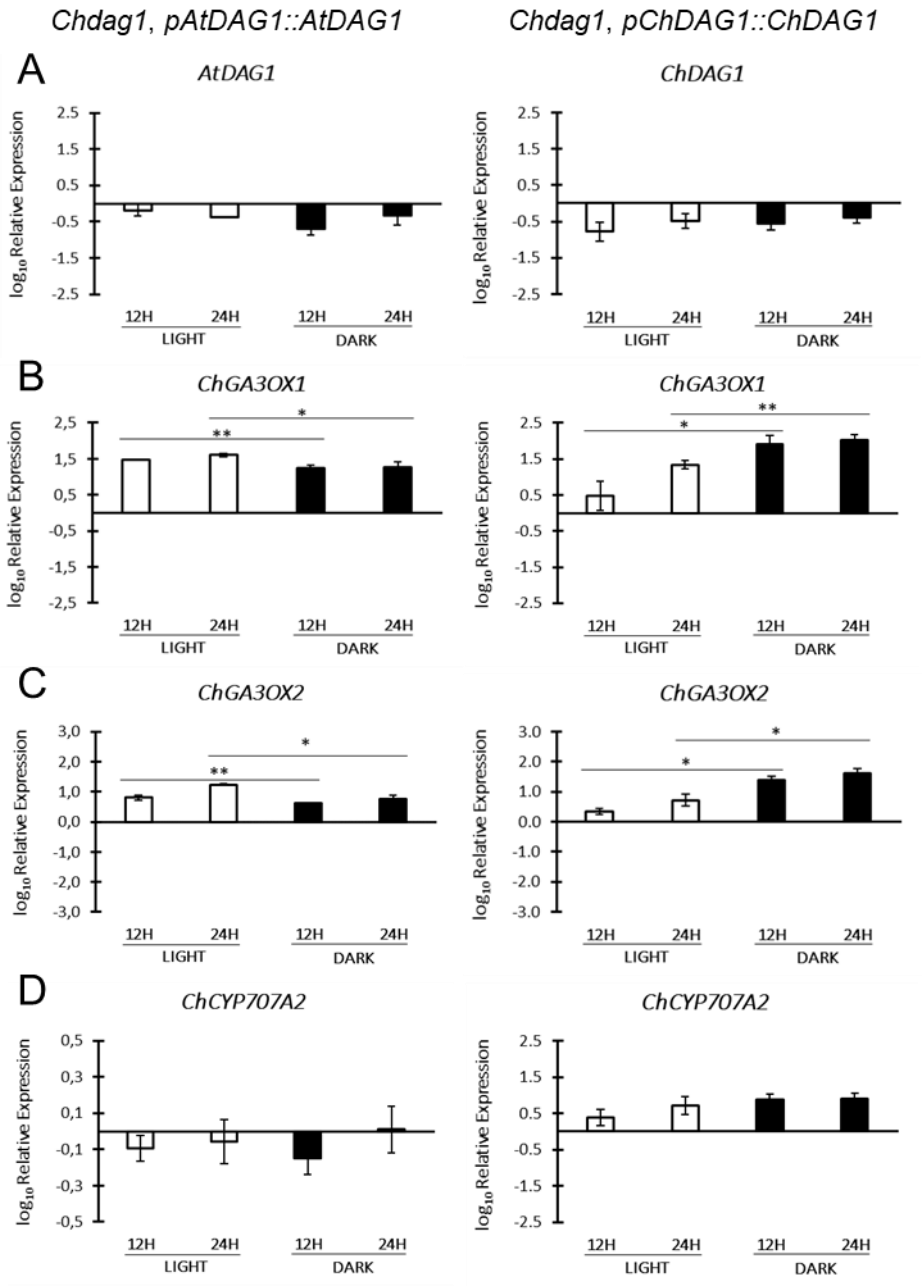
Chdag1, pAtDAG1::AtDAG1
Chdag1, pChDAG1::ChDAG1
A
AtDAG1
ChDAG1
B
ChGA3OX1
ChGA3OX1
C
ChGA3OX2
ChGA3OX2
D
ChCYP707A2
ChCYP707A2
log10 Relative Expression
12H
24H
LIGHT
DARK

Figure 23. Activity of AtDAG1 in the *Chdag1* background.
Relative expression levels of *ChDAG1* and *AtDAG1* (A), of *ChGA3OX1* (B), *ChGA3OX2* (C) and *ChCYP707A2* (D). Seeds of *Chdag1, pAtDAG1::AtDAG1* (left column) and *Chdag1,pChDAG1::ChDAG1* (right column) at 12 and 24 HAI, under light and dark conditions. Expression levels are presented as $\log_{10}$ respect to the dry condition, set to 0 (X axis). The values of relative expression levels are means of three biological replicates, with SD values. Significant differences were analysed by t-test (**p < 0.005, *p < 0.05).

Our analyses showed that ChDAG1 is unable to repress *AtGA3OX1* when expressed in the *Atdag1* mutant background, as AtDAG1 does. The Dof domains of ChDAG1 and AtDAG1 are identical, indicating that ChDAG1 should recognize the Dof binding sequences present on the *AtGA3OX1* promoter and bound by AtDAG1 [123], [124]. However, given that AtDAG1 negatively regulates *AtGA3OX1* by cooperating with AtGAI [123], one possibility is that ChDAG1 is unable to interact with AtGAI and, in turn, to bind Dof binding sites on the *AtGA3OX1* promoter to repress its expression.
Remarkably, expression of *ChDAG1* in the *Atdag1* background results in a striking and unexpected downregulation of *AtCYP707A2,* in imbibed seeds relative to dry seeds [125], different to the *Arabidopsis* complemented line (*Atdag1*,*pAtDAG1::AtDAG1*). Therefore, ChDAG1 is likely to induce an over-repression of *AtCYP707A2*, as it would bind *CYP707A2* promoter constitutively. It is well established that Dof proteins can interact with other regulatory factors and these interactions contribute to the specificity of DOF proteins [126]. We cannot rule out the hypothesis that ChDAG1 is unable to interact with a corepressor or that, rather it has an increased affinity for the *AtCYP707A2* promoter.

It should be noted that, in the *Atdag1* background, the expression profile of *ChDAG1* is different from the one of *AtDAG1* itself, indicating that: (1) the promoters of *ChDAG1* and *AtDAG1* do not share the same regulatory regions, (2) their expression is controlled by the same external/internal cues but in a different way, (3) other levels of regulation, namely epigenetic, could take place differentially on *ChDAG1* respect to *AtDAG1*.
As for the analysis of the transgenic lines expressing *AtDAG1* in the *Chdag1* background, the results allow to hypothesize that a species-specific regulatory context in *Cardamine* determines the extent of AtDAG1-mediated regulation of target genes. Indeed, in this background, AtDAG1 partially mirrors its physiological repression of *ChGA3OX1* in darkness, also reducing *ChCYP707A2* expression, whereas ChDAG1 was previously shown not to regulate ChCYP707A2; by contrast, *ChGA3OX2* shows a partial repression in darkness despite not being an AtDAG1 target in *Arabidopsis*, possibly suggesting an interaction of AtDAG1 with other *Cardamine* cofactors, allowing AtDAG1 to regulate such loci specifically in this context. The expression profile of *AtDAG1* in the *Cardamine* background is comparable to *ChDAG1* in the complementing line, possibly indicating that the transcriptional control is predominantly driven by the *Cardamine* genetic background.

Finally, the *AtDAG1* and *ChDAG1* promoters share two relevant regulatory domains, an E-box and a MADS-box, which, although both associated with seed dormancy and germination [41, 127] have not been linked to AtDAG1 by any evidence so far. Both *DAG1* loci are regulated by GAs, but in opposite ways; *AtDAG1* is positively controlled in the light by GAs (this work; [54]), while in *Cardamine* seeds GAs control the expression of *ChDAG1* positively in the dark and negatively in the light. These data highlight the hypothesis that GAs act as an internal signal, both in *Arabidopsis* and *Cardamine* seeds, but with opposite effects. Therefore, the *ChDAG1* locus, once in the presence of an increased amount of GAs, as in the *Atdag1*

background [54], will be repressed, as it is in the light-imbibed seeds of *Atdag1*,*pChDAG1::ChDAG1*. The extremely low expression level of *ChDAG1* in light imbibed *Atdag1* seeds is, at least partly, the reason why ChDAG1 is unable to complement any germination phenotypes of *Atdag1*.

Altogether, these observations support the idea that AtDAG1 and ChDAG1, despite having a partial context-dependent functional homology, might control homeostasis of GAs in a different fashion. Moreover, our results highlight the possibility that, despite orthologs, the regulation of the expression of *ChDAG1* and *AtDAG1* might differ in the two species.

5.1.5 Model of light-independent germination process

Adapted from Lepri et al., 2025

Taken together, our physiological and molecular data provide a solid framework for dark germination in *Cardamine* seeds and, possibly, in other Brassicaceae with light-independent germination. The phenotypic and molecular characterization of ChDAG1, both in its natural context, *Cardamine* seeds, and in the context of *Arabidopsis* seeds, as a light-dependent germination species, allowed us to outline a scheme which, although still representing a working model, represent a first important step in unveiling the mechanisms underlying light-independent and, possibly, light-inhibited germination.

Although many plant species, including *Arabidopsis*, can germinate in total darkness, the ecological context of their germination differ significantly from *Cardamine hirsuta*. Indeed, wild-type *Arabidopsis* seeds mainly depend on light-activated phytochrome pathways for germination, and, consistently, it was necessary to screen over 300 *Arabidopsis* accessions to identify three QTLs required for increasing germination under cold and dark [128].

Similarly to *Cardamine hirsuta*, *Aethionema arabicum* can germinate in darkness, but its utility as a model system is limited by the evolutionary distance from *Arabidopsis thaliana* and lack of genetic tractability. Comparative genomic studies suggest that *Cardamine hirsuta* shares approximately 85-90% genomic similarity with *A. thaliana* [72], while *Aethionema arabicum* shares 70-80% genomic similarity [64]. This restricts relevance of this species for direct comparative studies and functional genomic analyses. In contrast, *C. hirsuta* is evolutionarily closer to *Arabidopsis* and amenable to genetic transformation, making it a more suitable model for studying light-independent germination.

In this model, the amount of GAs in the dark plays a key role, and, in turn, the GA/ABA ratio which is higher in dark- than in light-imbibed seeds, eliciting seed germination (Fig. 24A). In this context, the importance of the role of ChDAG1 is highlighted by the control of its expression by GAs; indeed, GAs increase *ChDAG1* transcript level in the dark, while decreasing it in the light, a kind of control that mirrors what occurs in *Arabidopsis* seeds (Fig. 24B).

A crucial element of this scheme is related to the DELLA proteins GAI and RGA, and to their function with respect to GAs, and to their possible interaction with DAG1. Indeed, in *Cardamine* seeds in the dark, *GAI* and *RGA* are more expressed than in the light, similarly to *Arabidopsis*, but, unlike *Arabidopsis*, GA levels are as high as in the light. Remarkably, the inactivation of *ChDAG1* results in an increase of *GAI* and *RGA* transcript levels in the light but a decrease in the dark, thus suggesting that ChDAG1 has a prominent role in the control of GA homeostasis, also fine-tuning GAI and RGA levels. On the other hand, in *Arabidopsis* seeds, AtDAG1 and GAI mutually regulate their expression in order to cooperate in the repression of the GA biosynthetic gene *AtGA3OX1* [55].

Our data do not resolve the evolutionary and ecological reasons for the differences in light dependency germination among plants.

Cardamine is a broadly diffused species with higher potential for adaptation to diverse environments than *Arabidopsis* [77, 129]. *Cardamine* light-independent germination might have contributed to this adaptative potential permitting to colonize the most diverse environments. Future studies on seed germination of different *Cardamine* genotypes might help to uncover the evolutive history of this trait and how this contributed to colonization success. On a physiological point of view eventual differences in the composition of the cell wall might have evolved causing differences in the mechanical and chemical properties that are fundamental during seed germination in both light and dark conditions and are linked to GAs levels [130, 131, 132]. Considering this hypothesis, further studies utilizing *Cardamine* as a model system are required to provide evidence on this fundamental topic.

In conclusion our data represent a step forward in our understanding of dark germination, a topic of high interest in biotechnology including in all the conditions where light accessibility is limited.

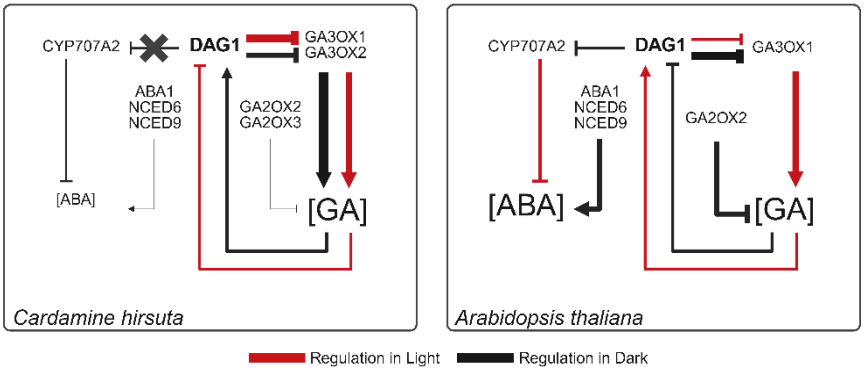

Figure 24. Scheme of the molecular mechanism underlying seed germination in *Cardamine*.
Scheme of the main elements involved in seed germination in *Cardamine hirsuta* (left) and *Arabidopsis thaliana* (right). Red and black arrows are referred to light and dark conditions, respectively. Arrows' thickness refers to the expression level of the corresponding genes. In *Cardamine* seeds, the transcript levels of *ChGA3OX1* and *ChGA3OX2* are higher in the dark than in the light, thus increasing GA levels. ChDAG1 represses these two GAs' biosynthetic genes which, in the absence of ChDAG1, are upregulated, particularly in light-imbibed seeds. The transcript level of *ChCYP707A2* is not altered by the inactivation of *ChDAG1*, suggesting that ChDAG1 is not involved in its regulation. GAs increase ChDAG1 transcript level in the dark, while decreasing it in the light. In *Arabidopsis* seeds, AtDAG1 represses both *AtGA3OX1* and *AtCYP707A2*, mainly in the dark [53, 54]. GAs increase *AtDAG1* transcript level in the light, while decreasing it in the dark. (Adapted from [112]).

5.2 The epigenetic side

5.2.1 H3K27me3/H3K4me3 dynamics uncoupled from light

Following the molecular characterisation of light-independent germination, we focused on the study of the epigenetic mechanisms that might contribute to integrate environmental and endogenous factors during the germination process. Given the involvement of the PRC2 complex and of its silencing mark H3K27me3 in the seed-to-seedling transition in *Arabidopsis*, we wondered whether, and eventually how, an alternative deployment of this PTM might support the light-independent germination ability of *Cardamine* seeds. To this end, we extracted total histones from dry and 24 hours imbibed seeds, in either light or dark conditions, and analysed the bulk level of H3K27me3 via immunoblot. Whether in dry seeds we observed high levels of the H3K27me3 mark, *Cardamine* seeds showed a significant decrease in H3K27me3 mark within the first 24 hours imbibition, 2-fold in light and 5-fold in darkness (Fig. 25A).

Since the epigenetic mark H3K4me3 is known to counteract H3K27me3 on most of its target loci, we also analysed this activating mark. We detected a statistically significant 1.5-fold increase in H3K4me3 levels only in darkness (Fig. 25B). This scenario is different from that proved in *Arabidopsis* [106], suggesting that the establishment of a different chromatin landscape in *Cardamine* might underpin the light-independent germination behaviour. It is possible that PRC2-mediated repression is relieved earlier and/or more broadly in *Cardamine* than in *Arabidopsis*, establishing a germination-permissive epigenetic state in light as well as in dark conditions. Moreover, the dark-specific gain of H3K4me3 might be coherent with the transcriptional activation of germination-promoting components (e.g. hormone metabolism) previously observed (Fig. 13).

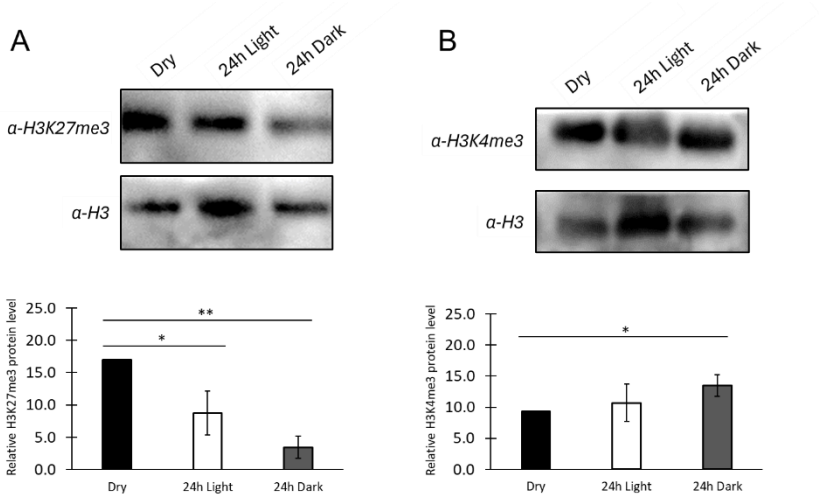

Figure 25. H3K27me3 decreases during imbibition.
Immunoblot of wild-type *Cardamine hirsuta* dry (Dry) and 24 hours imbibed seeds either in light or dark. Nuclear proteins were probed with H3K27me3 or H3K4me3 specific antibodies, with H3 as loading control. Immunoblot (top) and densitometric analysis (bottom). The protein levels are the mean of three biological replicates, presented with SD values. Significant differences were analysed by t-test (**$p < 0.005$, *$p < 0.05$).

5.2.2 PRC2 expression and activity during seed development

The significant level of H3K27me3 in dry seeds, prompted to a deeper analysis of chromatin dynamics during early seed developmental stages, to identify possible differences of the epigenetic landscape in *Cardamine* seeds.

To this end, we sampled flowers at 8-15 DAP to analyse maturing seeds (maturation), freshly harvested seeds, and 4-week stored seeds (stored), and assessed the expression levels of PRC2 catalytic

subunits. In *Arabidopsis thaliana*, three E(Z) homologues, CLF, MEA and SWN, provide the H3K27 methyltransferase activity within distinct PRC2 complexes. Our bioinformatic comparative analyses revealed four E(Z) homologues in *Cardamine*, possibly implying a duplication of *MEA*, based on the homologies. Expression analyses showed that all PRC2 catalytic subunits were strongly expressed during seed maturation, with a significant reduction in freshly harvested seeds (average of 5-fold), with a further reduction of *MEA* genes throughout dormancy (from "freshly harvested" to "stored" seeds) (Fig. 26).

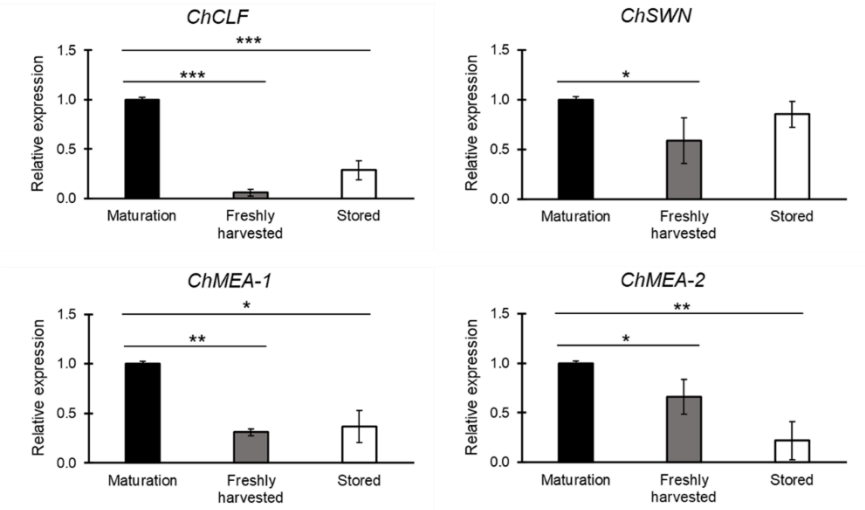

Figure 26. Expression of PRC2 catalytic subunits during seed development.
Relative expression levels of *ChCLF*, *ChSWN*, *ChMEA-1*, *ChMEA-2* in wild-type *Cardamine hirsuta* maturing seeds (maturation), freshly harvested seeds and 4-weeks stored seeds (stored). Expression levels are presented as the ratio of the corresponding mRNA level in seed maturation, which was set to 1. Relative expression levels were normalized with the *ChUBQ10* reference gene. The values are means of three biological replicates, presented with SD values. Significant differences were analysed by t-test (***$p < 0.001$, **$p < 0.005$, *$p < 0.05$).

From the same seeds developmental stages we extracted proteins enriched in histones and quantified global levels of H3K27me3 and H3K4me3, in order to have a broader scenario of chromatin dynamics, as for these epigenetic marks, during seed development. We observed an increase in H3K27me3 during dormancy, of 2- and 3-fold in freshly harvested and stored seeds, respectively (Fig. 27A), whereas H3K4me3 followed the opposite trend, with a statistically significant decrease of 1.5- and 2-fold in freshly harvested and stored seeds, respectively (Fig. 27B). We also examined the level of the histone variant H2A.Z, a conserved regulator of transcription whose deposition is mediated by the SWR1 complex and is associated with repression of inducible genes in *Arabidopsis*. It has been demonstrated that light-signalling factors play an important role in the dynamics of H2A.Z deposition, highlighting this histone variant as a negative regulator of transcriptional programs, relevant during the seed-to-seedling transition [133]. H2A.Z levels mirrored the H3K27me3 ones, progressively increasing during dormancy, with a statistically significant decrease of 1.5- and 3-fold in freshly harvested and 4-weeks stored seeds, respectively, though with an overall lower level (Fig. 27C).

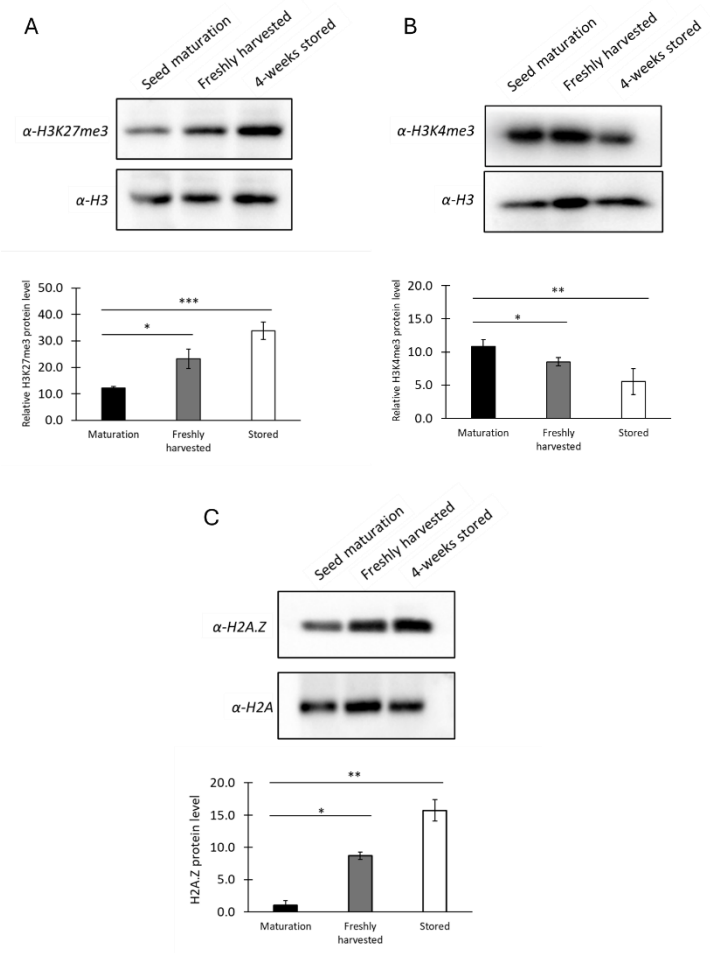

Figure 27. Profile of H3K27me3 through seed maturation.
Immunoblot of wild-type *Cardamine hirsuta* maturing seeds (maturation), freshly harvested seeds and 4-weeks stored seeds (stored). Nuclear proteins were probed with H3K27me3 (A), H3K4me3 (B) or H2A.Z (C) specific antibodies, and H3 or H2A used as loading control. Immunoblot (top) and densitometric analysis (bottom). The protein levels are the mean of three biological replicates, presented with SD values. Significant differences were analysed by t-test (***$p < 0.001$, **$p < 0.005$, *$p < 0.05$).

Consistently, expression levels of putative PRC2 target genes in *Cardamine* -namely *DOG1*, *DAG1*, *CHO1*, *ABI3*, *ABI4*, *ABI5*-, selected basing on *Arabidopsis* available data, were shown to be high in maturing seeds, with a progressive decrease during dormancy (Fig. 28).

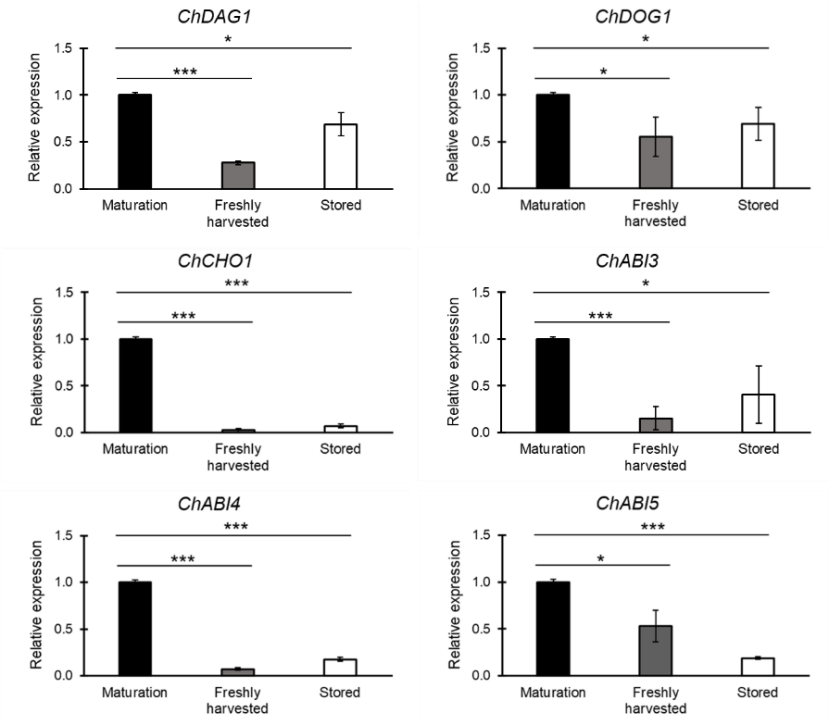

Figure 28. Expression levels of PRC2 putative target genes in *Cardamine.*

Relative expression levels of *ChDAG1*, *ChDOG1*, *ChCHO1*, *ChABI3*, *ChABI4*, *ChABI5* in wild-type *Cardamine hirsuta* maturing seeds (maturation), freshly harvested seeds and 4-weeks stored seeds (stored). Expression levels are presented as the ratio of the corresponding mRNA level in seed maturation, which was set to 1. Relative expression levels were normalized with the *ChUBQ10* reference gene. The values are means of three biological replicates, presented with SD values. Significant differences were analysed by t-test (***$p < 0.001$, *$p < 0.05$).

Curiously, transcript levels of PRC2 catalytic subunits decrease from maturation through dormancy, conversely to the increasing level of H3K27me3, thus implying that PRC2 activity is maintained despite the reduced expression of its catalytic subunit. This could be explained by a high protein stability, as PRC2 proteins produced in maturing seeds may be particularly stable in the dry state, where proteolysis is limited.

5.2.3 Pharmacological inhibition of PRC2 in *C. hirsuta*

To evaluate the contribution of PRC2 activity to the light-independent seed germination process, we used the small-molecule inhibitor RDS 3434, previously characterized in our laboratory, specifically targeting PRC2 catalytic domain, thus able to reduce H3K27me3 level in *Arabidopsis* seeds and to derepress PRC2 target genes in a dose-dependent manner [111].
Seeds of *Cardamine hirsuta* were imbibed in either light or dark conditions and treated with RDS 3434 (240 μM). Proteins enriched in histones extracted at 48 and 72 HAI, in either light or dark conditions, were analysed by immunoblot to assess H3K27me3 levels. RDS 3434 reduced efficiently the H3K27me3 mark respect to the control samples. In particular, at 48 HAI in dark, we observed a 2-fold reduction (Fig. 29B) and at 72 HAI light and dark 1.5-fold reduction (Fig. 29A and 29B). Surprisingly, at 48 HAI in light we observed an unexpected 1.5-fold increase of the H3K27me3 levels (Fig. 29A). In parallel, RDS 3434 delayed seeds germination in all treatments, with statistically significant reductions at 48 HAI, in both light and dark (35% and 38%, respectively); the inhibitory effect lasted at 72 HAI although with a higher variability across samples. This phenotype is similar to the delay in germination reported in *Arabidopsis* upon PRC2 inhibition by RDS 3434 [111].

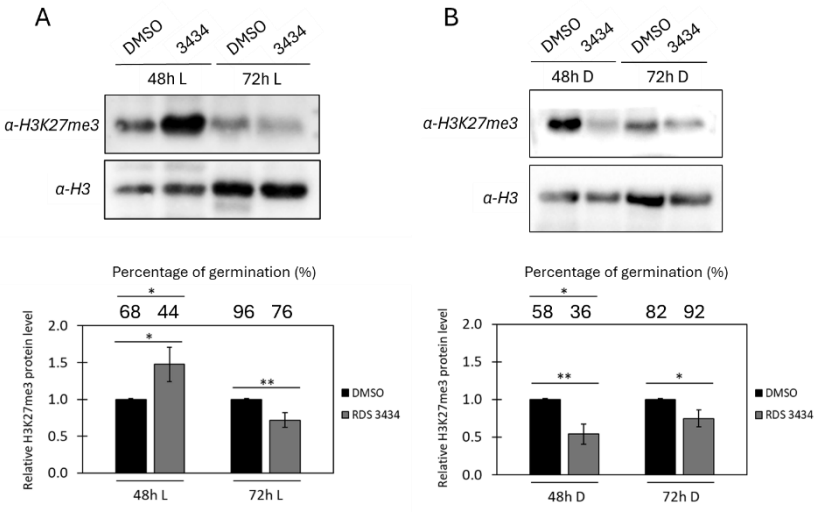

Figure 29. RDS 3434 effect on H2K27me3 levels.
Immunoblot of 48 and 72 hours imbibed wild-type *Cardamine* seeds, either in light (A) or dark (B), on media supplied with RDS 3434 or DMSO as control. Nuclear proteins were probed with H3K27me3 specific antibodies, with H3 as loading control. Western blot (top) and densitometric analysis (bottom). Results of seed germination assays, performed in the same conditions, are presented on top of densitometric analysis. Data represent the mean of three independent biological replicates, presented with SD values; for germination assays, 50 seeds for each replica were analysed. Significant differences were analysed by t-test (**p < 0.005, *p < 0.05).

Our results showed that chemical inhibition of PRC2 decreases H3K27me3 levels and delays germination in both light and dark conditions, indicating that a basal level of PRC2 activity is required for the seed-to-seedling transition state in *Cardamine* as in *Arabidopsis*. Our findings align with the framework previously

depicted and integrate with our earlier results: during post-harvest dormancy H3K27me3 likely accumulates on seed-specific and seed-dormancy related genes, while early imbibition is characterized by a rapid reduction of H3K27me3 and a gain of H3K4me3. Chemically reducing H3K27me3 in this window possibly disrupts the fine-tuned sequence of regulatory events, delaying germination regardless of light conditions.

To further characterise the effects of PRC2 inhibition, we employed the nuclear-localised GA biosensor nlsGPS2 in a *Cardamine hirsuta* wild-type background. FRET-based hormone biosensors, like nlsGPS2, have been used to monitor endogenous hormone dynamics *in vivo*, and their ratiometric readout allows straightforward, quantitative comparisons of gibberellin levels across conditions [134]. Since our epigenetic results indicate that PRC2 activity is involved in the germination process, imaging of nlsGPS2 upon RDS 3434 treatment allows to directly test whether perturbing the epigenetic dynamics reflects into altered GAs levels during germination and whether this depends on the light conditions. To this end, seeds of the *nlsGPS2* line were sown on media supplied with RDS 3434, either in light or dark conditions, and embryos were imaged at 48 and 72 HAI. In light at 48 HAI there was no significant difference between RDS 3434 and the control; at 72 HAI in light, RDS 3434 produced a significant increase in the nlsGPS2 emission ratio, indicating higher GA levels relative to the control (1.5-fold). In darkness, RDS 3434 significantly increased the emission ratio already at 48 HAI (1.3-fold), whereas at 72 HAI in darkness no significant difference was observed respect to the control. The pseudocolour maps below the scatter plot, reporting a representative embryo for each condition, qualitatively mirror the trends described (Fig. 30).

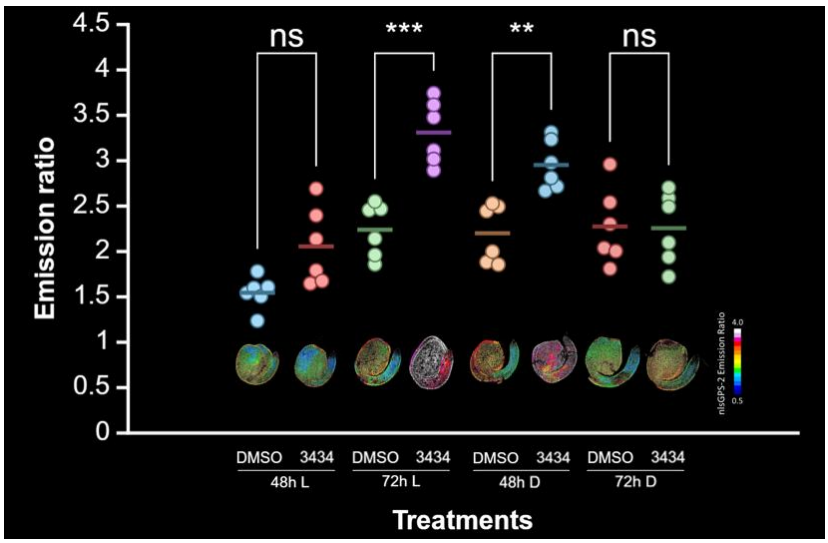

Figure 30. RDS 3434 treatment results in increased GA levels. Comparison of *Cardamine* transgenic embryos expressing the nlsGPS2 biosensor. Emission ratios at 48 and 72 HAI on media supplied with RDS 3434 or a DMSO were measured using FRETENATOR plugins for Fiji ImageJ. At the bottom of the scatter plot are reported the Max Z-projection of emission ratios of the embryos, extracted from the seed coats: the pseudocoloured maps indicate GA levels, with warm colours indicating higher levels. Data represent the mean of six independent biological replicates, presented with SD values. Significant differences were analysed by t-test (**$p < 0.005$, *$p < 0.05$, ns $p > 0.05$).

These results, increased GA at 48 HAI in darkness and 72 HAI in light, sound contradictory with the delay in germination following RDS 3434 treatment., Nevertheless, in *Cardamine* seed germination is controlled by the GA/ABA ratio rather than absolute GAs levels, as proved by our results.. Indeed, an increase in GA could be counterweighed by elevated ABA, such that the GA/ABA ratio required for germination is not reached. Thus, it will be interesting to analyse the ABA biosensor in the same conditions.

5.2.4 Nuclear profiling from seed maturation to germination

In *Arabidopsis thaliana*, DAPI-based nuclear profiling studies demonstrated that seed maturation is characterized by a significant reduction in embryonic cotyledon nuclear size, together with increased chromatin compaction: chromocenter number rises, the relative heterochromatic fraction increases, and pericentromeric and centromeric repeats become more condensed [135]. Upon germination and early seedling establishment, light further drives nuclear remodelling, as nuclei expand, chromocenters are re-organized and heterochromatin/euchromatin partitioning shifts in a coordinated manner during photomorphogenesis [136]. These studies provided quantitative traits that distinguish maturation-associated compaction from the light-promoted re-expansion and re-patterning of nuclear architecture. Based on these notions , we performed a time-resolved DAPI-based nuclear profiling in *Cardamine hirsuta* across seed maturation, dormancy ("freshly harvested" to "stored" seeds) and germination, to gain insights on how these nuclear features are configured during seed maturation and dormancy, and subsequently established upon imbibition in both light and darkness, exploiting *Cardamine hirsuta* as a ground breaking model.
To this end, we sampled flowers at 8-15 DAP to analyse maturing seeds (maturation), freshly harvested seeds, and 4-week stored seeds (stored); the seed coat was removed, and the cotyledons were dissected from the embryo. Cotyledon tissues were DAPI-stained and imaged using confocal microscopy (Fig. 31).

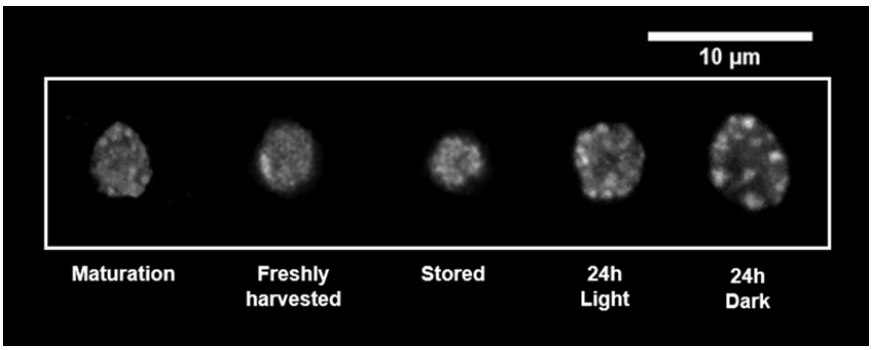

Figure 31. *Cardamine* wild-type cotyledons nuclei from seed maturation to seed germination.
Imaging of representative DAPI-stained cotyledon nuclei of maturing seeds (maturation), freshly harvested seeds, 4-weeks stored seeds (stored) and 24 hours imbibed seeds, either in light or in darkness. All the cotyledons have been dissected from embryos.

Nuclear parameters have been analysed using iCRAQ macro for Fiji ImageJ [137]. From seed maturation through dormancy, nuclear size progressively reduced, (1.5- and 1.8-fold in freshly harvested and stored seeds, respectively), similarly to *Arabidopsis*; upon imbibition, nuclear size increased, to a similar extent in both light and dark conditions, with an average increase of 4-fold respect to stored seeds (Fig. 32A). Chromocenters completely disappeared in dormant seeds, then increase during early imbibition similarly in both light and dark conditions (Fig. 32B).

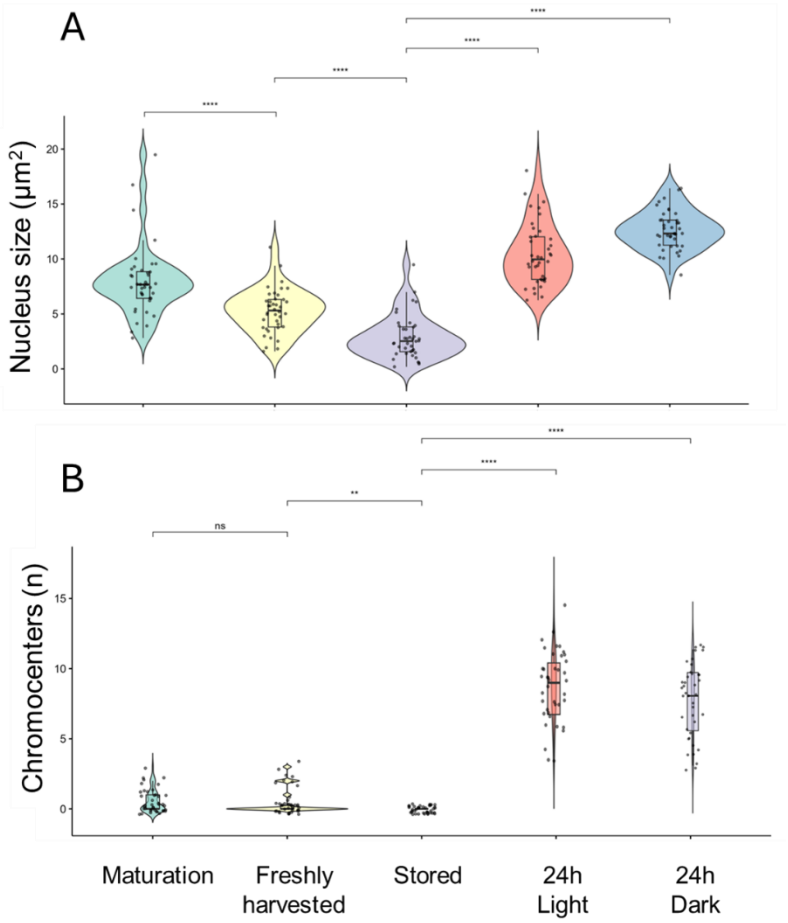

Figure 32. Nuclear profiling during seed maturation to seed germination in *Cardamine*.
Quantification of nuclear parameters obtained by DAPI-stained cotyledon nuclei of maturing seeds (maturation), freshly harvested seeds, 4-weeks stored seeds (stored) and 24 hours imbibed seeds, either in light or in darkness, dissected from embryos. Violin plots represent the distribution and median of the nuclear areas measured in 40 nuclei (A) and chromocenter number per nucleus (B) using iCRAQ macro for Fiji ImageJ. Significant differences were analysed by t-test (****$p < 0.0001$, **$p < 0.01$, ns $p > 0.05$)

This nuclear reorganization might be consistent with a repressed transcriptional state established from seed maturation throughout dormancy, with a subsequent rapid reactivation upon imbibition, regardless of light conditions. Thus, we next assessed RNAPII levels, by immunoblot analysis with both the elongating RNAPII-S2P form and the total RNAPII-TOT form, assessing also the *ChRNAPII* transcript levels by RT-qPCR.

Results showed distinct profiles for the two RNAPII forms across the developmental stages analysed. During seed maturation, although both forms showed high levels, RNAPII-S2P is significantly higher than RNAPII-TOT (2-fold), consistent with an elevated transcriptional activity at this stage. In freshly harvested seeds, the abundance of both forms declined respect to maturation, suggesting a general attenuation of polymerase activity. In stored seeds, RNAPII-S2P was significantly lower than total RNAPII (3-fold), marking the lowest abundance of the elongation-competent form and a pronounced reduction of genome-wide transcriptional activity (Fig. 33A).

Consistently, *ChRNAPII* mRNA showed a significant decrease from maturation through dormancy (12-fold), aligning transcript levels with the protein trends (Fig. 33B).

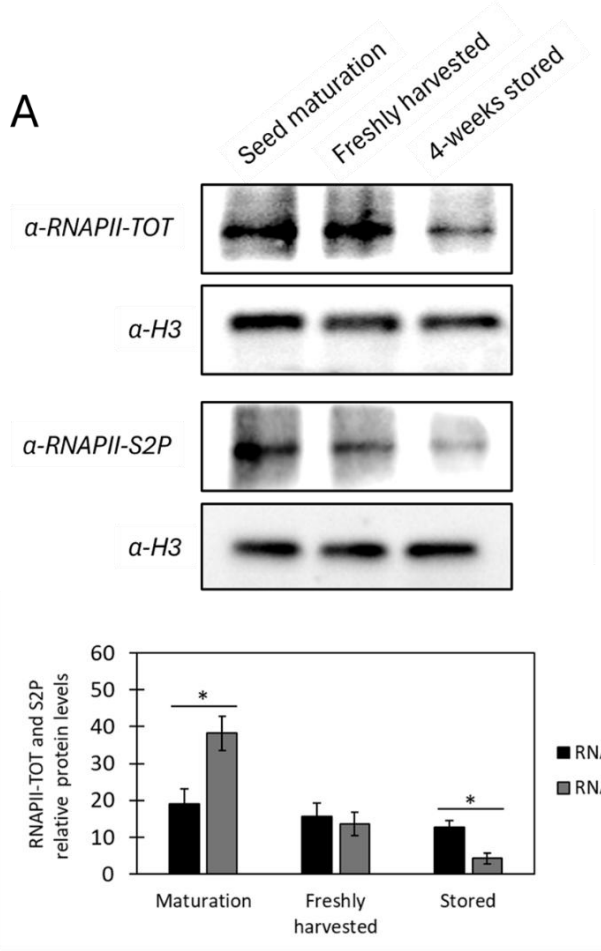
A
Seed maturation
Freshly harvested
4-weeks stored
α-RNAPII-TOT
α-H3
α-RNAPII-S2P
α-H3
RNAPII-TOT and S2P relative protein levels
60
50
40
30
20
10
0
*
*
Maturation
Freshly harvested
Stored
RNAPII-TOT
RNAPII-S2P

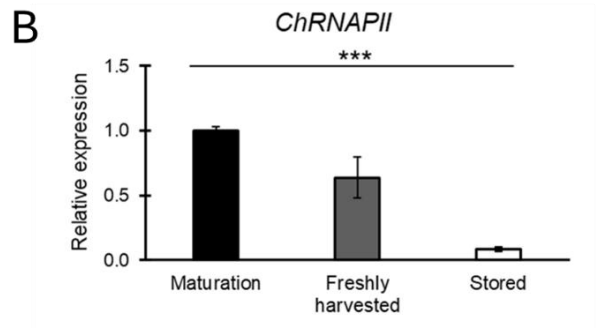
B
ChRNAPII
***
Relative expression
1.5
1.0
0.5
0.0
Maturation
Freshly harvested
Stored

Figure 33. Balance between RNAPII-S2P/total-RNAPII and expression of *RNAPII* through seed maturation in *Cardamine*.
(A) Immunoblot of wild-type *Cardamine hirsuta* maturing seeds (maturation), freshly harvested seeds and 4-weeks stored seeds (stored). Extracted nuclear proteins were probed with RNAPII-S2P and RNAPII specific antibodies, with H3 as loading control. Immunoblot (top) and densitometric analysis (bottom). The protein levels are the mean of three biological replicates, presented with SD values. Significant differences were analysed by t-test (*$p < 0.05$).
(B) Relative expression levels of *ChRNAPII* in wild-type *Cardamine hirsuta* maturing seeds (maturation), freshly harvested seeds and 4-weeks stored seeds (stored). Expression levels are presented as the ratio of the corresponding mRNA level in seed maturation, which was set to 1. Relative expression levels were normalized with the *ChUBQ10* reference gene. The values are means of three biological replicates, presented with SD values. Significant differences were analysed by t-test (***$p < 0.001$).

These data suggest a model in which dormancy is associated with a progressive reduction of RNAPII activity, consistent with the nuclear shrinkage and decreased chromocenters number observed, providing a baseline for the rapid nuclear reorganization observed during early germination (24 hours-imbibed seeds). In *Arabidopsis*, these changes are light-driven, while in *Cardamine* similar trends have been observed in both light and dark conditions.
Given these similar responses, we extended the nuclear profiling to germinating seeds, sampling from early (1, 24 and 48 HAI) to late (72, 96, 120 HAI) stages in both light and dark conditions (Fig. 34).

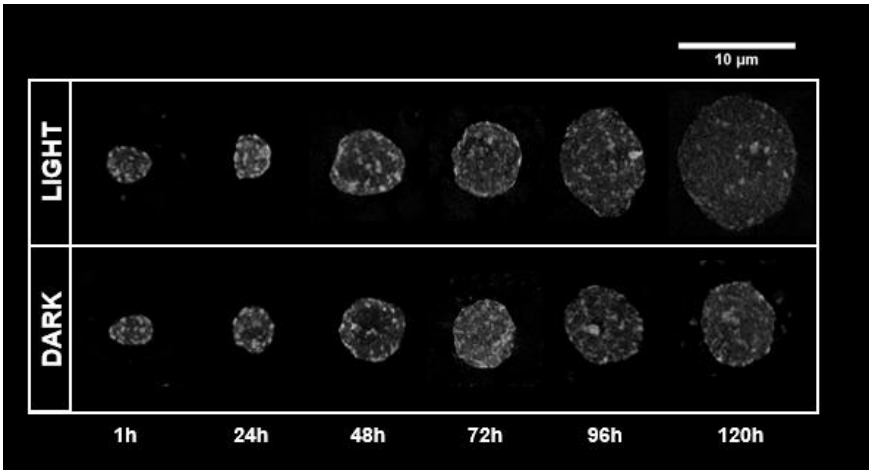

Figure 34. *Cardamine* wild-type cotyledons nuclei during early-to-late seed germination.
Representative DAPI-stained cotyledon nuclei of 1, 24, 48, 72, 96 120 hours imbibed seeds, either in light or dark conditions. The cotyledon have been dissected from embryos (1, 24 and 48 hours) or from seedlings (72, 96 and 120 hours).

Nuclear area progressively increased similarly in both light and dark conditions during early germination, with a larger expansion in light detected only from 72 HAI onward, possibly consistent with activation of photomorphogenesis, processes absent in darkness. In particular, we observed an average increase of 1.5-fold in light and of 1.3-fold in darkness, in each subsequent time point. Overall, the nuclear expansion progresses steadily in both light and dark conditions (Fig. 35A). Chromocenters formation showed a similar trend, outlining a light-independent increase during early-to-late germination, with the sole exception of 1 and 120 HAI (Fig. 35B): at these time points, the number of chromocenters resulted significantly higher in light than in darkness, with an increase of 1.7-fold in both conditions. While the increase at 120 HAI in light could

likewise be explained by the presence of mixed cell populations undergoing photomorphogenic differentiation, at 1 hour we cannot rule out a very early imbibition response taking place only in light. Moreover, conversely to the progressive nuclear expansion, chromocenters number in light remained stable up to 72 HAI, increasing of 1.5-fold and 1.4-fold only at 96 and 120 HAI, respectively. In darkness, instead, the first chromocenter spike-up at 1 HAI was less pronounced respect to the light condition but was later balanced by a progressive increase during early-to-late germination, with an average increase of 1.3-fold in each subsequent time point. Finally, the quantification of normalized euchromatin-rich nuclear regions, calculated as (nucleus size–chromocenters total)/nucleus size, revealed major fluctuations between the two light conditions, with a significant increase in darkness respect to light of 1.2-fold and 1-fold at 1 HAI and 24 HAI, respectively, and a significant increase in light respect to darkness at 120 HAI of 1.2-fold, plausibly reflecting cell-type diversification. Notably, early rise in euchromatin area in darkness deeply diverges from *Arabidopsis*, since in *Cardamine* the initial euchromatin expansion proceeds irrespective of light conditions, more strongly in darkness than in light, with a major light effect only in late germination.

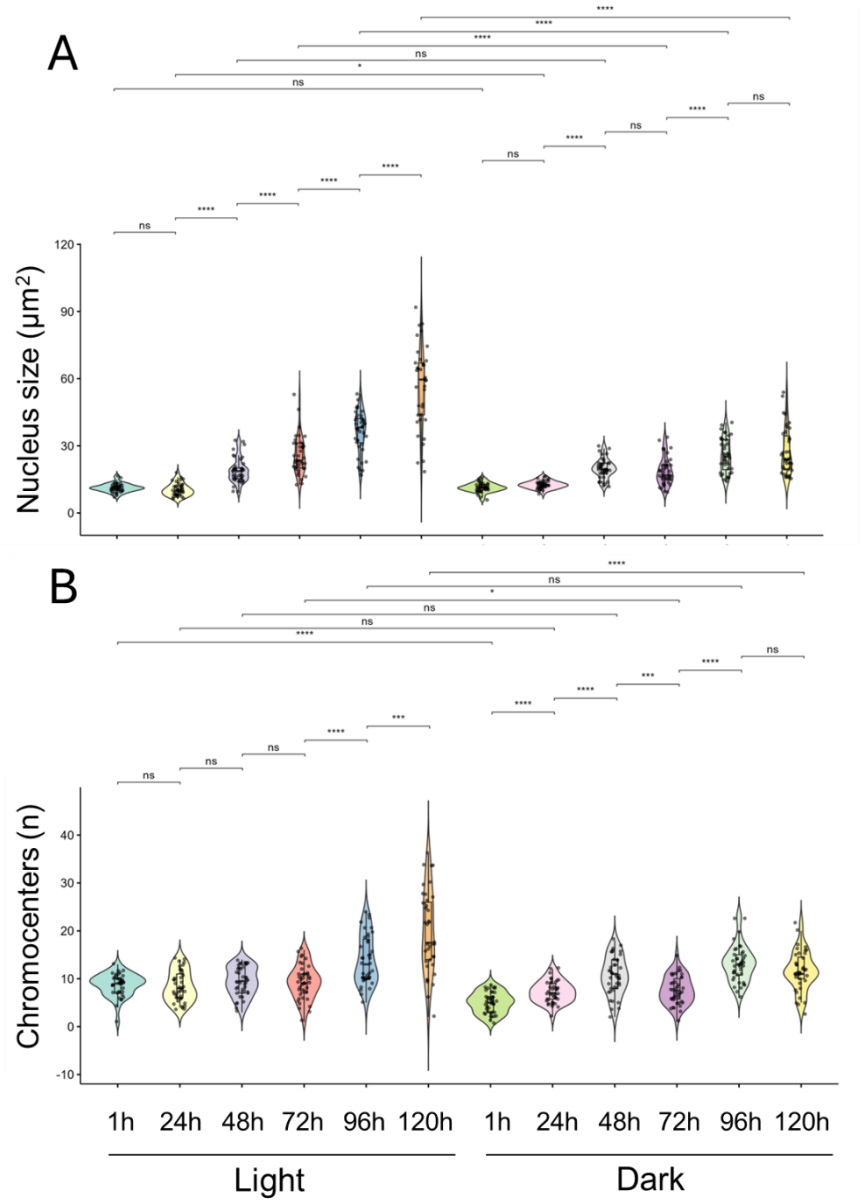
A
Nucleus size (µm²)
120
90
60
30
0
B
Chromocenters (n)
40
30
20
10
0
-10
1h
24h
48h
72h
96h
120h
1h
24h
48h
72h
96h
120h
Light
Dark

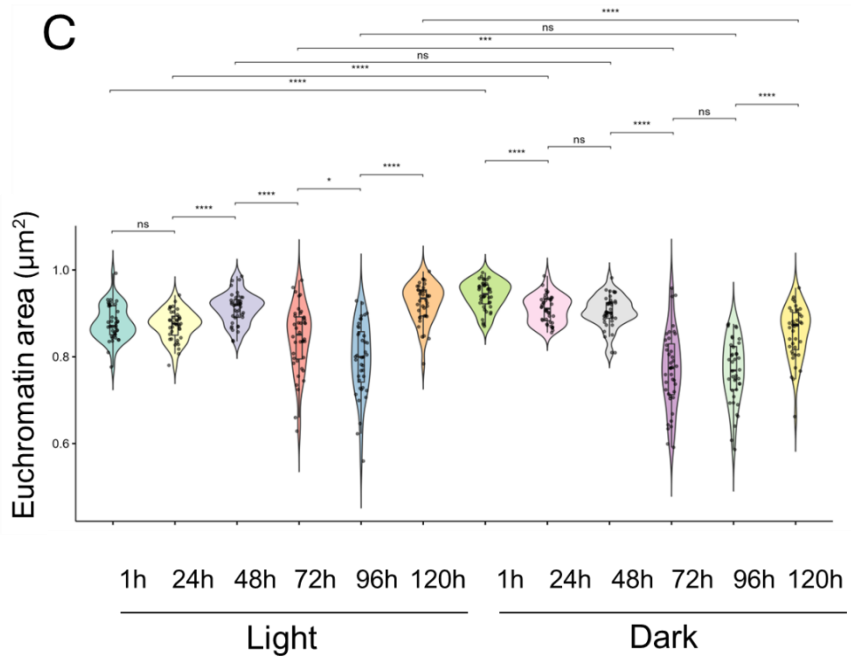

Figure 35. Nuclear profiling during seed imbibition in light and dark conditions in *Cardamine*.
Quantification of nuclear parameters obtained by DAPI-stained cotyledon nuclei dissected from embryos. Violin plots represent the distribution of the nuclear areas measured in 40 nuclei (A), chromocenter number per nucleus (B) and euchromatin area normalized by the nucleus size (C) using iCRAQ macro for Fiji ImageJ. Significant differences were analysed by t-test (****p < 0.0001, ***p < 0.001, **p < 0.01, *p < 0.05, ns p > 0.05)

Taken together, our results showed that nuclear dynamics from maturation through dormancy in *Cardamine*, such as nuclear shrinkage, reduced chromocenter and decline of RNAPII-S2P, mirrors what has been reported in *Arabidopsis*, indicating a

conserved entry into a transcriptionally restrained state during dormancy. However, in *Cardamine* seeds the earliest nuclear reorganization that drives the beginning of the germination process, such as early nuclear expansion, rapid reformation of chromocenters and increase of euchromatin domains, are largely light-independent, with light becoming modulatory, rather than permissive, only at later stages.

5.3 Future perspectives

Altogheter our data suggest that the key divergence between light-dependent and light-independent germination likely resides in locus-specific reprogramming of the epigenetic and transcriptional landscape during early imbibition, when also the major nuclear structural changes observed occur. On this basis, mapping H3K27me3, as a readout of PRC2-linked repression, and RNAPII-S2P, as an index of active transcription, by ChIP-seq during early germination, (1 HAI in darkness and at 24 and 48 HAI in either light or dark conditions), is the next step. This analysis will test (1) if there is a dynamic differential distribution of H3K27me3 in light and darkness on germination-related loci (2) if RNAPII recruitment precedes, coincides with, or follows H3K27me3 depletion at those loci and (3) if there is a subset of genes which shows light-independent RNAPII-S2P enrichment that could mechanistically account for *Cardamine* ability to germinate regardless of light conditions. In parallel, an RNA-seq experiment on the same time points will be performed, in order to define (1) differentially expressed genes and temporally resolved expression clusters and (2) light-independent co-expression networks associated with germination. Integrating ChIP-seq and RNA-seq results will allow us to define actual PRC2 targets and regulatory factors that act independently of light, refining the mechanistic model of *Cardamine* light-independent germination, finally determining a focused set of loci for subsequent functional analysis.

6. Materials and methods

6.1. Plant material and growth conditions

All the seeds from *Cardamine hirsuta* (ecotype Oxford), *Arabidopsis thaliana* (ecotype Wassilewskija), used in this work were grown in a growth chamber at 24°C/21°C with 16/8-h day/night cycles and light intensity of 300 mmol/m^{-2} s^{-1} (CCT 5700 K) as described previously [50]. The *Atdag1* mutant (Ws) is described by Papi et al. [50], *PHYB-9* and *PHYA-201* mutant alleles are described by Reed et al. [138], [139].

All seeds were harvested from completely dried mature plants grown at the same time, in the same conditions and stored for at least 4 weeks. For seed maturation samples, maturing seeds were extracted from the siliques 8-15 DAP and freshly harvested seeds were sampled immediately after silique explosion. These seeds have not been imbibed prior to analysis

As for the treatment with GA_{4+7}, seeds were sown on medium supplied with GA_{4+7} (Duchefa G0938) at the concentration 100 µM, or with an equal volume of its solvent Ethanol 96%, as control.

As for the treatment with RDS 3434, seeds were sown on medium supplied with RDS 3434 at the concentration 240 µM, or with an equal volume of its solvent, DMSO (Dimethyl sulfoxide), as control.

6.2. Seed germination assays

Twenty seeds for each genotype were sown on filter papers 595 (Schleicher & Schüll, Dassel, Germany), soaked with 5 ml water, under dim-green safe light. As for ABA and PAC assays, seeds were sown on medium containing ABA (Duchefa A0941) or PAC (Duchefa P0922), stratified, then transferred in the growth chamber and checked after 120 h. Seeds and seedlings pictures were taken

with a Leica MZ12 stereomicroscope using an AxioCam ERc5s camera. All the germination experiments were repeated with three different seed stocks.

For light-pulse experiments, stratified seeds were exposed to a pulse of red light (R, 660 nM) (40 μmol/m^{-2} s^{-1}), to a pulse of far-red light (FR, 735 nM) (10 μmol/$m^{-2}s^{-1}$) (mounting Heliospectra LX60 lamp), or to R-FR or R-FR-R 50 pulses, then grown in either continuous monochromatic white light (300 μmol/$m^{-2}s^{-1}$) (CCT 5700 K) or in the dark for 120 h. The images of the video of Arabidopsis and Cardamine germinating seeds were acquired at 1 h intervals, with a custom IR imaging setup.

The values are the average of three biological replicates, presented with SD values. Significant differences were analysed by t-test (***$p<0.001$, **$p<0.005$, *$p<0.05$).

6.3. RNA extraction and expression analysis

RNA was isolated according to Gabriele et al. [53]. Briefly, 50 mg of seed (based on dry seed weight) was ground and extracted with 1 ml of frozen XT buffer (0.2M sodium borate, 30 mM EGTA, 1% SDS, 1% sodium deoxycholate, 2% polyvinylpyrollidone, 10 mM DTT, and 1% IGEPAL [pH 9.0]) in a mortar. The samples were later treated with 10 µl of proteinase K (Roche) for 90 min at 42°C; precipitation on ice followed for 1 hour with 40 µl 2M potassium chloride. The supernatant was collected after centrifugation at 4°C. The RNA was precipitated from the supernatant at -20°C for 2 hours with 360 µl 8M lithium chloride. The RNA was collected by centrifugation at 4°C and redissolved in 100 ml water. The RNA was further purified via the clean-up protocol of the Total RNA Purification Kit (NORGEN 17200) according to the manufacturer's protocol. Total RNA was reverse transcribed using the PrimeScript RT reagent kit with gDNA Eraser (TaKaRa, San Jose, CA). Real-time qPCR was performed with SYBR green I master using the Rotor-Gene Q instrument (QIAGEN, Hilden, Germany). A total of

1 µl of the diluted cDNA was used, along with the specific primers (Table S1). Relative expression levels were normalized with the UBQ10 reference gene and, unless otherwise stated, were presented as log10 of relative expression compared to dry seeds, which was set to 0 (indicated by the X axis). The values are means of three biological replicates, with SD values. Significant differences were analyzed by t-test (***p<0.001, **p<0.005, *p<0.05).

6.4. Generation of transgenic plants

All The CRISPR-Cas9 mutant was obtained following the protocol of Schiml et al. [140]. A single-guide RNA (sgRNA) was designed using the CRISPR-Cas9 target online predictor ‘‘CCTop’’ (https://cctop.cos.uni-heidelberg.de/), and the sgRNA with low chance of causing off-target effects was selected. The sgRNA was assembled in a pEn-Chimera vector, then transferred by Gateway reaction to pmr284 vector, coding the Cas9 protein. Cardamine hirsuta Ox plants were transformed by Agrobacterium using the floral dip method. Sequences targeted by sgRNA of T1 mutant plants were examined by TIDE (Tracking of Indels by Decomposition) analysis. T3 progeny of Cas9-free homozygous plants were selected for both the Chdag1-1 and Chdag1-2 alleles.

For cloning of the constructs pAtDAG1::AtDAG1 and pChDAG1:: ChDAG1, the Gateway system (Invitrogen) was used. The genomic sequences of AtDAG1 and ChDAG1 and the 2 kb region upstream were amplified from Arabidopsis thaliana (Ws) and Cardamine hirsuta (Ox), respectively, using the primers listed in Table S1.

To generate ChUB10::GAL4 construct, pDONORP4P1-pChUB10 [141] and pDONOR221-GAL4 were recombined with pDONOR P2P3-NOS into a pB7m34GW destination vector via LR reaction (Invitrogen). The UBQ10::GAL4,UAS::GA2ox2 line for the transactivation assays was obtained by crossing the single homozygous lines.

The constructs were introduced in A. tumefaciens, GV301. Both Arabidopsis and Cardamine plants were transformed by floral dipping [142, 143]. For each construct, several transformants have been selected and analysed.

6.5. GUS construct and analysis

A 2.15-kb fragment of the ChDAG1 promoter region amplified by PCR with HindIII and BamHI restriction sites was cloned in HindIII-BamHI linearized binary vector pBI101. Cardamine wild-type plants were transformed and several independent transformants were selected on kanamycin (50 mg/ml). Seeds were imbibed for 24 h with/without GA4+7 100 mM, in dark or light conditions. GUS assay was performed according to Moubayidin et al. [144]. Samples were imaged with an Axioskop 2 plus microscope using the AxioCam ERc5s camera.

6.6. GA and ABA dosage

The analysis was performed on dry and 24-h imbibed seeds, either in light or dark conditions, for both Cardamine wild-type Ox and *Chdag1-1* mutant. Samples were analyzed for GA and ABA content according to Urbanová et al. [145] with some modifications.
For GA dosage, tissue samples of about 2 mg FW were ground to a fine consistency using 2.7-mm zirconium oxide beads (Retsch, Haan, Germany) and a Precellys homogenizer (Bertin Technologies, France) with 1 ml of ice-cold 80% acetonitrile containing 5% formic acid as extraction solution. The samples were then extracted overnight at 4°C using a benchtop laboratory rotator Stuart SB3 (Bibby Scientific, Staffordshire, UK) after adding internal gibberellins standards ($[^2H_2]GA_1$, $[^2H_2]GA_4$, $[^2H_2]GA_9$, $[^2H_2]GA_{19}$, $[^2H_2]GA_{20}$, $[^2H_2]GA_{24}$, $[^2H_2]GA_{29}$, $[^2H_2]GA_{34}$, and $[^2H_2]GA_{44}$) purchased from OlChemIm, Czech Republic. The homogenates were centrifuged at 36.670 g and 4°C for 10 min, and corresponding supernatants were further purified using mixed-mode SPE

cartridges (Waters, Milford, MA) and analyzed by ultra-high-performance liquid chromatography-tandem mass spectrometry (UHPLC-MS/MS) (Micromass, Manchester, UK). GAs were detected using multiple-reaction monitoring mode of the transition of the ion [M–H]- to the appropriate product ion. Masslynx 4.2 software (Waters) was used to analyze the data, and the standard isotope dilution method [146] was used to quantify the GA levels. The values are the mean of three biological replicates, presented with SD values. Significant differences were analysed by one way ANOVA with post hoc Tukey multiple comparison test (***p ≤0.001, **p ≤0.005, * p ≤0.05).

As for ABA dosage, about 5 mg of plant tissue per sample was homogenized using a bead mill (27 Hz, 10 min, 4°C; MixerMill, Retsch, Haan, Germany) and extracted in 1 ml of ice-cold methanol/water/acetic acid (10:89:1, v/v) and internal standard (+)-3',5',5',7',7',7'-$^{2}H_{6}$-ABA (Olchemim, Olomouc, Czech Republic). After 1 h of shaking in the dark at 4°C, the homogenates were centrifuged (36.670 g, 10 min, 4°C), and the pellets were then re-extracted in 0.5 ml extraction solvent for 30 min. The combined extracts were purified by solid-phase extraction on an Oasis HLB cartridges (60 mg, 3 ml, Waters), then evaporated to dryness in a Speed-Vac (UniEquip) and finally analyzed by UHPLC-ESI(–)-MS/MS. Data acquisition and analysis were performed using the MassLynx software (version 4.2, Waters). Significant differences were analysed by one way ANOVA with post hoc Tukey multiple comparison test (***p ≤0.001, **p ≤0.005, * p ≤0.05).

6.7. Protein extraction and immunoblot analysis

Proteins enriched in histones were isolated according to Ruta et al. [111]. Briefly, 80 mg of seeds were grinded with liquid nitrogen and dissolved in Chromatin Buffer Extraction (Sucrose 0,4 M; Tris Hcl pH 8 10 mM; β-mercaptoethanol 5 mM; PMSF 0,1 mM; Protease inhibitor cocktail 1X, Sigma-Aldrich P9599). The nuclei were pelleted at 4000 rpm for 20 min, at 4 °C, and dissolved in 800 µl

ddH2O. The proteins were precipitated with 150 µl of NaOH/ β-mercaptoethanol (138,7 µl 2N NaOH and 11,25 µl β-mercaptoethanol) and then with 55% TCA solution, for 15 min in ice. Following centrifugation for 20 min at 14000 rpm, 4 °C, the pellet was dissolved in HU Buffer (Urea 8 M; SDS 5%; TrisHCl pH 6,8 200 mM; EDTA 0,1 mM; DTT 100 mM; bromophenol blu) and boiled for 10 min at 65 °C. Proteins were separated on a 12% SDS-polyacrylamide gel (Bio-Rad) and blotted on a PVDF Immobilon-P Transfer membrane (Millipore). Detection of proteins was performed with specific antibodies against H3K27me3 (Millipore #07–449), H3K4me3 (Abcam - ab8580), RNA Pol II (Santa Cruz - N20 SC-899), RNA Pol II-S2P (Abcam - ab238146) and against histone H3 (Biorbyt orb10805) as a loading control. The anti-rabbit IgG conjugated to peroxidase was used as a secondary antibody and the signal was detected with ECL system. The values are the average of three biological replicates, presented with SD values. Significant fold enrichments were analysed by t-test (***$p<0.001$, **$p<0.005$, *$p<0.05$).

6.8. DAPI staining

Biological samples, either seeds or seedlings, were fixed in 4% (wt/vol) paraformaldehyde for 3 h under the appropriate light condition and treated with a solution containing 6% cellulose Onozuka R10 (Yakult), 0.5% macerozyme R10 (Duchefa), and 0.1% Triton X-100 for 3 h. Upon seed coat dissection, cotyledons were isolated and squashed on a glass slide, flash frozen in liquid nitrogen, and incubated with PEMSB (50 mM Pipes pH 7.3, 5 mM EGTA pH 7.1, 5 mM MgSO4, 0.05% saponin, 5% (wt/vol) BSA) before being mounted with Vectashield (Vector laboratories) supplemented with 2 µg·mL−1 DAPI (4′,6′-diamidino-2-phenylindole) at room temperature.

6.9. Confocal acquisition of DAPI-stained nuclei

DAPI-stained nuclei were imaged using a Zeiss LSM 710 confocal laser-scanning microscope, equipped with a Plan-Apochromat 63×/1.40 Oil DIC M27 objective. Image acquisition was performed in frame scan mode, with a frame size of 1024 × 1024 pixels and a pixel dwell time of 3.15 µs. A 2× digital zoom was applied, resulting in a final image field of view of 67.4 × 67.4 µm. DAPI fluorescence was excited using a 405 nm diode laser, and emission was collected in the 410–460 nm spectral window. Images were acquired at 16-bit depth to maximize dynamic range and intensity resolution. For three-dimensional analysis, Z-stacks were acquired with a Z-step interval of 0.26 µm, ensuring adequate axial resolution for volumetric measurements and chromatin segmentation. All acquisition parameters were kept constant across samples and conditions to ensure quantitative comparability. Image acquisition was conducted using the ZEN Black software suite (Carl Zeiss), and the images were further analysed using Fiji ImageJ software with the iCRAQ macro.

6.10. Deconvolution of DAPI-stained nuclei images

All images were deconvolved with Huygens Professional version 24.10 (Scientific Volume Imaging, The Netherlands, http://svi.nl), using the GMLE algorithm, SNR:15, 10.000 maximum iterations, quality change threshold:0.001, PSF mode:theoretical.

6.11. Analysis of DAPI-stained nuclei

For each condition, 40 nuclei have been analysed. The nuclei analysis has been carried out using iCRAQ, a tool written in ImageJ macro language that relies on the FeatureJ and Interactive H_Watershed plugins [137]. Nuclei were detected via global thresholding of the median filtered z-projection (maximum

intensity) of the stack and the corresponding regions were saved as ImageJ regions of interest (ROIs). Incorrectly detected nucleus ROIs were suppressed manually. Likewise, missed nuclei were added manually. The input stack was cropped around each nucleus ROI. For chromocenter segmentation, the largest 3D structure tensor eigenvalue was calculated using the FeatureJ plugin, and its z-projection served as an input for the interactive H-watershed plugin. Image regions labeled as chromocenters were also saved as ROIs. Chromocenter ROIs could also be manually added or removed. Finally, binary masks of nucleus and chromocenter ROIs were used to produce an annotated image with three gray levels: 0 for the background, 128 for the nucleus and 255 for the chromocenters.

All the data provided by iCRAQ for nuclei and chromocenters were Data manipulation, statistical analysis, and figure generation of the nuclei and chromocenters parameters provided by iCRAQ were conducted using RStudio (Posit Software, PBC, 2024), version 2023.12.1 Build 402, “Ocean Storm” release, on a Windows platform. Data were imported from and exported to Excel files using the *readxl* (Wickham & Bryan, 2023) and *writexl* (Ooms, 2023) packages, respectively. Core data wrangling operations, such as filtering, transformation, grouping, and joining, were performed using *dplyr* [147], while data reshaping was carried out with the *reshape2* package [148]. Visualization was implemented using *ggplot2* [148], and plots were styled using customized themes and palettes from *RColorBrewer* [149]. Statistical significance between experimental conditions was assessed using the *stat_compare_means()* function from the *ggpubr* package [150]. The error bars represent SD values. Significant differences were analyzed by t-test (****$p<0.0001$, ***$p<0.001$, **$p<0.01$, *$p<0.05$, ns $p>0.05$).

6.12. Confocal acquisition of nlsGPS2 biosensor

Embryos were mounted in liquid ¼ × MS medium (1/4 × MS salts, 0.025% MES (w/v), pH 5.7), covered with a coverslip and imaged. All confocal images were acquired as z-stacks in 16-bit mode, with a ×20 dry 0.70 HC PLAN APO objective on an upright Leica SP8-Fliman confocal microscope. Typical settings were as follows: sequential scanning was used with the following laser/detector settings: sequence 1: 442 excitation 5–30%, HYD1: 460–500 nm, 100 gain; HYD2 525–560 nm, 100 gain. Sequence 2: 514 excitation 5–30%, HYD2 525–560 nm, 100 gain. Scan speed 400, line averaging: 2–4, bidirectional X: on, pinhole: 1 airy unit, Z-step size: equal to the optical section thickness, zoom: 0.75 or 1, acquisition interval: 5–10 min, pixel size: 0.49–1 µm.

6.13. Image processing and analysis of nlsGPS2 biosensor

Image processing and analysis were conducted using a streamlined yet adaptable pipeline to analyse biosensor data efficiently. The FRETENATOR plugins [151] were employed for this purpose, with segmentation settings optimized for each experiment while maintaining consistency within individual experiments. Two key plugins were used: “FRETENATOR segment and ratio 1.5” for segmenting punctate structures, performing ratio calculations, and exporting data as both images and results tables, and “FRETENATOR ROI labeler” for assigning specific labels to regions of interest (ROIs) generated by the segmentation process and incorporating this information into the results table. Data manipulation, statistical analysis, and figure generation of the resulting tables were conducted using RStudio (Posit Software, PBC, 2024), version 2023.12.1 Build 402, “Ocean Storm” release, on a Windows platform, as specified in “Analysis of DAPI-stained nuclei”. The values are the median of six biological replicates, presented with SD values. Significant differences were analysed by t-test (***$p<0.001$, **$p<0.005$, *$p<0.05$).

Table S1

Arabidopsis thaliana	
At_ABA1_for	GATGCAGCCAAATATGGGTCAAGG
At_ABA1_rev	GCCATTGCATGGATAATAGCGACTC
At_CYP707A2_for	ATGGGCTTGCCTTACATCGGAGA
At_CYP707A2_rev	TGGCTTGAACAAGTGAGCTTTGCT
At_DAG1_for	TGTCGAAGGTATTGGACCGAA
At_DAG1_rev	TCCGACTGGGACGTTACGA
At_GA2OX2_for	TGCCAAACACCAGATCTCAC
At_GA2OX2_rev	AGGCCATTGACATGGTCTTG
At_GA2OX3_for	CCAAAACCCAAATCGTCAAGGC
At_GA2OX3_rev	TTGATGGCTTCTTGCTCCAACTG
At_GA3OX1_for	GCTTAAGTCTGCTCGGTCGG
At_GA3OX1_rev	AGATGCGATACGAGCGACG
At_GA3OX2_for	ACGTCGGTGACTTGCTCCA
At_GA3OX2_rev	GTTAACCCTGGCTCGGTGAA
At_GAPDH_for	GCTGAGGAAGTCAACGCTGC
At_GAPDH_rev	CGGACACTAGTGGCTCATCG
At_NCED6_for	ACCGGGTCGGATATAAATTGGGTTG
At_NCED6_rev	CCCGGGTTGGTTCTCCTGATTC
At_NCED9_for	AACCGCCGCTATGGTTTTAGACG
At_NCED9_rev	CCAGTCACCGGAAGGTTATGCAC
At_UBQ10_for	GGCCTTGTATAATCCCTGATGAATAAG
At_UBQ10_rev	AAAGAGATAACAGGAACGGAAACATAGT
Cardamine hirsuta	
Ch_ABA1_for	TAAAAGCGGCGAGGCTCTG
Ch_ABA1_rev	AACCTCCGATTCCACCTCCG
Ch_ABA2_for	GAGTGTTGCGGCTGAGCTTG
Ch_ABA2_rev	CAGGCAAATGAGCCAAAGCGA
Ch_ABA3_for	AAAGGCTCTGCGACACTCCC
Ch_ABA3_rev	CAAGGAGAGCACCAAGCCCA

Ch_ABI3_for	TTGAAGCAAAGCGACGTGGG
Ch_ABI3_rev	GCCTCTAGCTCCGGCAAGT
Ch_ABI4_for	CAAGTTCCGTTACCGTGGCG
Ch_ABI4_rev	CCACTTGCGAGTGCGCTTAC
Ch_ABI5_for	CATAACGGCGGTGAGAGTGC
Ch_ABI5_rev	CCACACCAGCCTTCACCAAG
Ch_CHO1_for	TACCCCGGCGGTCCTAAACT
Ch_CHO1_rev	CGGAAGAGAAGACAACGCCG
Ch_CLF_for	CCCGATGGCTCTGCCAAGTT
Ch_CLF_rev	GCGACGCACTTTGCCTCTTC
Ch_CYP707A1_for	GGCGGCGAAGTTTGTTCTGG
Ch_CYP707A1_rev	GGCTTGTTTCCCCAGCATCC
Ch_CYP707A2_for	TTGGCCTTACATCGGAGAGA
Ch_CYP707A2_rev	TGGACTGCTTATCATCACGC
Ch_CYP707A3_for	TCTCAAGCCCAGAAGCTGCG
Ch_CYP707A3_rev	GCATCCTCTCTTTGCTCGCC
Ch_DAG1_for	CGATGGAAACAAGAAAGGCG
Ch_DAG1_rev	ACCTTCGACAACCTTTGCAG
Ch_DOG1_for	CGTGTGACTCAGTTCCTCCGT
Ch_DOG1_rev	GCTCCGCCGTTAGATCGCTA
Ch_GA20OX1_for	AGGCGAGAGTTGTGGCTACG
Ch_GA20OX1_rev	GAGCGGTTCTTCTCGTCGCT
Ch_GA20OX2_for	CCGAAGCTCACCGTTTCACG
Ch_GA20OX2_rev	AGCGTAGCCACTGCTCTCAC
Ch_GA20OX3_for	GTATGGCCCGACCACGACAA
Ch_GA20OX3_rev	CGGAAAGGAATCCGGCGAGA
Ch_GA2OX2_for	ATCTGTGTGAAAGATGGAAGTTG
Ch_GA2OX2_rev	TAACACTCTTGAACCTCCCGT
Ch_GA2OX3_for	CCAAAACCCAAATCGTCAAGGC
Ch_GA2OX3_rev	TTGATGGCTTCTTGCTCCAACTG
Ch_GA3OX1_for	CAACCTGACTTCACAGCTCT

Ch_GA3OX1_rev	ATGAGAGGGATGGTTTCACC
Ch_GA3OX2_for	CCCTGGTTCACTCGTGGTCA
Ch_GA3OX2_rev	GCCGTGGAGAAGCGAGATCT
Ch_GA3OX3_for	ACATCCCCGTGAACCGTGAC
Ch_GA3OX3_rev	AGGCTCGGGTTCAGGTTTGG
Ch_GAI_for	TCCGCCATTTCAGATGACCT
Ch_GAI_rev	CACAAGACGACGATGAAAGG
Ch_GAPDH_for	TGACCACCGTCCACTCCATCAC
Ch_GAPDH_rev	GCTCTTCCACCTCTCCAGTCCTCC
Ch_MEA1_for	CACACCATGCACTTGCACGTC
Ch_MEA1_rev	GCACAATTACATCCTCCAAAACG
Ch_MEA2_for	GCTTATGGAGAAAAAAGGTGTCCG
Ch_MEA2_rev	GCACAACTACATCCTTCAAAGCG
Ch_NCED5_for	ACCCGGAGACGAAGGAGCTAT
Ch_NCED5_rev	AACGTCCGGCGATTTCTCCC
Ch_NCED6_for	AACCAAGCTGGGACGATCGG
Ch_NCED6_rev	ATCCACGAGGCCGATCCTAG
Ch_NCED9_for	ATGATCTCCCACGAACGCCG
Ch_NCED9_rev	ATGCTGGACTGGTTGCTCCG
Ch_PIL5_for	CGTGTTCTGCTGTGTCAAAG
Ch_PIL5_rev	CTTCCTCAGTGGCTTCTCTT
Ch_RGA_for	CAACCTCGCTACTGAGACCG
Ch_RGA_rev	CCGCGTTAGAAGACGGTGGA
Ch_RNAPII_for	CGGGGGATACTCAAGTGCGA
Ch_RNAPII_rev	GACGTGCACCAGACTCCCAT
Ch_SOM_for	GTCTGAGCAATCAGCGTCTCCA
Ch_SOM_rev	CTTGGAGTGGAAGGCGAAAGAG
Ch_SWN_for	ACAGAAGACCGCAGCCTCAG
Ch_SWN_rev	CCCGCTGTGCTATCCAATGC
Ch_UBQ10_for	GCCAAGATCCAGGATAAGGA
Ch_UBQ10_rev	GGGTAGATTCCTTCTGGATG

Ch_WRKY70_for	ACTGGTGTGGCCAGAAATGG
Ch_WRKY70_rev	ATCGCTGGCAACTCCGAACA
GUS	
pChDAG1::GUS_for	AAGCTTTCTAGGACGTGATCTTTT
pChDAG1::GUS_rev	TCTCTTTGTCCAAGTTCGGATCC
Transgenic plants	
geneAtDAG1_for	ATGGATGCTACGAAGTGGACTCAG
geneAtDAG1_rev	CAGGAGGATCTTCATGGTGA
geneChDAG1_for	ATGGATGCTACGAAGTGGACGCAG
geneChDAG1_rev	TAATACAGGAGGATCCTCGTGGTAA
pAtDAG1_for	AGTTTCGAATTCTGGTGGCTA
pAtDAG1_rev	GCCTTTCTCTTTGTTGAAGTTC
pChDAG1_for	CATATGTACATACCTTCTTAAGCCC
pChDAG1_rev	CTCTGCCTTTCTCTTTGTCCAAGT

7. References

[1] K. A. Franklin and P. H. Quail, “Phytochrome functions in Arabidopsis development,” Jan. 2010, *J Exp Bot*. doi: 10.1093/jxb/erp304.

[2] M. Ahmad and A. R. Cashmore, “HY4 gene of A. thaliana encodes a protein with characteristics of a blue-light photoreceptor,” *Nature*, vol. 366, no. 6451, pp. 162–166, 1993, doi: 10.1038/366162A0.

[3] J. M. Christie, M. Salomon, K. Nozue, M. Wada, and W. R. Briggs, “LOV (light, oxygen, or voltage) domains of the blue-light photoreceptor phototropin (nph1): Binding sites for the chromophore flavin mononucleotide,” *Proc Natl Acad Sci U S A*, vol. 96, no. 15, pp. 8779–8783, Jul. 1999, doi: 10.1073/pnas.96.15.8779.

[4] J. A. Jarillo, H. Gabrys, J. Capel, J. M. Alonso, J. R. Ecker, and A. R. Cashmore, “Phototropin-related NPL1 controls chloroplast relocation induced by blue light,” *Nature*, vol. 410, no. 6831, pp. 952–954, Apr. 2001, doi: 10.1038/35073622.

[5] T. Kagawa, M. Kasahara, T. Abe, S. Yoshida, and M. Wada, “Function analysis of phototropin2 using fern mutants deficient in blue light-induced chloroplast avoidance movement,” *Plant Cell Physiol*, vol. 45, no. 4, pp. 416–426, Apr. 2004, doi: 10.1093/pcp/pch045.

[6] J. J. Favory *et al.*, “Interaction of COP1 and UVR8 regulates UV-B-induced photomorphogenesis and stress acclimation in Arabidopsis,” *EMBO Journal*, vol. 28, no. 5, pp. 591–601, Mar. 2009, doi: 10.1038/emboj.2009.4.

[7] L. Rizzini *et al.*, “Perception of UV-B by the arabidopsis UVR8 protein,” *Science (1979)*, vol. 332, no. 6025, pp. 103–106, Apr. 2011, doi: 10.1126/science.1200660.

[8] V. Gawande *et al.*, “Artificial Light Spectra and Its Impact on Plant Physiological Processes and Secondary Metabolism,” *Int J Plant Soil Sci*, vol. 35, no. 18, pp. 2060–2070, 2023, doi: 10.9734/ijpss/2023/v35i183492.

[9] L. C. Roden, H. R. Song, S. Jackson, K. Morris, and I. A. Carre, “Floral responses to photoperiod are correlated with the timing of rhythmic expression relative to dawn and dusk in Arabidopsis,” *Proc Natl Acad Sci U S A*, vol. 99, no. 20, pp. 13313–13318, Oct. 2002, doi: 10.1073/pnas.192365599.

[10] C. L. Ballaré and R. Pierik, “The shade-avoidance syndrome: Multiple signals and ecological consequences,” 2017, *Plant Cell Environ*. doi: 10.1111/pce.12914.
[11] K. A. Franklin, S. J. Davis, W. M. Stoddart, R. D. Vierstra, and G. C. Whitelam, “Mutant analyses define multiple roles for phytochrome C in Arabidopsis photomorphogenesis,” *Plant Cell*, vol. 15, no. 9, pp. 1981–1989, Sep. 2003, doi: 10.1105/tpc.015164.
[12] S. Lorrain, T. Allen, P. D. Duek, G. C. Whitelam, and C. Fankhauser, “Phytochrome-mediated inhibition of shade avoidance involves degradation of growth-promoting bHLH transcription factors,” *Plant Journal*, vol. 53, no. 2, pp. 312–323, Jan. 2008, doi: 10.1111/j.1365-313X.2007.03341.x.
[13] P. Leivar *et al.*, “Dynamic antagonism between phytochromes and PIF family basic helix-loop-helix factors induces selective reciprocal responses to light and shade in a rapidly responsive transcriptional network in Arabidopsis,” *Plant Cell*, vol. 24, no. 4, pp. 1398–1419, 2012, doi: 10.1105/tpc.112.095711.
[14] T. Kagawa *et al.*, “Arabidopsis NPL1: A phototropin homolog controlling the chloroplast high-light avoidance response,” *Science (1979)*, vol. 291, no. 5511, pp. 2138–2141, Mar. 2001, doi: 10.1126/science.291.5511.2138.
[15] M. Kasahara, T. Kagawa, K. Olkawa, N. Suetsugu, M. Miyao, and M. Wada, “Chlomplast avoidance movement reduces photodamage in plants,” *Nature*, vol. 420, no. 6917, pp. 829–832, Dec. 2002, doi: 10.1038/nature01213.
[16] N. E. Holt, G. R. Fleming, and K. K. Niyogi, “Toward an understanding of the mechanism of nonphotochemical quenching in green plants,” Jul. 06, 2004, *Biochemistry*. doi: 10.1021/bi0494020.
[17] T. Barros and W. Kühlbrandt, “Crystallisation, structure and function of plant light-harvesting Complex II,” Jun. 2009, *Biochim Biophys Acta*. doi: 10.1016/j.bbabio.2009.03.012.
[18] X. P. Li *et al.*, “A pigment-binding protein essential for regulation of photosynthetic light harvesting,” *Nature*, vol. 403, no. 6768, pp. 391–395, Jan. 2000, doi: 10.1038/35000131.
[19] M. Exposito-Rodriguez, P. P. Laissue, G. Yvon-Durocher, N. Smirnoff, and P. M. Mullineaux, “Photosynthesis-dependent H2O2 transfer from chloroplasts to nuclei provides a high-light signalling mechanism,” *Nat Commun*, vol. 8, no. 1, Dec. 2017, doi: 10.1038/s41467-017-00074-w.
[20] P. L. Keun, C. Kim, F. Landgraf, and K. Apel, “EXECUTER1- and EXECUTER2-dependent transfer of stress-related signals from the

plastid to the nucleus of Arabidopsis thaliana," *Proc Natl Acad Sci U S A*, vol. 104, no. 24, pp. 10270–10275, Jun. 2007, doi: 10.1073/pnas.0702061104.

[21] I. Adamska, I. Ohad, and K. Kloppstech, "Synthesis of the early light-inducible protein is controlled by blue light and related to light stress," *Proc Natl Acad Sci U S A*, vol. 89, no. 7, pp. 2610–2613, 1992, doi: 10.1073/pnas.89.7.2610.

[22] R. G. Walters and P. Horton, "Acclimation of Arabidopsis thaliana to the light environment: regulation of chloroplast composition," *Planta*, vol. 197, no. 3, pp. 475–481, Oct. 1995, doi: 10.1007/BF00196669.

[23] S. Bailey, R. G. Walters, S. Jansson, and P. Horton, "Acclimation of Arabidopsis thaliana to the light environment: The existence of separate low light and high light responses," *Planta*, vol. 213, no. 5, pp. 794–801, 2001, doi: 10.1007/s004250100556.

[24] L. Dietzel, K. Bräutigam, and T. Pfannschmidt, "Photosynthetic acclimation: State transitions and adjustment of photosystem stoichiometry - Functional relationships between short-term and long-term light quality acclimation in plants," Mar. 2008, *FEBS J.* doi: 10.1111/j.1742-4658.2008.06264.x.

[25] A. Oravecz *et al.*, "CONSTITUTIVELY PHOTOMORPHOGENIC1 is required for the UV-B response in Arabidopsis," *Plant Cell*, vol. 18, no. 8, pp. 1975–1990, 2006, doi: 10.1105/tpc.105.040097.

[26] N. Li *et al.*, "UV-B-induced CPD photolyase gene expression is regulated by UVR8-dependent and-independent pathways in arabidopsis," *Plant Cell Physiol*, vol. 56, no. 10, pp. 2014–2023, Jan. 2015, doi: 10.1093/pcp/pcv121.

[27] S. Hayes, C. N. Velanis, G. I. Jenkins, and K. A. Franklin, "UV-B detected by the UVR8 photoreceptor antagonizes auxin signaling and plant shade avoidance," *Proc Natl Acad Sci U S A*, vol. 111, no. 32, pp. 11894–11899, Aug. 2014, doi: 10.1073/pnas.1403052111.

[28] B. A. Brown and G. I. Jenkins, "UV-B signaling pathways with different fluence-rate response profiles are distinguished in mature arabidopsis leaf tissue by requirement for UVR8, HY5, and HYH," *Plant Physiol*, vol. 146, no. 2, pp. 576–588, 2008, doi: 10.1104/pp.107.108456.

[29] R. B. Goldberg, G. de Paiva, and R. Yadegari, "Plant Embryogenesis: Zygote to Seed," *Science (1979)*, vol. 266, no. 5185, pp. 605–614, Oct. 1994, doi: 10.1126/science.266.5185.605.

[30] J. D. Bewley, "Seed germination and dormancy," *Plant Cell*, vol. 9, no. 7, pp. 1055–1066, 1997, doi: 10.1105/tpc.9.7.1055.

[31] W. E. Finch-Savage and G. Leubner-Metzger, “Seed dormancy and the control of germination,” Aug. 2006, *New Phytol*. doi: 10.1111/j.1469-8137.2006.01787.x.
[32] L. Bentsink, J. Jowett, C. J. Hanhart, and M. Koornneef, “Cloning of DOG1, a quantitative trait locus controlling seed dormancy in Arabidopsis,” *Proc Natl Acad Sci U S A*, vol. 103, no. 45, pp. 17042–17047, Nov. 2006, doi: 10.1073/pnas.0607877103.
[33] S. L. Kendall, A. Hellwege, P. Marriot, C. Whalley, I. A. Graham, and S. Penfield, “Induction of dormancy in Arabidopsis summer annuals requires parallel regulation of DOG1 and hormone metabolism by low temperature and CBF transcription factors,” *Plant Cell*, vol. 23, no. 7, pp. 2568–2580, 2011, doi: 10.1105/tpc.111.087643.
[34] S. Footitt, Z. Huang, H. A. Clay, A. Mead, and W. E. Finch-Savage, “Temperature, light and nitrate sensing coordinate Arabidopsis seed dormancy cycling, resulting in winter and summer annual phenotypes,” *Plant Journal*, vol. 74, no. 6, pp. 1003–1015, Jun. 2013, doi: 10.1111/tpj.12186.
[35] H. He *et al.*, “Interaction between parental environment and genotype affects plant and seed performance in Arabidopsis,” *J Exp Bot*, vol. 65, no. 22, pp. 6603–6615, Dec. 2014, doi: 10.1093/jxb/eru378.
[36] V. Springthorpe and S. Penfield, “Flowering time and seed dormancy control use external coincidence to generate life history strategy,” *Elife*, vol. 2015, no. 4, Mar. 2015, doi: 10.7554/eLife.05557.
[37] W. E. Finch-Savage and S. Footitt, “Seed dormancy cycling and the regulation of dormancy mechanisms to time germination in variable field environments,” Feb. 01, 2017, *J Exp Bot*. doi: 10.1093/jxb/erw477.
[38] L. Yang, S. Liu, and R. Lin, “The role of light in regulating seed dormancy and germination,” Sep. 01, 2020, *J Integr Plant Biol*. doi: 10.1111/jipb.13001.
[39] A. Carta, E. Skourti, E. Mattana, F. Vandelook, and C. A. Thanos, “Photoinhibition of seed germination: Occurrence, ecology and phylogeny,” 2017. doi: 10.1017/S0960258517000137.
[40] E. Oh *et al.*, “PIL5, a phytochrome-interacting bHLH protein, regulates gibberellin responsiveness by binding directly to the GAI and RGA promoters in Arabidopsis seeds,” *Plant Cell*, vol. 19, no. 4, pp. 1192–1208, 2007, doi: 10.1105/tpc.107.050153.
[41] E. Oh *et al.*, “Genome-wide analysis of genes targeted by PHYTOCHROME INTERACTING FACTOR 3-LIKE5 during seed

germination in arabidopsis," *Plant Cell*, vol. 21, no. 2, pp. 403–419, 2009, doi: 10.1105/tpc.108.064691.

[42] E. Oh, J. Kim, E. Park, J. Il Kim, C. Kang, and G. Choi, "PIL5, a phytochrome-interacting basic helix-loop-helix protein, is a key negative regulator of seed germination in Arabidopsis thaliana," *Plant Cell*, vol. 16, no. 11, pp. 3045–3058, 2004, doi: 10.1105/tpc.104.025163.

[43] E. Oh, S. Yamaguchi, Y. Kamiya, G. Bae, W. Il Chung, and G. Choi, "Light activates the degradation of PIL5 protein to promote seed germination through gibberellin in Arabidopsis," *Plant Journal*, vol. 47, no. 1, pp. 124–139, Jul. 2006, doi: 10.1111/j.1365-313X.2006.02773.x.

[44] Y. Yamauchi *et al.*, "Contribution of gibberellin deactivation by AtGA2ox2 to the suppression of germination of dark-imbibed Arabidopsis thaliana seeds," *Plant Cell Physiol*, vol. 48, no. 3, pp. 555–561, Mar. 2007, doi: 10.1093/pcp/pcm023.

[45] K. Sakamoto and A. Nagatani, "Nuclear localization activity of phytochrome B," *Plant Journal*, vol. 10, no. 5, pp. 859–868, Nov. 1996, doi: 10.1046/j.1365-313X.1996.10050859.x.

[46] L. Zhu *et al.*, "CUL4 forms an E3 ligase with COP1 and SPA to promote light-induced degradation of PIF1," *Nat Commun*, vol. 6, Jun. 2015, doi: 10.1038/ncomms8245.

[47] M. Ogawa, A. Hanada, Y. Yamauchi, A. Kuwahara, Y. Kamiya, and S. Yamaguchi, "Gibberellin biosynthesis and response during Arabidopsis seed germination," *Plant Cell*, vol. 15, no. 7, pp. 1591–1604, Jul. 2003, doi: 10.1105/tpc.011650.

[48] M. Okamoto *et al.*, "CYP707A1 and CYP707A2, which encode abscisic acid 8′-hydroxylases, are indispensable for proper control of seed dormancy and germination in Arabidopsis," *Plant Physiol*, vol. 141, no. 1, pp. 97–107, 2006, doi: 10.1104/pp.106.079475.

[49] V. Ruta *et al.*, "The DOF transcription factors in seed and seedling development," Feb. 01, 2020, *Plants (Basel)*. doi: 10.3390/plants9020218.

[50] M. Papi, S. Sabatini, D. Bouchez, C. Camilleri, P. Costantino, and P. Vittorioso, "Identification and disruption of an Arabidopsis zinc finger gene controlling seed germination," *Genes Dev*, vol. 14, no. 1, pp. 28–33, 2000, doi: 10.1101/gad.14.1.28.

[51] M. Papi *et al.*, "Inactivation of the phloem-specific Dof zinc finger gene DAG1 affects response to light and integrity of the testa of Arabidopsis seeds," *Plant Physiol*, vol. 128, no. 2, pp. 411–417, 2002, doi: 10.1104/pp.010488.

[52] G. Gualberti *et al.*, “Mutations in the Dof zinc finger genes DAG2 and DAG1 influence with opposite effects the germination of Arabidopsis seeds,” *Plant Cell*, vol. 14, no. 6, pp. 1253–1263, 2002, doi: 10.1105/tpc.010491.

[53] S. Gabriele, A. Rizza, J. Martone, P. Circelli, P. Costantino, and P. Vittorioso, “The Dof protein DAG1 mediates PIL5 activity on seed germination by negatively regulating GA biosynthetic gene AtGA3ox1,” *Plant Journal*, vol. 61, no. 2, pp. 312–323, Jan. 2010, doi: 10.1111/j.1365-313X.2009.04055.x.

[54] A. Boccaccini *et al.*, “The DAG1 transcription factor negatively regulates the seed-to-seedling transition in Arabidopsis acting on ABA and GA levels,” *BMC Plant Biol*, vol. 16, no. 1, Sep. 2016, doi: 10.1186/s12870-016-0890-5.

[55] A. Boccaccini *et al.*, “The DOF protein DAG1 and the della protein GAI cooperate in negatively regulating the AtGA3ox1 gene,” Sep. 01, 2014, *Cell Press*. doi: 10.1093/mp/ssu046.

[56] M. Negbi and D. Koller, “Dual Action of White Light in the Photocontrol of Germination of Oryzopsis miliacea,” *Plant Physiol*, vol. 39, no. 2, pp. 247–253, Mar. 1964, doi: 10.1104/pp.39.2.247.

[57] C. A. Thanos, K. Georghiou, and P. Delipetrou, “Photoinhibition of seed germination in the maritime plant matthiola tricuspidata,” *Ann Bot*, vol. 73, no. 6, pp. 639–644, 1994, doi: 10.1006/anbo.1994.1080.

[58] C. A. Thanos, K. Georghiou, D. J. Douma, and C. J. Marangaki, “Photoinhibition of seed germination in mediterranean maritime plants,” *Ann Bot*, vol. 68, no. 5, pp. 469–475, 1991, doi: 10.1093/oxfordjournals.aob.a088280.

[59] Z. Yaniv and A. L. Mancinelli, “Phytochrome and Seed Germination. IV. Action of Light Sources With Different Spectral Energy Distribution on the Germination of Tomato Seeds,” *Plant Physiol*, vol. 43, no. 1, pp. 117–120, Jan. 1968, doi: 10.1104/pp.43.1.117.

[60] F. C. Botha and J. G. Chris Small, “The Germination Response of the Negatively Photoblastic Seeds of Citrullus lanatus to Light of Different Spectral Compositions,” *J Plant Physiol*, vol. 132, no. 6, pp. 750–753, 1988, doi: 10.1016/S0176-1617(88)80240-2.

[61] K. J. Appenroth, G. Lenk, L. Goldau, and R. Sharma, “Tomato seed germination: Regulation of different response modes by phytochrome B2 and phytochrome A,” *Plant Cell Environ*, vol. 29, no. 4, pp. 701–709, Apr. 2006, doi: 10.1111/j.1365-3040.2005.01455.x.

[62] C. Shichijo, K. Katada, O. Tanaka, and T. Hashimoto, “Phytochrome A-mediated inhibition of seed germination in tomato,” *Planta*, vol. 213, no. 5, pp. 764–769, 2001, doi: 10.1007/s004250100545.
[63] J. M. Barrero, A. B. Downie, Q. Xu, and F. Gubler, “A role for barley CRYPTOCHROME1 in light regulation of grain dormancy and germination,” *Plant Cell*, vol. 26, no. 3, pp. 1094–1104, 2014, doi: 10.1105/tpc.113.121830.
[64] Z. Mérai *et al.*, “Aethionema arabicum: A novel model plant to study the light control of seed germination,” *J Exp Bot*, vol. 70, no. 12, pp. 3313–3328, Jun. 2019, doi: 10.1093/jxb/erz146.
[65] H. A. Borthwick, S. B. Hendricks, M. W. Parker, E. H. Toole, and V. K. Toole, “A Reversible Photoreaction Controlling Seed Germination,” *Proceedings of the National Academy of Sciences*, vol. 38, no. 8, pp. 662–666, Aug. 1952, doi: 10.1073/pnas.38.8.662.
[66] M. Seo *et al.*, “Regulation of hormone metabolism in Arabidopsis seeds: Phytochrome regulation of abscisic acid metabolism and abscisic acid regulation of gibberellin metabolism,” *Plant Journal*, vol. 48, no. 3, pp. 354–366, Nov. 2006, doi: 10.1111/j.1365-313X.2006.02881.x.
[67] N. Fernandez-Pozo *et al.*, “Aethionema arabicum genome annotation using PacBio full-length transcripts provides a valuable resource for seed dormancy and Brassicaceae evolution research,” *Plant Journal*, vol. 106, no. 1, pp. 275–293, Apr. 2021, doi: 10.1111/tpj.15161.
[68] Z. Mérai, F. Xu, A. Hajdu, L. Kozma-Bognár, and L. Dolan, “Phytochrome A is required for light-inhibited germination of Aethionema arabicum seed,” *New Phytologist*, vol. 247, no. 5, pp. 2134–2146, Sep. 2025, doi: 10.1111/nph.70344.
[69] Z. Mérai *et al.*, “Phytochromes mediate germination inhibition under red, far-red, and white light in Aethionema arabicum,” *Plant Physiol*, vol. 192, no. 2, pp. 1584–1602, Jun. 2023, doi: 10.1093/plphys/kiad138.
[70] D. Koenig and D. Weigel, “Beyond the thale: Comparative genomics and genetics of Arabidopsis relatives,” May 21, 2015, *Nat Rev Genet*. doi: 10.1038/nrg3883.
[71] U. Krämer, “Planting molecular functions in an ecological context with arabidopsis thaliana,” *Elife*, vol. 2015, no. 4, Mar. 2015, doi: 10.7554/elife.06100.
[72] X. Gan *et al.*, “The Cardamine hirsuta genome offers insight into the evolution of morphological diversity,” *Nat Plants*, vol. 2, no. 11, Oct. 2016, doi: 10.1038/nplants.2016.167.

[73] J. Lihová, K. Marhold, H. Kudoh, and M. A. Koch, “Worldwide phylogeny and biogeography of Cardamine flexuosa (Brassicaceae) and its relatives,” *Am J Bot*, vol. 93, no. 8, pp. 1206–1221, 2006, doi: 10.3732/ajb.93.8.1206.

[74] C. Canales, M. Barkoulas, C. Galinha, and M. Tsiantis, “Weeds of change: Cardamine hirsuta as a new model system for studying dissected leaf development,” Jan. 2010, *J Plant Res*. doi: 10.1007/s10265-009-0263-3.

[75] M. A. Beilstein, I. A. Al-Shehbaz, S. Mathews, and E. A. Kellogg, “Brassicaceae phylogeny inferred from phytochrome A and ndhF sequence data: Tribes and trichomes revisited,” *Am J Bot*, vol. 95, no. 10, pp. 1307–1327, Oct. 2008, doi: 10.3732/ajb.0800065.

[76] T. L. P. Couvreur, A. Franzke, I. A. Al-Shehbaz, F. T. Bakker, M. A. Koch, and K. Mummenhoff, “Molecular phylogenetics, temporal diversification, and principles of evolution in the mustard family (Brassicaceae),” *Mol Biol Evol*, vol. 27, no. 1, pp. 55–71, Jan. 2010, doi: 10.1093/molbev/msp202.

[77] A. S. Hay *et al.*, “Cardamine hirsuta: A versatile genetic system for comparative studies,” *Plant Journal*, vol. 78, no. 1, pp. 1–15, 2014, doi: 10.1111/tpj.12447.

[78] D. Vlad *et al.*, “Leaf shape evolution through duplication, regulatory diversification and loss of a homeobox gene,” *Science (1979)*, vol. 343, no. 6172, pp. 780–783, 2014, doi: 10.1126/science.1248384.

[79] A. Sicard *et al.*, “Repeated evolutionary changes of leaf morphology caused by mutations to a homeobox gene,” *Current Biology*, vol. 24, no. 16, pp. 1880–1886, Aug. 2014, doi: 10.1016/j.cub.2014.06.061.

[80] C. L. A. Kamei, B. Pieper, S. Laurent, M. Tsiantis, and P. Huijser, “CRISPR/Cas9-mediated mutagenesis of RCO in cardamine hirsuta,” *Plants*, vol. 9, no. 2, Feb. 2020, doi: 10.3390/plants9020268.

[81] A. Hay and M. Tsiantis, “The genetic basis for differences in leaf form between Arabidopsis thaliana and its wild relative Cardamine hirsuta,” *Nat Genet*, vol. 38, no. 8, pp. 942–947, Aug. 2006, doi: 10.1038/ng1835.

[82] B. J. M. Tremblay and J. I. Qüesta, “Non-coding and epigenetic mechanisms in the regulation of seed germination in Arabidopsis thaliana,” Jun. 17, 2025, *J Exp Bot*. doi: 10.1093/jxb/eraf051.

[83] M. Tanaka, A. Kikuchi, and H. Kamada, “The arabidopsis histone deacetylases HDA6 and HDA19 contribute to the repression of embryonic properties after germination,” *Plant Physiol*, vol. 146, no. 1, pp. 149–161, 2008, doi: 10.1104/pp.107.111674.

[84] M. Van Zanten *et al.*, "HISTONE DEACETYLASE 9 represses seedling traits in Arabidopsis thaliana dry seeds," *Plant Journal*, vol. 80, no. 3, pp. 475–488, Nov. 2014, doi: 10.1111/tpj.12646.
[85] Z. Wang *et al.*, "Arabidopsis seed germination speed is controlled by SNL histone deacetylase-binding factor-mediated regulation of AUX1," *Nat Commun*, vol. 7, Nov. 2016, doi: 10.1038/ncomms13412.
[86] Y. Han *et al.*, "Arabidopsis histone deacetylase HD2A and HD2B regulate seed dormancy by repressing DELAY OF GERMINATION 1," *Front Plant Sci*, vol. 14, 2023, doi: 10.3389/fpls.2023.1124899.
[87] Y. Liu, M. Koornneef, and W. J. J. Soppe, "The absence of histone H2B monoubiquitination in the Arabidopsis hub1 (rdo4) mutant reveals a role for chromatin remodeling in seed dormancy," *Plant Cell*, vol. 19, no. 2, pp. 433–444, 2007, doi: 10.1105/tpc.106.049221.
[88] A. M. Molitor, Z. Bu, Y. Yu, and W. H. Shen, "Arabidopsis AL PHD-PRC1 Complexes Promote Seed Germination through H3K4me3-to-H3K27me3 Chromatin State Switch in Repression of Seed Developmental Genes," *PLoS Genet*, vol. 10, no. 1, Jan. 2014, doi: 10.1371/journal.pgen.1004091.
[89] C. Yang, F. Bratzel, N. Hohmann, M. Koch, F. Turck, and M. Calonje, "VAL-and AtBMI1-Mediated H2Aub initiate the switch from embryonic to postgerminative growth in arabidopsis," *Current Biology*, vol. 23, no. 14, pp. 1324–1329, Jul. 2013, doi: 10.1016/j.cub.2013.05.050.
[90] J. Zheng *et al.*, "A novel role for histone methyltransferase KYP/SUVH4 in the control of Arabidopsis primary seed dormancy," *New Phytologist*, vol. 193, no. 3, pp. 605–616, Feb. 2012, doi: 10.1111/j.1469-8137.2011.03969.x.
[91] D. Gu *et al.*, "Arabidopsis histone methyltransferase SUVH5 is a positive regulator of light-mediated seed germination," *Front Plant Sci*, vol. 10, May 2019, doi: 10.3389/fpls.2019.00841.
[92] J. Goodrich, P. Puangsomlee, M. Martin, D. Long, E. M. Meyerowitz, and G. Coupland, "A Polycomb-group gene regulates homeotic gene expression in Arabidopsis," *Nature*, vol. 386, no. 6620, pp. 44–51, Mar. 1997, doi: 10.1038/386044a0.
[93] U. Grossniklaus, J. P. Vielle-Calzada, M. A. Hoeppner, and W. B. Gagliano, "Maternal control of embryogenesis by MEDEA, a Polycomb group gene in Arabidopsis," *Science (1979)*, vol. 280, no. 5362, pp. 446–450, Apr. 1998, doi: 10.1126/science.280.5362.446.
[94] M. Luo, P. Bilodeau, A. Koltunow, E. S. Dennis, W. J. Peacock, and A. M. Chaudhury, "Genes controlling fertilization-independent seed

development in Arabidopsis thaliana," *Proc Natl Acad Sci U S A*, vol. 96, no. 1, pp. 296–301, Jan. 1999, doi: 10.1073/pnas.96.1.296.
[95] Y. Chanvivattana *et al.*, "Interaction of Polycomb-group proteins controlling flowering in Arabidopsis," *Development*, vol. 131, no. 21, pp. 5263–5276, Nov. 2004, doi: 10.1242/dev.01400.
[96] N. Yoshida *et al.*, "EMBRYONIC FLOWER2, a Novel Polycomb Group Protein Homolog, Mediates Shoot Development and Flowering in Arabidopsis," *Plant Cell*, vol. 13, no. 11, pp. 2471–2481, Nov. 2001, doi: 10.1105/tpc.010227.
[97] A. R. Gendall, Y. Y. Levy, A. Wilson, and C. Dean, "The VERNALIZATION 2 gene mediates the epigenetic regulation of vernalization in Arabidopsis," *Cell*, vol. 107, no. 4, pp. 525–535, Nov. 2001, doi: 10.1016/S0092-8674(01)00573-6.
[98] R. A. Ach, P. Taranto, and W. Gruissem, "A conserved family of WD-40 proteins binds to the retinoblastoma protein in both plants and animals," *Plant Cell*, vol. 9, no. 9, pp. 1595–1606, 1997, doi: 10.1105/tpc.9.9.1595.
[99] A. L. Kenzior and W. R. Folk, "AtMSI4 and RbAp48 WD-40 repeat proteins bind metal ions," *FEBS Lett*, vol. 440, no. 3, pp. 425–429, Dec. 1998, doi: 10.1016/S0014-5793(98)01500-2.
[100] L. Hennig, R. Bouveret, and W. Gruissem, "MSI1-like proteins: An escort service for chromatin assembly and remodeling complexes," Jun. 2005, *Trends Cell Biol*. doi: 10.1016/j.tcb.2005.04.004.
[101] C. Spillane *et al.*, "Interaction of the Arabidopsis Polycomb group proteins FIE and MEA mediates their common phenotypes," *Current Biology*, vol. 10, no. 23, pp. 1535–1538, Nov. 2000, doi: 10.1016/S0960-9822(00)00839-3.
[102] R. Yadegari *et al.*, "Mutations in the FIE and MEA genes that encode interacting polycomb proteins cause parent-of-origin effects on seed development by distinct mechanisms," *Plant Cell*, vol. 12, no. 12, pp. 2367–2381, 2000, doi: 10.1105/tpc.12.12.2367.
[103] T. Kinoshita, J. J. Harada, R. B. Goldberg, and R. L. Fischer, "Polycomb repression of flowering during early plant development," *Proc Natl Acad Sci U S A*, vol. 98, no. 24, pp. 14156–14161, Nov. 2001, doi: 10.1073/pnas.241507798.
[104] N. Ohad *et al.*, "Mutations in FIE, a WD polycomb group gene, allow endosperm development without fertilization," *Plant Cell*, vol. 11, no. 3, pp. 407–415, 1999, doi: 10.1105/tpc.11.3.407.
[105] K. Müller, D. Bouyer, A. Schnittger, and A. R. Kermode, "Evolutionarily Conserved Histone Methylation Dynamics during

Seed Life-Cycle Transitions," *PLoS One*, vol. 7, no. 12, Dec. 2012, doi: 10.1371/journal.pone.0051532.
[106] D. Bouyer *et al.*, "Polycomb repressive complex 2 controls the embryo-to-seedling phase transition," *PLoS Genet*, vol. 7, no. 3, Mar. 2011, doi: 10.1371/journal.pgen.1002014.
[107] B. Xu *et al.*, "Selective inhibition of EZH2 and EZH1 enzymatic activity by a small molecule suppresses MLL-rearranged leukemia," *Blood*, vol. 125, no. 2, pp. 346–357, Aug. 2015, doi: 10.1182/blood-2014-06-581082.
[108] K. D. Konze *et al.*, "An orally bioavailable chemical probe of the lysine methyltransferases EZH2 and EZH1," *ACS Chem Biol*, vol. 8, no. 6, pp. 1324–1334, Jun. 2013, doi: 10.1021/cb400133j.
[109] A. Lepri *et al.*, "Plants and Small Molecules: An Up-and-Coming Synergy," Apr. 01, 2023, *Plants (Basel)*. doi: 10.3390/plants12081729.
[110] S. Valente *et al.*, "Identification of PR-SET7 and EZH2 selective inhibitors inducing cell death in human leukemia U937 cells," *Biochimie*, vol. 94, no. 11, pp. 2308–2313, Nov. 2012, doi: 10.1016/j.biochi.2012.06.003.
[111] V. Ruta *et al.*, "Inhibition of Polycomb Repressive Complex 2 activity reduces trimethylation of H3K27 and affects development in Arabidopsis seedlings," *BMC Plant Biol*, vol. 19, no. 1, Oct. 2019, doi: 10.1186/s12870-019-2057-7.
[112] A. Lepri *et al.*, "A DOF transcriptional repressor-gibberellin feedback loop plays a crucial role in modulating light-independent seed germination," *Plant Commun*, vol. 6, no. 4, Apr. 2025, doi: 10.1016/j.xplc.2025.101262.
[113] S. G. Thomas, A. L. Phillips, and P. Hedden, "Molecular cloning and functional expression of gibberellin 2- oxidases, multifunctional enzymes involved in gibberellin deactivation.," *Proc Natl Acad Sci U S A*, vol. 96, no. 8, pp. 4698–4703, Apr. 1999, doi: 10.1073/pnas.96.8.4698.
[114] G. Bertolotti *et al.*, "A PHABULOSA-Controlled Genetic Pathway Regulates Ground Tissue Patterning in the Arabidopsis Root.," *Curr Biol*, vol. 31, no. 2, pp. 420-426.e6, Jan. 2021, doi: 10.1016/j.cub.2020.10.038.
[115] T. Sun and F. Gubler, "MOLECULAR MECHANISM OF GIBBERELLIN SIGNALING IN PLANTS," *Annu Rev Plant Biol*, vol. 55, no. Volume 55, 2004, pp. 197–223, 2004, doi: https://doi.org/10.1146/annurev.arplant.55.031903.141753.

[116] P. Hedden, “The genes of the Green Revolution,” *Trends in Genetics*, vol. 19, no. 1, pp. 5–9, 2003, doi: https://doi.org/10.1016/S0168-9525(02)00009-4.
[117] C. Schwechheimer and B. C. Willige, “Shedding light on gibberellic acid signalling.,” *Curr Opin Plant Biol*, vol. 12, no. 1, pp. 57–62, Feb. 2009, doi: 10.1016/j.pbi.2008.09.004.
[118] N. Nishimura, T. Yoshida, N. Kitahata, T. Asami, K. Shinozaki, and T. Hirayama, “ABA-Hypersensitive Germination1 encodes a protein phosphatase 2C, an essential component of abscisic acid signaling in Arabidopsis seed.,” *Plant J*, vol. 50, no. 6, pp. 935–949, Jun. 2007, doi: 10.1111/j.1365-313X.2007.03107.x.
[119] T. Yoshida *et al.*, “ABA-hypersensitive germination3 encodes a protein phosphatase 2C (AtPP2CA) that strongly regulates abscisic acid signaling during germination among Arabidopsis protein phosphatase 2Cs.,” *Plant Physiol*, vol. 140, no. 1, pp. 115–126, Jan. 2006, doi: 10.1104/pp.105.070128.
[120] G. Née *et al.*, “DELAY OF GERMINATION1 requires PP2C phosphatases of the ABA signalling pathway to control seed dormancy,” *Nat Commun*, vol. 8, no. 1, p. 72, 2017, doi: 10.1038/s41467-017-00113-6.
[121] N. Nishimura *et al.*, “Control of seed dormancy and germination by DOG1-AHG1 PP2C phosphatase complex via binding to heme,” *Nat Commun*, vol. 9, no. 1, p. 2132, 2018, doi: 10.1038/s41467-018-04437-9.
[122] J.-M. Davière and P. Achard, “Gibberellin signaling in plants.,” *Development*, vol. 140, no. 6, pp. 1147–1151, Mar. 2013, doi: 10.1242/dev.087650.
[123] A. Boccaccini *et al.*, “The DOF protein DAG1 and the DELLA protein GAI cooperate in negatively regulating the AtGA3ox1 gene.,” *Mol Plant*, vol. 7, no. 9, pp. 1486–1489, Sep. 2014, doi: 10.1093/mp/ssu046.
[124] S. Gabriele, A. Rizza, J. Martone, P. Circelli, P. Costantino, and P. Vittorioso, “The Dof protein DAG1 mediates PIL5 activity on seed germination by negatively regulating GA biosynthetic gene AtGA3ox1.,” *Plant J*, vol. 61, no. 2, pp. 312–323, Jan. 2010, doi: 10.1111/j.1365-313X.2009.04055.x.
[125] A. Boccaccini *et al.*, “The DAG1 transcription factor negatively regulates the seed-to-seedling transition in Arabidopsis acting on ABA and GA levels.,” *BMC Plant Biol*, vol. 16, no. 1, p. 198, Sep. 2016, doi: 10.1186/s12870-016-0890-5.

[126] S. Yanagisawa, "The transcriptional activation domain of the plant-specific Dof1 factor functions in plant, animal, and yeast cells.," *Plant Cell Physiol*, vol. 42, no. 8, pp. 813–822, Aug. 2001, doi: 10.1093/pcp/pce105.
[127] L.-H. Yu *et al.*, "Arabidopsis MADS-Box Transcription Factor AGL21 Acts as Environmental Surveillance of Seed Germination by Regulating ABI5 Expression.," *Mol Plant*, vol. 10, no. 6, pp. 834–845, Jun. 2017, doi: 10.1016/j.molp.2017.04.004.
[128] P.-H. Meng, A. Macquet, O. Loudet, A. Marion-Poll, and H. M. North, "Analysis of natural allelic variation controlling Arabidopsis thaliana seed germinability in response to cold and dark: identification of three major quantitative trait loci.," *Mol Plant*, vol. 1, no. 1, pp. 145–154, Jan. 2008, doi: 10.1093/mp/ssm014.
[129] L. Baumgarten *et al.*, "Pan-European study of genotypes and phenotypes in the Arabidopsis relative Cardamine hirsuta reveals how adaptation, demography, and development shape diversity patterns.," *PLoS Biol*, vol. 21, no. 7, p. e3002191, Jul. 2023, doi: 10.1371/journal.pbio.3002191.
[130] F. Chen and K. J. Bradford, "Expression of an expansin is associated with endosperm weakening during tomato seed germination.," *Plant Physiol*, vol. 124, no. 3, pp. 1265–1274, Nov. 2000, doi: 10.1104/pp.124.3.1265.
[131] S. A. Sinclair *et al.*, "Etiolated Seedling Development Requires Repression of Photomorphogenesis by a Small Cell-Wall-Derived Dark Signal.," *Curr Biol*, vol. 27, no. 22, pp. 3403-3418.e7, Nov. 2017, doi: 10.1016/j.cub.2017.09.063.
[132] H. Xu *et al.*, "A Molecular Signal Integration Network Underpinning Arabidopsis Seed Germination.," *Curr Biol*, vol. 30, no. 19, pp. 3703-3712.e4, Oct. 2020, doi: 10.1016/j.cub.2020.07.012.
[133] H. Chen *et al.*, "PIFs interact with SWI2/SNF2-related 1 complex subunit 6 to regulate H2A.Z deposition and photomorphogenesis in Arabidopsis," *Journal of Genetics and Genomics*, vol. 50, no. 12, pp. 983–992, Dec. 2023, doi: 10.1016/j.jgg.2023.04.008.
[134] A. Rizza, A. Walia, V. Lanquar, W. B. Frommer, and A. M. Jones, "In vivo gibberellin gradients visualized in rapidly elongating tissues," *Nat Plants*, vol. 3, no. 10, pp. 803–813, Oct. 2017, doi: 10.1038/s41477-017-0021-9.
[135] M. Van Zanten *et al.*, "Seed maturation in Arabidopsis thaliana is characterized by nuclear size reduction and increased chromatin condensation," *Proc Natl Acad Sci U S A*, vol. 108, no. 50, pp. 20219–20224, Dec. 2011, doi: 10.1073/pnas.1117726108.

[136] C. Bourbousse *et al.*, "Light signaling controls nuclear architecture reorganization during seedling establishment," *Proc Natl Acad Sci U S A*, vol. 112, no. 21, pp. E2836–E2844, May 2015, doi: 10.1073/pnas.1503512112.
[137] P. Johann to Berens *et al.*, "Advanced Image Analysis Methods for Automated Segmentation of Subnuclear Chromatin Domains," *Epigenomes*, vol. 6, no. 4, Dec. 2022, doi: 10.3390/epigenomes6040034.
[138] J. W. Reed, A. Nagatani, T. D. Elich, M. Fagan, and J. Chory, "Phytochrome A and Phytochrome B Have Overlapping but Distinct Functions in Arabidopsis Development," *Plant Physiol*, vol. 104, no. 4, pp. 1139–1149, 1994, doi: 10.1104/PP.104.4.1139.
[139] J. W. Reed, P. Nagpal, D. S. Poole, M. Furuya, and J. Chory, "Mutations in the gene for the red/far-red light receptor phytochrome B alter cell elongation and physiological responses throughout arabidopsis development," *Plant Cell*, vol. 5, no. 2, pp. 147–157, 1993, doi: 10.1105/tpc.5.2.147.
[140] S. Schiml, F. Fauser, and H. Puchta, "CRISPR/Cas-mediated site-specifi c mutagenesis in arabidopsis thaliana using Cas9 nucleases and paired nickases," in *Methods in Molecular Biology*, vol. 1469, Methods Mol Biol, 2016, pp. 111–122. doi: 10.1007/978-1-4939-4931-1_8.
[141] G. Di Ruocco *et al.*, "Differential spatial distribution of miR165/6 determines variability in plant root anatomy," *Development*, vol. 145, no. 1, Jan. 2018, doi: 10.1242/dev.153858.
[142] S. J. Clough and A. F. Bent, "Floral dip: A simplified method for Agrobacterium-mediated transformation of Arabidopsis thaliana," *Plant Journal*, vol. 16, no. 6, pp. 735–743, Dec. 1998, doi: 10.1046/j.1365-313X.1998.00343.x.
[143] X. Zhang, R. Henriques, S. S. Lin, Q. W. Niu, and N. H. Chua, "Agrobacterium-mediated transformation of Arabidopsis thaliana using the floral dip method," *Nat Protoc*, vol. 1, no. 2, pp. 641–646, Jul. 2006, doi: 10.1038/nprot.2006.97.
[144] L. Moubayidin *et al.*, "Spatial coordination between stem cell activity and cell differentiation in the root meristem," *Dev Cell*, vol. 26, no. 4, pp. 405–415, Aug. 2013, doi: 10.1016/j.devcel.2013.06.025.
[145] T. Urbanová, D. Tarkowská, O. Novák, P. Hedden, and M. Strnad, "Analysis of gibberellins as free acids by ultra performance liquid chromatography-tandem mass spectrometry," *Talanta*, vol. 112, pp. 85–94, Aug. 2013, doi: 10.1016/j.talanta.2013.03.068.

[146] D. Rittenberg and G. L. Foster, “A New Procedure For Quantitative Analysis By Isotope Dilution, With Application To The Determination Of Amino Acids And Fatty Acids,” *Journal of Biological Chemistry*, vol. 133, no. 3, pp. 737–744, May 1940, doi: 10.1016/s0021-9258(18)73304-8.
[147] H. Wickham, “Reshaping data with the reshape package,” *J Stat Softw*, vol. 21, no. 12, pp. 1–20, 2007, doi: 10.18637/jss.v021.i12.
[148] W. C. Hadley Wickham, *RStudio Create Elegant Data Visualisations Using the Grammar of Graphics*. 2016. Accessed: Oct. 22, 2025. [Online]. Available: https://cir.nii.ac.jp/crid/1883118016368358400
[149] E. Neuwirth, “Package ‘rcolorbrewer,’” *mirror.niser.ac.in*, 2014, Accessed: Oct. 22, 2025. [Online]. Available: https://mirror.niser.ac.in/cran/web/packages/RColorBrewer/RColorBrewer.pdf
[150] A. Kassambara, “Ggpubr:’Ggplot2’Based Publication Ready Plots,” *R package version*, p. 2, 2023, Accessed: Oct. 21, 2025. [Online]. Available: https://cir.nii.ac.jp/crid/1370861707141778052
[151] J. H. Rowe, A. Rizza, and A. M. Jones, “Quantifying Phytohormones in Vivo with FRET Biosensors and the FRETENATOR Analysis Toolset,” in *Methods in Molecular Biology*, vol. 2494, Methods Mol Biol, 2022, pp. 239–253. doi: 10.1007/978-1-0716-2297-1_17.

8. List of publications

Lepri, A., Kazmi, H., Bertolotti, G., Longo, C., Occhigrossi, S., Quattrocchi, L., De Vivo, M., Scintu, D., Svolacchia, N., Tarkowska, D., Tureckova, V., Strnad, M., Del Bianco, M., Di Mambro, R., Costantino, P., Sabatini, S., Dello Ioio, R., & Vittorioso, P. (2025). A DOF transcriptional repressor-gibberellin feedback loop plays a crucial role in modulating light-independent seed germination. *Plant communications*, *6*(4), 101262.

Boccaccini, A., Cimini, S., Kazmi, H., Lepri, A., Longo, C., Lorrai, R., & Vittorioso, P. (2024). When Size Matters: New Insights on How Seed Size Can Contribute to the Early Stages of Plant Development. *Plants (Basel, Switzerland)*, *13*(13), 1793.

Lepri, A., Longo, C., Messore, A., Kazmi, H., Madia, V. N., Di Santo, R., Costi, R., & Vittorioso, P. (2023). Plants and Small Molecules: An Up-and-Coming Synergy. *Plants (Basel, Switzerland)*, *12*(8), 1729.

Longo, C., Lepri, A., Paciolla, A., Messore, A., De Vita, D., Bonaccorsi di Patti, M. C., Amadei, M., Madia, V. N., Ialongo, D., Di Santo, R., Costi, R., & Vittorioso, P. (2022). New Inhibitors of the Human p300/CBP Acetyltransferase Are Selectively Active against the Arabidopsis HAC Proteins. *International journal of molecular sciences*, *23*(18), 10446.

Longo, C., Holness, S., De Angelis, V., Lepri, A., Occhigrossi, S., Ruta, V., & Vittorioso, P. (2021). From the Outside to the Inside: New Insights on the Main Factors That Guide Seed Dormancy and Germination. *Genes*, *12*(1), 52.

Ruta, V., Longo, C., Lepri, A., De Angelis, V., Occhigrossi, S., Costantino, P., & Vittorioso, P. (2020). The DOF Transcription Factors in Seed and Seedling Development. *Plants (Basel, Switzerland)*, *9*(2), 218.